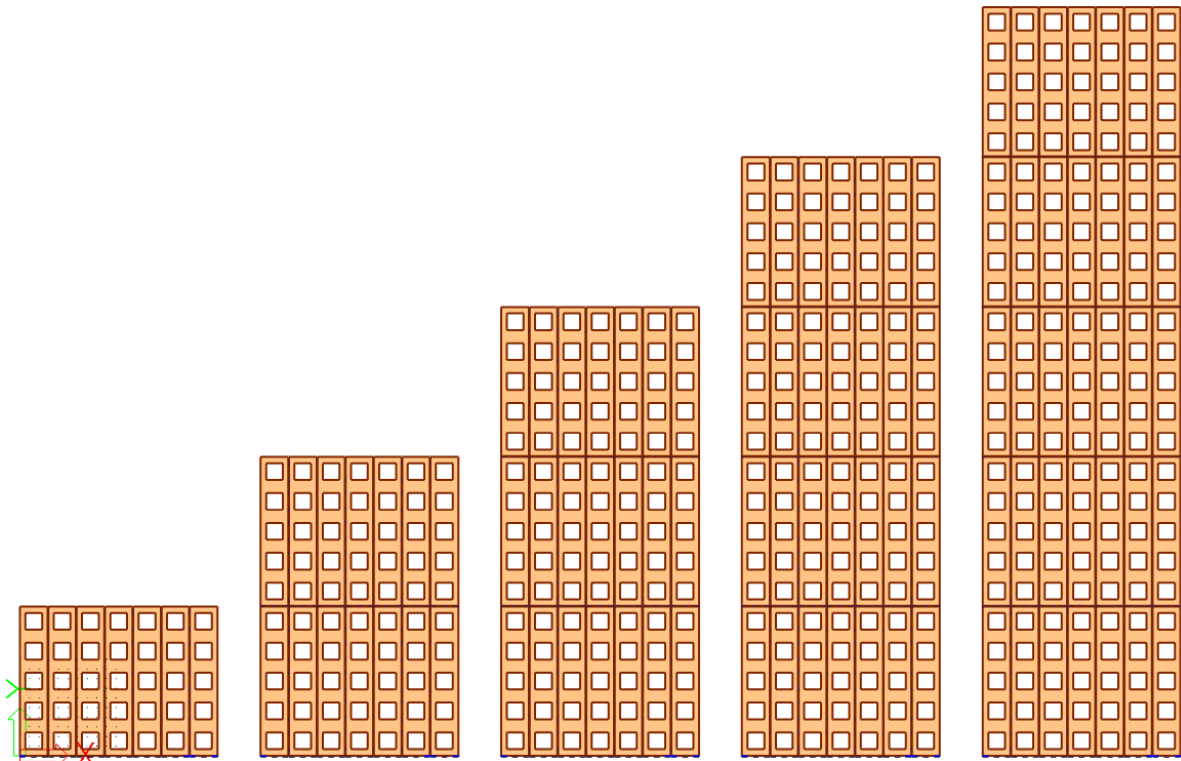


Structural analysis of CLT walls in façades of a multistory building

Appendices



Pim Mol

February 2023

Content

A1	Appendices	4
A2	Chapter 2 appendices	5
A2.1	Method of Schelling.....	5
A2.2	Method of Schelling - forces.....	7
A2.3	Method of Schelling derivation	8
A2.4	Effective moment of inertia for CLT panels.....	10
A2.5	Buckling of CLT	13
A2.6	CLT panel properties	15
A2.7	Comparisson of test results	18
A2.8	Effective number of fasteners (stiffness)	19
A2.9	Single shear plane steel-to-timber connections.....	21
A2.10	Brittle failure modes of multi-fastener connections.....	23
A3	Chapter 3 appendices	26
A3.1	Loads on the structure	26
A3.2	c_{s,c_d} factor calculation.....	28
A3.3	Detail of the façade-floor connection.....	30
A3.4	2nd order calculation for the structure	31
A4	Chapter 4 appendices	32
A4.1	Façade view and deflection components	32
A4.2	Shear stiffness of fenestrated panels	42
A4.3	Theoretical hand calculations	43
A4.4	Theoretical top deformation without connection stiffness.....	46
A4.5	Maple script for the top deformation due to deformation of the lintels.....	47
A4.6	Theoretical top deformation - results	48
A4.7	Forces on the connections – additional bending moment.....	49
A5	Chapter 5 appendices	51
A5.1	Detail drawings of the connections at the foundation.....	51
A5.2	Detail drawings of the connections at the fifth floor	58
A5.3	Calculation of the bolt resistance of a M16 bolt.....	63
A5.4	Maximum force on bolts of shear key connections on vertical edges of the panels....	65
A6	Chapter 6 appendices	66
A6.1	Validation of the model	66
A6.2	Validation of connections (with linear stiffness)	70

A6.3	Modelling of the transversal façade	83
A7	Chapter 7 appendices	84
A7.1	Theoretical top deformation including connection stiffness.....	84
A7.2	Theoretical top deformation including connection stiffness and slip	89
A7.3	Addition of a concrete core.....	92
A7.4	Theoretical contribution of the effective width.....	94
A7.5	Reduced top deformation – theoretical calculation without connection stiffnesses ..	100

A1 Appendices

This report contains the appendices for the main thesis report “CLT façade structures; study on the influence of mechanical connections on the strength and stiffness of CLT façades that function as the main stability system”. Each chapter will have its dedicated appendices with same chapter number.

A2 Chapter 2 appendices

A2.1 Method of Schelling

The method of Schelling will be derived for a structure with 7 elements using maple. It can be derived by solving the differential equation below.

$$EI \frac{d^4 w}{dx^4} = q(x) \quad (1)$$

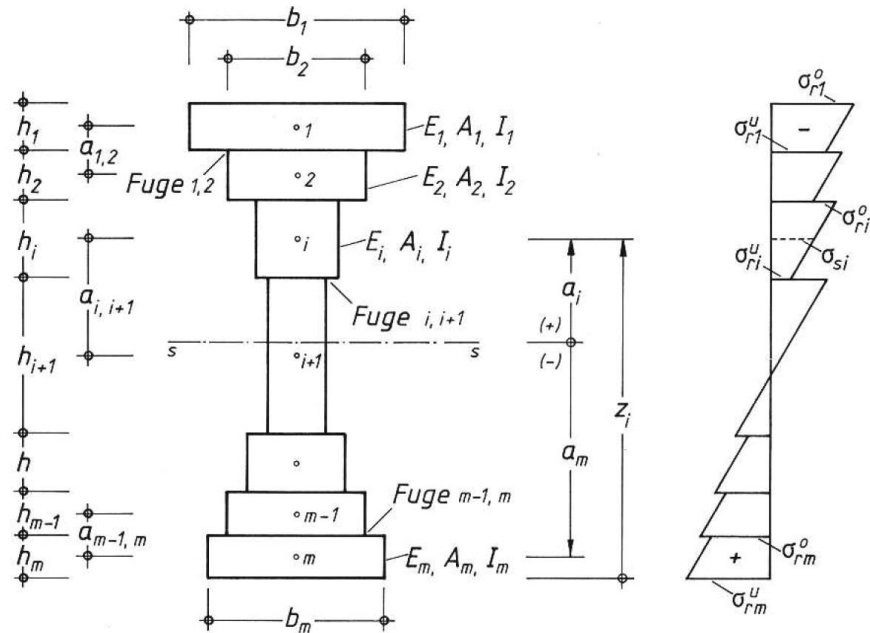


Figure 1, variables for the calculation of the gamma-values (Schelling, W. 1982)

$$\begin{bmatrix}
 v_{1,1} & v_{1,2} & 0 & 0 & 0 & 0 & 0 \\
 v_{2,1} & v_{2,2} & v_{2,3} & 0 & 0 & 0 & 0 \\
 0 & \cdot & \cdot & \cdot & 0 & 0 & 0 \\
 0 & 0 & v_{i,i-1} & v_{i,i} & v_{i,i+1} & 0 & 0 \\
 0 & 0 & 0 & \cdot & \cdot & \cdot & 0 \\
 0 & 0 & 0 & 0 & v_{m-1,m-2} & v_{m-1,m-1} & v_{m-1,m} \\
 0 & 0 & 0 & 0 & 0 & v_{m,m-1} & v_{m,m}
 \end{bmatrix}
 *
 \begin{bmatrix}
 \gamma_1 \\
 \gamma_2 \\
 \cdot \\
 \gamma_i \\
 \cdot \\
 \gamma_{m-1} \\
 \gamma_m
 \end{bmatrix}
 =
 \begin{bmatrix}
 s_1 \\
 s_2 \\
 \cdot \\
 s_i \\
 \cdot \\
 s_{m-1} \\
 s_m
 \end{bmatrix}$$

$$v_{i,i-1} = -\bar{C}_{i-1,i} * a_{i-1}$$

$$v_{i,i} = \left(\bar{C}_{i-1,i} + \bar{C}_{i,i+1} + \frac{\pi^2}{l^2} * E_v * \bar{A}_i \right) * a_{i-1}$$

$$v_{i,i+1} = -\bar{C}_{i,i+1} * a_{i+1}$$

$$s_i = \bar{C}_{i,i+1} * a_{i,i+1} - \bar{C}_{i-1,i} * a_{i-1,i}$$

Where,

- $\bar{C}_{i,i+1}$ is the stiffness per meter length of the connection between member i and member i+1
- a_i is the distance between the center of gravity of the member and that of the total element
- $v_{i,i}$ is an abbreviation for easier computing
- s_i is an abbreviation for easier computing

The maple script to calculate the γ -factors is shown in A2.3.

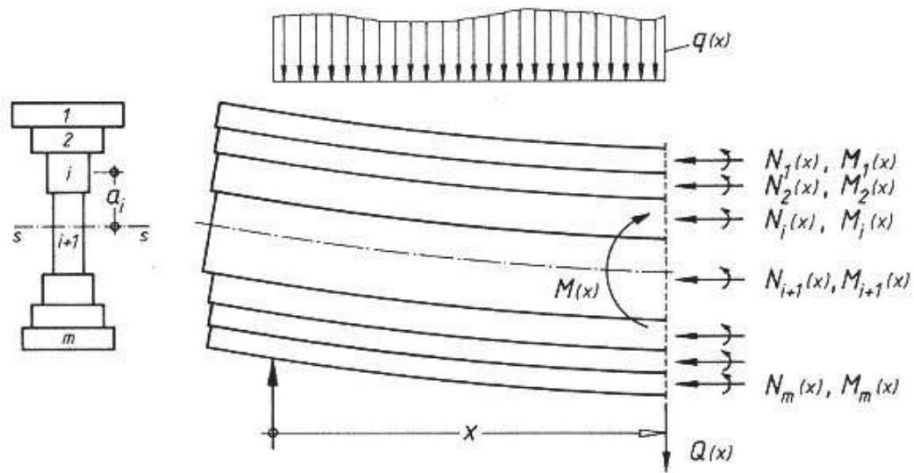


Figure 2, side view with section forces

A2.2 Method of Schelling - forces

The method of Schelling can be used to calculate the bending stiffness but also to calculate the forces on the elements. The bending stress in the middle of an element is calculated as:

$$\sigma_{si} = -\frac{M}{I_{ef}} * \gamma_i * a_i \quad (2)$$

And the bending stress at the ends of an element is calculated according to the method of Schelling as:

$$\sigma_{ri} = -\frac{M}{I_{ef}} * \gamma_i * (a_i \pm \frac{h_i}{2}) \quad (3)$$

Where,

M	is the bending moment on the façade
I_{ef}	is the effective bending stiffness according to the method
γ_i	is the gamma-value of element i
a_i	is the distance of element i to the center
h_i	is the height of element i
σ_{si}	is the stress due to bending in the center of the element
σ_{ri}	is the stress due to bending at the edges of the element

However, equation (3) does not correlate to Figure 2 as the bending moment $M_i(x)$ on each individual member has not been accounted for in the method of Schelling and will add a bending stress on each individual element.

A2.2.1 Section force equilibrium

The bending moment on the façade is calculated as the sum of all bending moments on the panels and the normal forces in each panel multiplied with its distance to the center of the façade (Figure 2). The bending moment on each panel can be derived from this as well.

$$M = \sum_{i=1}^n M_i(x) + \sum_{i=1}^n N_i(x) * a_i \quad (4)$$

In case all elements are symmetrical.

$$M_i(x) = \frac{M - \sum_{i=1}^n N_i(x) * a_i}{n} \quad (5)$$

$$N_i(x) = \sigma_{si} * b \quad (6)$$

M_i	is the bending moment on element i
N_i	is the axial force in element i
n	is the number of elements

A2.3 Method of Schelling derivation

```

> restart;
>
Calculation of the bending stiffness of a façade with the method of Schelling.
The height is multiplied by 2 as the method of Schelling is derived for a beam on two supports,
whereas the
façade is schematized as a cantilever.

The following equation is derived for 7 identical elements with the following parameters
>
> A := b·t :
> t := 't':
> b := 'b':
> h := 'h':
> E := 'E':
> K := 'K':
> L := 2·h :
>
> a1 := 3·b : a2 := 2·b : a3 := 1·b : a4 := 0 : a5 := -b : a6 := -2·b : a7 := -3·b :
>
> v11 :=  $\left( K + \frac{\text{Pi}^2}{L^2} \cdot E \cdot A \right) \cdot a1 : v12 := -K \cdot a2 :$ 
> v21 := -K·a1 : v22 :=  $\left( K + K + \frac{\text{Pi}^2}{L^2} \cdot E \cdot A \right) \cdot a2 : v23 := -K \cdot a3 :$ 
> v32 := -K·a2 : v33 :=  $\left( K + K + \frac{\text{Pi}^2}{L^2} \cdot E \cdot A \right) \cdot a3 : v34 := -K \cdot a4 :$ 
> v43 := -K·a3 : v44 :=  $\left( K + K + \frac{\text{Pi}^2}{L^2} \cdot E \cdot A \right) \cdot a4 : v45 := -K \cdot a5 :$ 
> v54 := -K·a4 : v55 :=  $\left( K + K + \frac{\text{Pi}^2}{L^2} \cdot E \cdot A \right) \cdot a5 : v56 := -K \cdot a6 :$ 
> v65 := -K·a5 : v66 :=  $\left( K + K + \frac{\text{Pi}^2}{L^2} \cdot E \cdot A \right) \cdot a6 : v67 := -K \cdot a7 :$ 
> v76 := -K·a6 : v77 :=  $\left( K + \frac{\text{Pi}^2}{L^2} \cdot E \cdot A \right) \cdot a7 :$ 
>
> s1 := K·b : s2 := 0 : s3 := 0 : s4 := 0 : s5 := 0 : s6 := 0 : s7 := -K·b :
>
> with(linalg) :
> Amatrix := matrix( [ [v11, v12, 0, 0, 0, 0, 0], [v21, v22, v23, 0, 0, 0, 0], [0, v32, v33, v34, 0, 0, 0],
0], [0, 0, v43, v44, v45, 0, 0], [0, 0, 0, v54, v55, v56, 0], [0, 0, 0, 0, v65, v66, v67], [0, 0, 0, 0, 0, v76, v77]] ) :
> S := vector( [s1, s2, s3, s4, s5, s6, s7] ) :
> gama := evalf( linsolve( Amatrix, S ) ) :

```

The solution holds the gamma-factors for each element.
 gama[1] is the first gamma-factor and-so-on.
 the moment of inertia is calculated for the façade without openings.
 First the I-value including stiffness is calculated, then the I-value without stiffness is calculated.
 This factor is then multiplied with the moment of inertia for the façade with openings to find the bending stiffness of the façade.

```

>
> gama[1]; gama[7]:
      1.333333333 K h2 (97.40909108 E2 b2 t2 + 157.9136705 E K b h2 t + 48. K2 h4)
      961.3891943 E3 b3 t3 + 1948.181822 E2 K b2 h2 t2 + 947.4820228 E K2 b h4 t + 64. K3 h6
> gama[2]; gama[6]:
      8. K2 h4 (9.869604404 E b t + 8. K h2)
      961.3891943 E3 b3 t3 + 1948.181822 E2 K b2 h2 t2 + 947.4820228 E K2 b h4 t + 64. K3 h6
> gama[3]; gama[5]:
      64. K3 h6
      961.3891943 E3 b3 t3 + 1948.181822 E2 K b2 h2 t2 + 947.4820228 E K2 b h4 t + 64. K3 h6
> gama[4];
      -t1
>
> Ief :=  $\frac{7 \cdot t \cdot b^3}{12} + 2 \cdot \text{gama}[1] \cdot t \cdot b \cdot a l^2 + 2 \cdot \text{gama}[2] \cdot t \cdot b \cdot a 2^2 + 2 \cdot \text{gama}[3] \cdot t \cdot b \cdot a 3^2$ ;
> Imax :=  $\frac{7 \cdot t \cdot b^3}{12} + 2 \cdot t \cdot b \cdot a l^2 + 2 \cdot t \cdot b \cdot a 2^2 + 2 \cdot t \cdot b \cdot a 3^2$ ; evalf(Ifull);
> gamma_red :=  $\frac{Ief}{Imax}$ ;
>
  
```

The presented equations have been rewritten below

$$\gamma_1 = \gamma_7 = \frac{(A^2 * E^2 * \pi^2 + 4 * A * k * E * L^2 * \pi^2 + 3 * k^2 * L^4) * k * L^2}{3 * (A^3 * E^3 * \pi^6 + 5 * A^2 * k * E^2 * L^2 * \pi^4 + 6 * A * k^2 * E * L^4 * \pi^2 + k^3 * L^6)}$$

$$\gamma_2 = \gamma_6 = \frac{(A * E * \pi^2 + 2 * k * L^2) * k^2 * L^4}{2 * (A^3 * E^3 * \pi^6 + 5 * A^2 * k * E^2 * L^2 * \pi^4 + 6 * A * k^2 * E * L^4 * \pi^2 + k^3 * L^6)}$$

$$\gamma_3 = \gamma_5 = \frac{k^3 * L^6}{1 * (A^3 * E^3 * \pi^6 + 5 * A^2 * k * E^2 * L^2 * \pi^4 + 6 * A * k^2 * E * L^4 * \pi^2 + k^3 * L^6)}$$

$$\gamma_4 = 1$$

A2.4 Effective moment of inertia for CLT panels

The effective moment of inertia for CLT panels has been calculated. For panels with two transverse layers, the gamma method as given in Eurocode 5 can be used. For panels with more transverse layers a method as presented in “Cross-Laminated Timber Structural Design” by Proholz has been applied. This is related to the method of Schelling where the stiffness between layers is dependent on the stiffness of the transverse layer due to rolling shear. Two exemplary calculations are shown on the following pages.

The resulting factors are shown in the table below

Table 1, bending stiffness of each CLT panel

	$I_{0,\text{net}}$ $\times 10^9 \text{ mm}^4$	γ_{red} -	$I_{0,\text{eff}}$ $\times 10^9 \text{ mm}^4$
LL-190/7s	0,485	0,881	0,46
LL-260/7s	1,387	0,801	1,11
LL-300/9s	2,099	0,560	1,18
LL-360/9s	3,360	0,391	1,31
LL-400/11s	4,589	0,462	2,12

CLT panel LL-190/7s

$E := 11000$	N/mm ²
$G_R := 50$	N/mm ²
$b := 1000$	mm
$L_{ref} := 3100$	mm

LL-190-7s

$t_0 := 30$	mm
$t_{g0} := 20$	mm

$$Y_1 := \frac{1}{1 + \frac{\pi^2 \cdot E \cdot b \cdot t_0}{L_{ref}^2} \cdot \frac{t_{g0}}{b \cdot G_R}} = 0,881 \quad a_1 := 1,5 \cdot t_0 + t_{g0} = 65 \quad \text{mm}$$

$$I_{0,ef} := 2 \cdot \frac{b \cdot (2 \cdot t_0)^3}{12} + \frac{b \cdot t_0^3}{12} + 2 \cdot Y_1 \cdot b \cdot 2 \cdot t_0 \cdot a_1^2 = 4,8472 \cdot 10^8$$

$$I_{0,net} := 2 \cdot \frac{b \cdot (2 \cdot t_0)^3}{12} + \frac{b \cdot t_0^3}{12} + 2 \cdot b \cdot 2 \cdot t_0 \cdot a_1^2 = 5,4525 \cdot 10^8$$

$$reduction := \frac{I_{0,ef}}{I_{0,net}} = 0,889$$

$$t_0 := 150$$

$$I_{eff} := 0,485 \cdot 10^9$$

$$A_{net} := t_0 \cdot 1000$$

$$l_{cr} := 3100$$

$$f_{c,0,k} := 26,4$$

$$E_{0,05} := 9670$$

$$i := \sqrt{\frac{I_{eff}}{A_{net}}} = 56,9$$

$$\lambda := \frac{l_{cr}}{i} = 54,5$$

$$\lambda_{rel} := \frac{\lambda}{\pi} \cdot \sqrt{\frac{f_{c,0,k}}{E_{0,05}}} = 0,91$$

$$k_y := 0,5 \cdot \left(1 + 0,1 \cdot (\lambda_{rel} - 0,3) + \lambda_{rel}^2 \right) = 0,94$$

$$k_c := \frac{1}{k_y + \sqrt{k_y^2 - \lambda_{rel}^2}} = 0,84$$

CLT panel LL-400/11s

```

> restart;
> t0 := 40 : t90 := 30 : E := 11000 : L := 3100 : b := 1000 : Gr := 50 :
> a1 := 2.5·t0 + 2·t90 : a2 := t0 + t90 : a3 := 0 : a4 := -a2 : a5 := -a1 :
> C :=  $\frac{b \cdot Gr}{t90}$  : C12 := C : C23 := C : C34 := C : C45 := C :
> Di :=  $\frac{\text{Pi}^2 \cdot E \cdot b \cdot t0}{L^2}$  : D1 := 2·Di : D2 := Di : D3 := D2 : D4 := D2 : D5 := D1 :
> v11 := (C12 + D1)·a1 : v12 := -C12·a2 : v21 := -C12·a1 :
> v22 := (C12 + C23 + D2)·a2 : v23 := -C23·a3 : v32 := -C23·a2 :
> v33 := (C23 + C34 + D3)·a3 : v34 := -C34·a4 :
> v43 := -C34·a3 : v44 := (C34 + C45 + D4)·a4 : v45 := -C45·a5 :
> v54 := -C45·a4 : v55 := (C45 + D5)·a5 :
>
> s1 := -C12·(a2 - a1) :
> s2 := C12·(a2 - a1) - C23·(a3 - a2) :
> s3 := C23·(a3 - a2) - C34·(a4 - a3) :
> s4 := C34·(a4 - a3) - C45·(a5 - a4) :
> s5 := C45·(a5 - a4) :
> with(linalg) :
> Amatrix := matrix([ [v11, v12, 0, 0, 0], [v21, v22, v23, 0, 0], [0, v32, v33, v34, 0], [0, 0, v43,
v44, v45], [0, 0, 0, v54, v55] ]) :
> S := vector([s1, s2, s3, s4, s5]) :
> gama := linsolve(Amatrix, S) :
> I0ef :=  $2 \cdot \frac{b \cdot (2 \cdot t0)^3}{12} + 3 \cdot \frac{b \cdot t0^3}{12} + \text{gama}[1] \cdot 2 \cdot b \cdot (2 \cdot t0) \cdot a1^2 + \text{gama}[2] \cdot 2 \cdot b \cdot t0 \cdot a2^2$ ;
>
> I0net :=  $2 \cdot \frac{b \cdot (2 \cdot t0)^3}{12} + 3 \cdot \frac{b \cdot t0^3}{12} + 2 \cdot b \cdot (2 \cdot t0) \cdot a1^2 + 2 \cdot b \cdot t0 \cdot a2^2$ ;
>
> gamma_ef :=  $\frac{I0ef}{I0net}$ 

```

2.12×10^9
 4.59×10^9
0.462

```

t0 := 280
I_eff := 2,12·109
A_net := t0·1000
l_cr := 3100

f_c,0,k := 26,4
E_0,05 := 9670

i :=  $\sqrt{\frac{I_{eff}}{A_{net}}}$  = 87
λ :=  $\frac{l_{cr}}{i}$  = 35,6

λ_rel :=  $\frac{\lambda}{\pi} \cdot \sqrt{\frac{f_{c,0,k}}{E_{0,05}}}$  = 0,59
k_y := 0,5 ·  $\left( 1 + 0,1 \cdot (\lambda_{rel} - 0,3) + \lambda_{rel}^2 \right)$  = 0,69
k_c :=  $\frac{1}{k_y + \sqrt{k_y^2 - \lambda_{rel}^2}}$  = 0,96

```

A2.5 Buckling of CLT

Stability of a panel has to be checked when both bending stresses and normal stresses occur. Buckling of the CLT is checked by including a k_c factor in the unity check calculation.

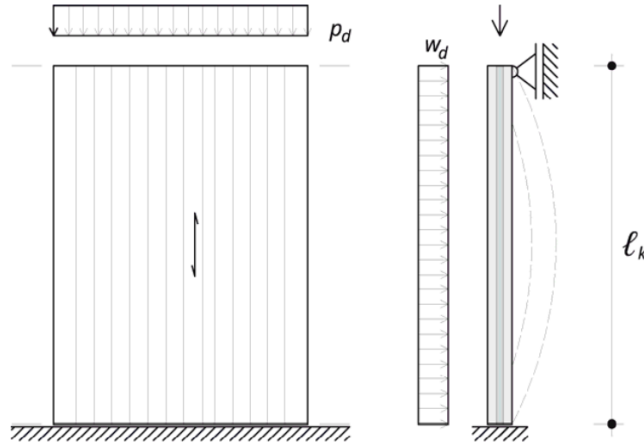


Figure 3, buckling of the panel [Proholz,2014]

$$\frac{\sigma_{c,0,d}}{k_{c,y} f_{c,0,d}} + \frac{\sigma_{m,d}}{f_{m,d}} \leq 1,0 \quad (7)$$

$$k_{c,y} = \frac{1}{k_y + \sqrt{k_y^2 - \lambda_{rel,y}^2}} \quad (8)$$

$$k_y = 0,5(1 + \beta_c(\lambda_{rel,y} - 0,3) + \lambda_{rel,y}^2) \quad (9)$$

β_c Coefficient for imperfection 0,1 for CLT

$$\lambda_{rel,y} = \frac{\lambda_y}{\pi} \sqrt{\frac{f_{c,0,k}}{E_{0,05}}} \quad (10)$$

$$\lambda_y = \frac{l_{cr}}{i_{y,0,eff}} \quad (11)$$

$$i_{y,0,eff} = \sqrt{\frac{I_{y,0,eff}}{A_{0,net}}} \quad (12)$$

Table 2, compression resistance of the CLT panel including buckling

Panel	t_0	$A_{0,net}$	I_{eff}	k_c	$N_{c,Rd}$
	<i>mm</i>	<i>mm²</i>	<i>x10⁹ mm⁴</i>	-	<i>kN</i>
LL-190/7s	150	150.000	0,49	0,84	2395
LL-260/7s	200	200.000	1,11	0,93	3535
LL-300/9s	240	240.000	1,18	0,92	4197
LL-360/9s	240	240.000	1,31	0,93	4243
LL-400/11s	280	280.000	2,12	0,96	5109

$$t_0 := 280$$

$$I_{eff} := 2,12 \cdot 10^9$$

$$A_{net} := t_0 \cdot 1000$$

$$l_{cr} := 3100$$

$$f_{c,0,k} := 26,4$$

$$E_{0,05} := 9670$$

$$i := \sqrt{\frac{I_{eff}}{A_{net}}} = 87$$

$$\lambda := \frac{l_{cr}}{i} = 35,6$$

$$\lambda_{rel} := \frac{\lambda}{\pi} \cdot \sqrt{\frac{f_{c,0,k}}{E_{0,05}}} = 0,59$$

$$k_y := 0,5 \cdot \left(1 + 0,1 \cdot (\lambda_{rel} - 0,3) + \lambda_{rel}^2 \right) = 0,69$$

$$k_c := \frac{1}{k_y + \sqrt{k_y^2 - \lambda_{rel}^2}} = 0,96$$

A2.6 CLT panel properties

Several type of CLT panels will be used for this thesis. The panels are based on the available panels at Derix. This is a CLT producer based in Germany, but has provided CLT panels for Dutch building projects as well. LL-type panels have been chosen, which have two layers in longitudinal direction on the outside of the panel. These panels have a large net area orientated in the vertical orientation.

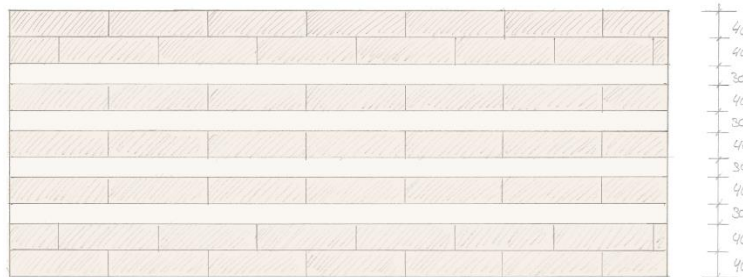


Figure 4, cross-section of an LL-type CLT panel (LL-400/11s)

Cross-sectional values follow from the properties of the base material. Most properties are defined based on the net cross-section. Only for bending out of plane, the effective moment of inertia has to be used in SLS. The net cross-section in the strong direction is the sum of the boards orientated in strong direction. Similarly, the net cross-section in the weak direction is the sum of the boards orientated in the weak direction. In the image below, the light grey hatched layers (numbered 1, 2 and 3) indicate the considered boards. All boards have the same modulus of elasticity.

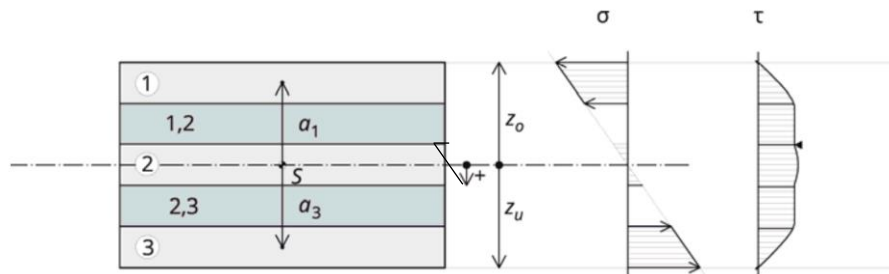


Figure 5, CLT cross-section [Proholz, Cross-Laminated Timber Structural Design, 2014]

Cross-sectional values have been calculated for five panels. The results are shown in the tables below. Table 5 shows the net thickness of the panel in 0-direction and 90-direction and the corresponding values for net area, section modulus and moment of inertia. The effective moment of inertia $I_{0,eff}$ has been calculated as the net moment of inertia multiplied with an effective gamma value as calculated in A2.4. The buckling factor k_c has been calculated with a buckling length of one story height (3,1 meter)

Three main stiffness parameters can be described. The first is the axial stiffness in 0-direction. The second is the axial stiffness in 90-direction. The third and final stiffness parameter is the shear stiffness. The shear stiffness takes into account the gross cross-section. This is the total cross-section of the panel, indifferent of the grain direction of the boards.

$$K_0 = E_{0,mean} A_{0,net} \quad (13)$$

$$K_{90} = E_{0,mean} A_{90,net} \quad (14)$$

$$K_s = G_{s,mean} A_{gross} \quad (15)$$

Table 3, orthotropic stiffness values per meter width

	K₀	K₉₀	K_s
	<i>kN/mm</i>	<i>kN/mm</i>	<i>kN/mm</i>
LL-190/7s	1740	464	86
LL-260/7s	2320	696	117
LL-300/9s	2784	696	135
LL-360/9s	2784	1392	162
LL-400/11s	3248	1392	180

The different directions of a CLT plate are defined based on the strong direction of the grain. Most boards are directed in the 0°-direction. This indicates that most of the grains are parallel to the considered direction. Perpendicular to this direction is then the 90°-direction. The resistance of the CLT panels to compression forces, tensile forces and shear forces can be calculated based on the presented formulas. The buckling factor k_c has been calculated in chapter A2.5.

$$N_{c,Rd} = A_{0,net} * k_c * f_{c,0,d} \quad (16)$$

$$N_{t,Rd} = A_{0,net} * f_{t,0,d} \quad (17)$$

$$V_{Rd} = A_{i,net} * f_{v,d} \quad (18)$$

Table 4, resistance values per meter width

	t₀	A_{0,net}	A_{90,net}	k_c	N_{c,Rd}	N_{t,Rd}	V_{0,Rd}	V_{90,Rd}
	<i>mm</i>	<i>mm²</i>	<i>mm²</i>		<i>kN/m</i>	<i>kN/m</i>	<i>kN/m</i>	<i>kN/m</i>
LL-190/7s	150	150.000	40.000	0,84	2395	1725	594	159
LL-260/7s	200	200.000	60.000	0,93	3535	2300	792	238
LL-300/9s	240	240.000	60.000	0,92	4197	2756	950	238
LL-360/9s	240	240.000	120.000	0,93	4243	2756	950	475
LL-400/11s	280	280.000	120.000	0,96	5109	3222	1109	475

The net area can be found by:

$$A_{net} = \sum_{i=1}^n b * d_i \quad (19)$$

The net moment of inertia is the sum of the individual moment of inertias of each layer, summed with their contribution according to the parallel axis theorem. Assuming there is full transfer of shear, the formula states:

$$I_{net} = \sum_{i=1}^n \frac{b * d_i^3}{12} + \sum_{i=1}^n b * d_i * a_i^2 \quad (20)$$

The effective moment of inertia is only taken into consideration in SLS for out of plane bending and buckling of the CLT panel. Rolling shear deformation reduces the stiffness of the cross section. The gamma method is used to calculate the effective moment of inertia. A gamma factor is calculated to include the additional shear deformation. The Steiner part of the bending stiffness of each layer is then multiplied with the corresponding gamma factor. For panels where more than two layers undergo rolling shear deformation, the gamma value is found using the method of Schelling. This method can be best explained as the gamma method (as given in Eurocode 5) for more than three members that are to be connected.

$$\gamma_i = \frac{1}{\left(1 + \frac{\pi^2 E_i A_i}{l_{ref}^2} * \frac{d_{i,j}}{b G_{R,i,j}}\right)} \quad (21)$$

$$I_{ef} = \sum_{i=1}^3 \frac{b * d_i^3}{12} + \sum_{i=1}^n \gamma_i * b * d_i * a_i^2 \quad (22)$$

Table 5, cross-sectional values per meter width

	t_0	t_{90}	t	$A_{0,net}$	$A_{90,net}$	$W_{0,net}$	$I_{0,net}$	γ_{red}	$I_{0,eff}$
	<i>mm</i>	<i>mm</i>	<i>mm</i>	<i>mm²</i>	<i>mm²</i>	<i>mm³</i>	<i>mm⁴</i>	-	<i>x10⁹ mm⁴</i>
LL-190/7s	150	40	190	150.000	40.000	5,74 E6	0,485 E9	0,881	0,46
LL-260/7s	200	60	260	200.000	60.000	10,7 E6	1,387 E9	0,801	1,11
LL-300/9s	240	60	300	240.000	60.000	14,0 E6	2,099 E9	0,560	1,18
LL-360/9s	240	120	360	240.000	120.000	18,7 E6	3,360 E9	0,391	1,31
LL-400/11s	280	120	400	280.000	120.000	23,0 E6	4,589 E9	0,462	2,12

A2.7 Comparisson of test results

Results from three researches regarding timber-to-steel dowelled fastener connections have been gathered. Results were taken from Liu et al. (2020), Dobes et al. (2022) and Sandhaas (2012). The load-deformation curves from tests have been plotted in the figure below for dowelled type fasteners.

Table 6, sources of load-deformation curves

Source	Year	Diameter	No. fasteners
Liu et al.	2020	M16 bolts	1
Dobes et al.	2022	M20 bolts	1
Sandhaas	2012	M12 dowels	1, 3 and 5

Results from Dobes and Sandhaas have been adjusted for dowel diameter given that these did not use a 16 mm diameter. The European Yield Method equations have been used to adjust the force observed in the connection to that what would be expected for a 16 mm fastener. The failure mode for all adjustments remained the same (ductile) failure mode.

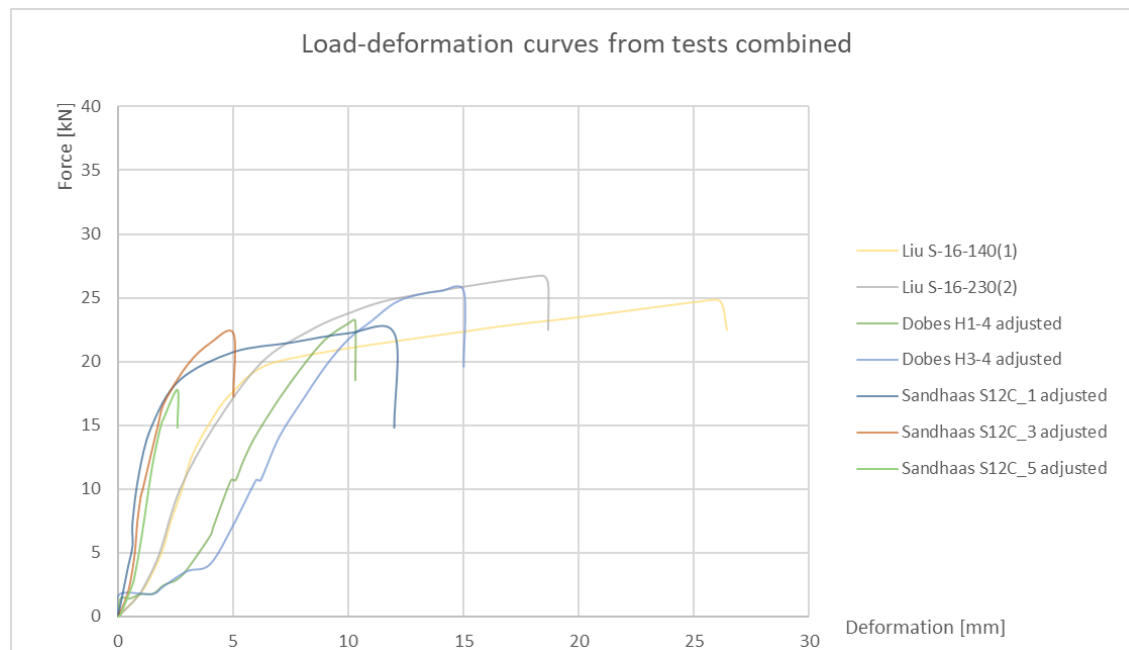


Figure 6, test results combined

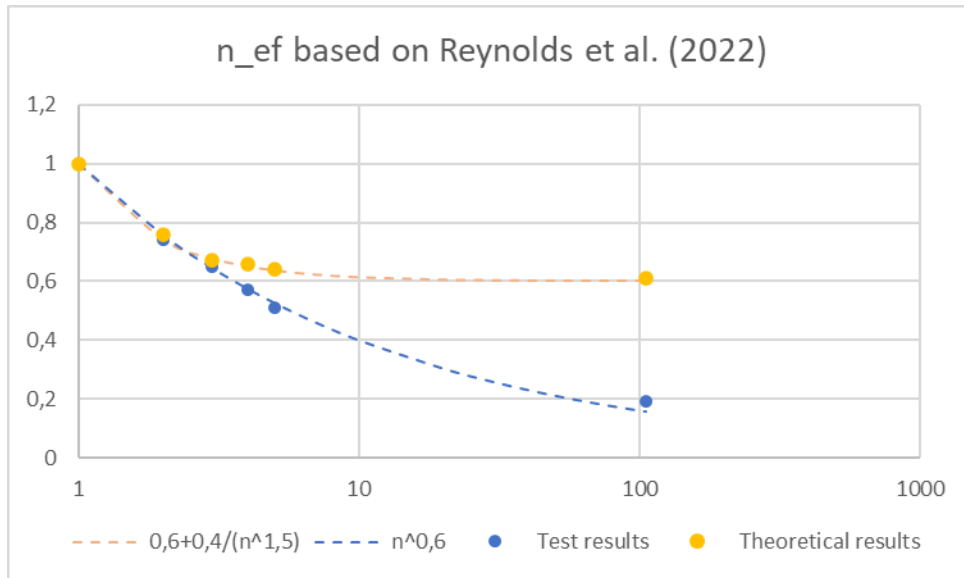
A2.8 Effective number of fasteners (stiffness)

Reynolds et al. researched the effective number of dowels for load-reload stiffness (elastic stiffness K_e). Theoretical results indicated that the first added dowel would have the largest influence on the effective stiffness (33% to 40% reduction). This has been supported by test results. The theoretical results also indicated that the effective number of dowels quickly settle at 0,60. This however is not supported in test results. The effective number of dowels for 105 dowels was theoretically found to be 64,3 dowels whereas the actual test results found an effective number of 20,2 (19%). Reynolds et al. indicate that this suggests that additional processes are restricting the number of dowels contributing to the connection stiffness. In larger specimen, “misalignment along the length of the dowel through the multiple plates may be important.” (Reynolds et al., 2022).

Table 7, effective number of dowels according to Reynolds et al. (2022)

Number of dowels applied	n_{ef} based on elastic stress field (theory)	n_{ef} based on dowel misalignment (theory) For 10 mm dowels	n_{ef} based on dowel misalignment (theory) For 12 mm dowels	Test results 12 mm	Test results 10 mm
1	1	1	1	1	1
2	0,75	0,71	0,76	0,74	0,75
3	0,64	0,63	0,67	0,65	0,65
4	0,60	0,59	0,66	0,57	0,56
5	0,61	0,56	0,64	0,51	0,47
7 ^a	0,46				
105 ^b			0,61	0,19	

The results by Reynolds have been shown in the table and graph. Theoretical results have been shown in yellow whereas test results are shown in blue. Two curves have been defined in order to indicate the trend line that is observed. These do not represent an actual definition for n_{ef} , but do indicate clear differences between the theoretical results and test results.



Jorissen presented several equations to represent the effective number of bolts in timber-to-timber connections. Provided that there was a minimum spacing $a_1 > 7d$, the following equation was found.

$$n_{ef} = 0,85 * n^{0,90} \quad (23)$$

$$m_{ef} = 0,90 * m \quad \text{for } m = 2 \quad (24)$$

A2.9 Single shear plane steel-to-timber connections

There are several failure modes defined in Eurocode 5. These are specified for thin plates and thick plates. Figure 7 shows all these failure mechanisms. Thin plates have a thickness less than half the diameter of the dowel. Thick plates have a thickness larger than the diameter of the dowel. For steel plates with a thickness between half the diameter and one times the diameter of the dowels, linear interpolation can be used.

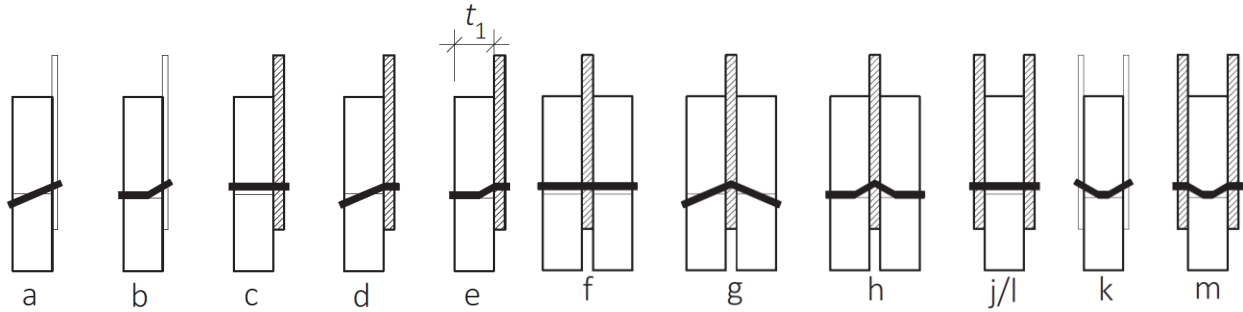


Figure 7, failure mechanisms (Timber engineering book V2)

Thin plate failure modes are failure of timber embedment and formation of a plastic hinge.

$$\text{Mode a} \quad F_{v,Rk,a} = 0,4 * f_{h,k} * t_1 * d \quad (25)$$

$$\text{Mode b} \quad F_{v,Rk,b} = 1,15 * \sqrt{2 * M_{y,k} * f_{h,k} * d} + \frac{F_{ax,Rk}}{4} \quad (26)$$

Thick plate failure modes are also failure of the timber embedment and formation of a plastic hinge.

$$\text{Mode c} \quad F_{v,Rk,c} = f_{h,k} * t_1 * d \quad (27)$$

$$\text{Mode d} \quad F_{v,Rk,d} = f_{h,k} * t_1 * d * \left[\sqrt{2 + \frac{4 * M_{y,k}}{f_{h,k} * d * t_1^2}} - 1 \right] + \frac{F_{ax,Rk}}{4} \quad (28)$$

$$\text{Mode e} \quad F_{v,Rk,e} = 2,3 * \sqrt{M_{y,k} * f_{h,k} * d} + \frac{F_{ax,Rk}}{4} \quad (29)$$

$F_{v,Rk,a}$ and $F_{v,Rk,c}$ are brittle failure modes as the timber fails in a brittle manner (timber embedment failure). The other three failure modes form at least one hinge before failure, which indicates a more ductile failure. This is preferred, hence the required failure mode should be mode b, d or e.

A2.9.1 Double shear plane steel-to-timber connections

Failure modes f, g, h, j/l, k and m are modes for double shear plane connections. However, the corresponding equations are similar to the ones for single shear plane connections (due to symmetry).

Considered mode	Comparable to
Mode f	Mode c
Mode g	Mode d
Mode h	Mode e
Mode j	Mode c with t_1 as 50% of t
Mode k	Mode b
Mode l	Mode c with t_1 as 50% of t
Mode m	Mode e

Mode j and mode l are similar to one another, but are named individually. Mode j is failure of the embedment strength of the timber for thin plate connections whereas mode l is failure of the embedment strength for thick plate connections. So the separation is only to indicate the thickness of the steel plates. These modes are calculated as 50% of mode c, as the result is the resistance per shear plane and only half the timber thickness contributes to each shear plane.

A2.10 Brittle failure modes of multi-fastener connections

Five types of brittle failure modes of timber have been defined in the new Eurocode 5 draft (2022). These failures apply to standard timber and parallel laminated timber. They are not mentioned to be applicable for CLT although Brown and Li (2020) and Azinovic et al. (2022) observed brittle failure in CLT for grouped fasteners.

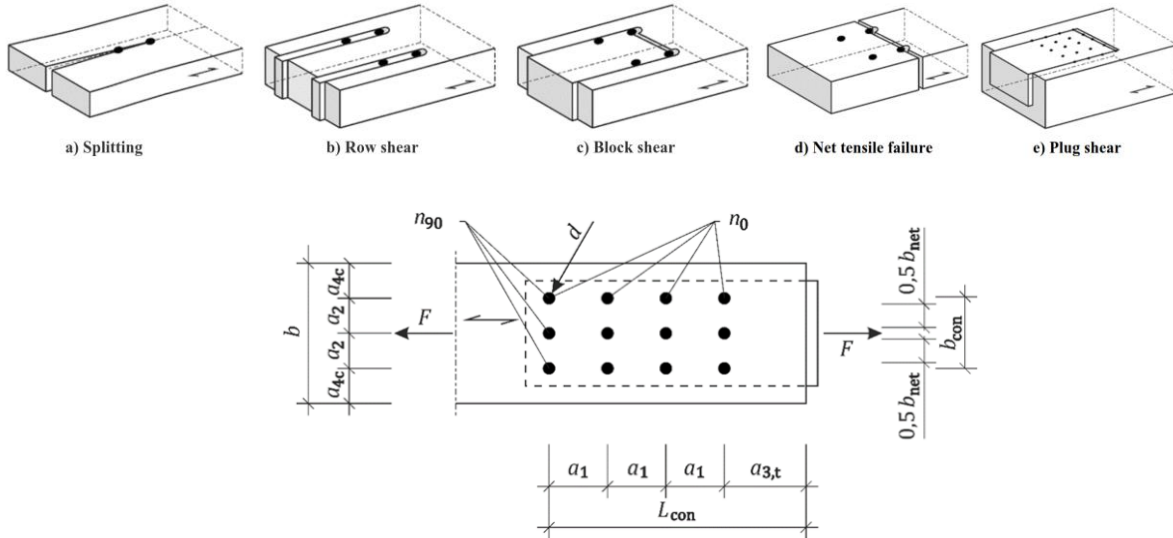


Figure 8, brittle failure modes of multi-fastener connections

The brittle failure of an LL-400/11s panel is calculated for a connection as shown in A5.1.2.

Row shear failure

$$F_{rs,d} = 2 * n_{90} * F_{v,l,d} = 2 * 8 * 332 = 5312 \text{ kN} \quad (30)$$

Block shear failure

$$F_{bs,d} = \max(2 * F_{v,l,d}; F_{t,d}) = \max(2 * 332; 1811) = 1811 \text{ kN} \quad (31)$$

Plug shear failure

$$F_{ps,d} = \max(2 * F_{v,b,d}; F_{t,d} + F_{v,b,d}) = \max(2 * 894; 1811 + 406) = 2217 \text{ kN} \quad (32)$$

Net tensile failure

$$F_{t,net,d} = k_t * F_{t,d} = 1,1 * 1811 = 1992 \text{ kN} \quad (33)$$

The brittle resistance of the connection in the CLT panel is found to be 1811 kN as the result of block shear failure. Ductile failure of this connection is $(40 \times 68 =) 2720$ kN. This shows that there is a potential for brittle failure (brittle failure is 67% of ductile failure). However, it is not clearly specified in the Eurocode draft whether the brittle failure should be accounted for in CLT, nor how the different shear planes in a CLT panel should be defined. Given the fact that CLT has two different orientations of the fiber, each orientation may have a contribution for each shear plane of the panel.

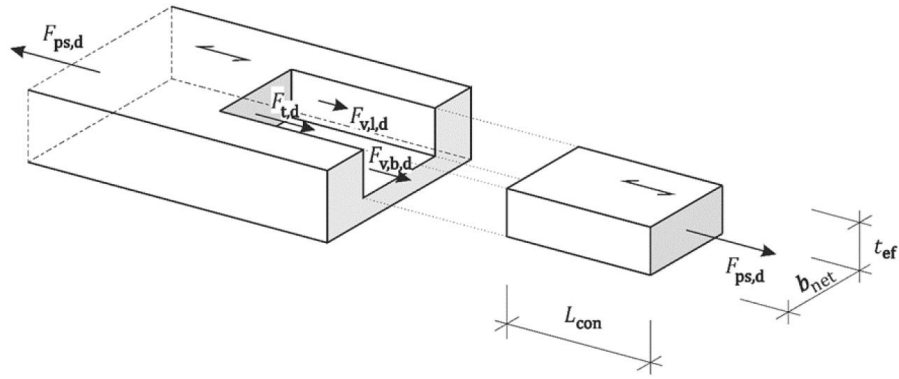


Figure 9, definitions of shear resistance for different shear planes

- $F_{v,l,d}$ design shear resistance per side shear plane in the timber member
 $F_{v,b,d}$ design shear resistance of the bottom shear plane in the timber member
 $F_{t,d}$ design tensile failure resistance of the head plane

$$F_{v,l,d} = k_v * t_{ef} * L_{con} * f_{v,d} \quad (34)$$

$$k_v = 0,4 + 1,4 \sqrt{\frac{G_{mean}}{E_{0,mean}}} = 0,4 + 1,4 \sqrt{\frac{450}{11600}} = 0,68 \quad (35)$$

$$L_{con} = 4 * 80 + 80 = 400 \text{ mm} \quad (36)$$

$$F_{v,l,d} = 0,68 * 280 * 440 * 3,96 = 332 \text{ kN} \quad (37)$$

$$F_{v,b,d} = k_v * L_{con} * b_{net} * f_{v,d} \quad (38)$$

$$b_{net} = 8 * 80 + 48 = 688 \text{ mm} \quad (39)$$

$$F_{v,b,d} = 0,68 * 488 * 680 * 3,96 = 894 \text{ kN} \quad (40)$$

$$F_{t,d} = k_t * t_{ef} * b_{net} * f_{t,0,d} \quad (41)$$

$$k_t = 0,9 + 1,4 \sqrt{\frac{G_{mean}}{E_{0,mean}}} = 0,9 + 1,4 \sqrt{\frac{450}{11600}} = 1,18 \quad (42)$$

$$F_{t,d} = 1,18 * 194 * 688 * 11,5 = 1811 \text{ kN} \quad (43)$$

The effective thickness of the fastener to calculate $F_{t,d}$ is calculated below.

Inner member

$$t_{ef,el} = \max\left\{\left(2 - \frac{t_{h,i}}{11d}\right); 0,65\right\} * \alpha_{cl} * t_{h,i} \quad \text{if } \frac{t_{h,i}}{d} > 11 \alpha_{cl} \quad (44)$$

$$t_{ef,el} = \left(2 - \frac{190}{176}\right) * 0,65 * 190 = 114 \text{ mm} \quad (45)$$

$$t_{ef,pl} = \sqrt{\frac{M_{y,k}}{2 d f_{h,0,k}}} + \frac{t_h}{2} \quad (46)$$

$$t_{ef,pl} = \sqrt{\frac{0,3 * 800 * 16^{2,6}}{2 * 16 * \frac{0,035 * (1 - 0,015 * 16) * 385^{1,16}}{1,1}}} + \frac{200}{2} = 120 \text{ mm} \quad (47)$$

$$t_{ef,ps} = \min\{t_{ef,el}; t_{ef,pl}\} \quad (48)$$

$$t_{ef,ps} = \min\{114; 120\} = 114 \text{ mm} \quad (49)$$

Outer member

$$t_{ef,el} = \max\left\{\left(1,17 - \frac{t_{h,o}}{18d}\right); 0,35\right\} * \alpha_{cl} * t_{h,i} \quad \text{if } \frac{t_{h,i}}{d} > 3 \alpha_{cl} \quad (50)$$

$$t_{ef,el} = \left(1,17 - \frac{65}{288}\right) * 0,65 * 65 = 40 \text{ mm} \quad (51)$$

$$t_{ef,pl} = 20 + \frac{65}{2} = 53 \text{ mm} \quad (52)$$

$$t_{ef,ps} = \min\{40; 53\} = 40 \text{ mm} \quad (53)$$

$$t_{ef} = 114 + 2 * 40 = 194 \text{ mm} \quad (54)$$

A3 Chapter 3 appendices

A3.1 Loads on the structure

A3.1.1 Floor loads

Vertical loads are the result of floor loads transferred to the façade and self weight of the façade. The weight of the floor depends on the lay-up. Especially the use of a concrete screed can influence this weight. As many literature indicates that a lightweight structure has many difficulties it was decided to assume a timber concrete composite floor. The concrete can be replaced by gravel if disassembly is requested. However, this would mean that the thickness of the CLT floor panel needs to increase as it no longer functions as a timber concrete composite floor. A detail of the floor lay-up is given in appendix NR.

Table 8, floor lay-up

Material	Thickness	Unit	Weight	Unit	Weight	Unit
Floor finishing	15	mm			0,10	kN/m ²
Double fermacel	25	mm			0,30	kN/m ²
Insulation	40	mm			0,05	kN/m ²
Concrete	80	mm	25	kN/m ³	2,00	kN/m ²
CLT	280	mm	4,5	kN/m ³	1,26	kN/m ²
Total	440	mm			3,71	kN/m ²

The main variable load on the floor is the usage of the apartments. This is specified in Table 9. Internal walls will be accounted for by a variable load of 0,8 kN/m². This represents movable walls with a dead load of at most 2,0 kN/m.

Table 9, variable load apartments

Category	Function	q _k [kN/m ²]	Q _k [kN]	Ψ ₀	Ψ ₁	Ψ ₂
A	Apartments (including walls)	2,55	3,00	0,40	0,50	0,30
A	Hallways	2,00	3,00	0,40	0,50	0,30

Roof loads are not specified as they contribute very little to the overall behavior of the structure.

The floor load per story are found to be (based on a measured span of 8 m)

$$g_k = 14,82 \text{ kN/m}$$

$$q_k = 4,08 \text{ kN/m} \quad \text{including } \psi_0 = 0,4$$

A3.1.2 Façade loads

The façade is made from CLT panels. Openings have been used to allow for daylight entry. This takes up 34% of the area of the panel. The self-weight of the façade is calculated as the average between the weight of the closed façade and the weight of the windows. The weight of the CLT panels is separated from the façade load as it can be generated in the computer, based on the thickness of the panel.

Table 10, façade lay-up (inside to outside)

Material	Thickness	Weight	Weight
	<i>kN/m³</i>	<i>kN/m³</i>	<i>kN/m²</i>
Wall finishing	10		0,10
Gypsumboard	12		0,15
Insulation (fire resistant)	100		0,10
CLT	Variable	4,2	-
Insulation (thermal)	100		0,10
Façade cladding	40		0,50
Total	222 excl. CLT		0,95

Table 11, window lay-up (inside to outside)

Material	Thickness	Weight	Weight
	mm	<i>kN/m³</i>	<i>kN/m²</i>
Glass (triple glazing)	15	25	0,38
Hardwood window frame			0,18
Total			0,56

It is given that 34% of the façade is transparent (window) and therefor the weight of the façade then becomes 0,82 kN/m² or 2,54 kN/m¹ for each story.

Table 12, self weight of the CLT panels per story

Panel	Thickness	Weight	Weight
	mm	<i>kN/m²</i>	<i>kN/m</i>
LL-190/7s	190	0,80	1,63
LL-260/7s	260	1,09	2,24
LL-300/9s	300	1,26	2,58
LL-360/9s	360	1,51	3,10
LL-400/11s	400	1,68	3,44

A3.2 $c_s c_d$ factor calculation

$b := 27,0$ bouwwerkbreedte

$d := 20,3$ bouwwerkdiepte

$h := 77,5$ bouwwerkhoopte

$c_{dir} := 1,0$ windrichtingsfactor

$c_{season} := 1,0$ seizoensfactor

$v_{b,0} := 27,0$

$z_0 := 0,3$ voor windgebied II afhankelijk van locatie 0,003; 0,01; 0,05; 0,3; 1,0

$z_s := 0,6 \cdot h$ ruwheidslengte

$z := z_s$

$z_{0,II} := 0,05$

$$k_r := 0,19 \cdot \left(\frac{z_0}{z_{0,II}} \right)^{0,07} = 0,2154$$

$$c_r := k_r \cdot \ln \left(\frac{z}{z_0} \right) = 1,0863 \quad \text{ruwheidsfactor}$$

$c_o := 1,0$ orografiefactor voor vlakke gebieden 1,0

$$v_b := c_{dir} \cdot c_{season} \cdot v_{b,0} = 27$$

$$v_m := c_r \cdot c_o \cdot v_b = 29,3301$$

$k_1 := 1,0$ turbulentiefactor 1,0

$$I_v := \frac{k_1}{c_o \cdot \ln \left(\frac{z}{z_0} \right)} = 0,1983 \quad \text{turbulentie-intensiteit}$$

$L_t := 300$ referentielengteschaal

$z_t := 200$ referentiehoogte

$$\alpha := 0,67 + 0,05 \cdot \ln(z_0) = 0,6098$$

$$L := L_t \cdot \left(\frac{z}{z_t} \right)^\alpha = 123,2438 \quad \text{turbulentiengteschaal}$$

$$B := \frac{1}{\sqrt{1 + 1,5 \cdot \sqrt{\left(\frac{b}{L} \right)^2 + \left(\frac{h}{L} \right)^2 + \left(\frac{b}{L} \cdot \frac{h}{L} \right)^2}}} = 0,7036 \quad \text{achtergrondresponsfactor (eigenlijk } B^2)$$

De keuze $B^2 = 1$ is aan de veilige kant

$\delta_{tot} := 0,06$

$\phi := \frac{z}{h} = 0,6$ afmetingsreductiefunctie

Resonantieresponsfactor (eigenlijk R^2)

Tabel 4.1 — Terreincategorieën en terreinparameters

Terreincategorie	z_0 m	z_{min} m
0 Zee of kustgebied met wind aanstromend over open zee	0,003	1
I Meren of vlak en horizontaal gebied met verwaarloosbare vegetatie en zonder obstakels	0,01	1
II Gebied met lage begroeiing als gras en vrijstaande obstakels (bomen, gebouwen) met een tussenruimte van ten minste 20 obstakelhoogtes	0,05	2
III Gebied met regelmatige begroeiing of gebouwen of vrijstaande obstakels met een tussenruimte van ten hoogste 20 obstakelhoogtes (zoals dorpen, voorstedelijk terrein, blijvend bos)	0,3	5
IV Gebied waar ten minste 15 % van de oppervlakte is bedekt met gebouwen met een gemiddelde hoogte boven 15 m	1,0	10

De terreincategorieën zijn geïllustreerd in A.1.

$G_y := 0,375$ waarde G: indien uniform 0,5; indien lineair 0,375; indien parabolisch 0,278
 $G_z := 0,375$ waarde K: indien uniform 1,000; indien lineair 1,500; indien parabolisch 1,667

$K_y := 1,00$

$K_z := 1,00$

$c_y := 11,5$ vervalconstant

$c_z := 11,5$ vervalconstant

$n := \frac{46}{h} = 0,5935$ eerste eigenfrequentie

$\phi_y := \frac{c_y \cdot b \cdot n}{v_m} = 6,2835$ $\phi_z := \frac{c_z \cdot h \cdot n}{v_m} = 18,0361$

$K_s := \frac{1}{1 + \sqrt{\left(G_y \cdot \phi_y \right)^2 + \left(G_z \cdot \phi_z \right)^2 + \left(\frac{2}{\pi} \cdot G_y \cdot \phi_y \cdot G_z \cdot \phi_z \right)^2}} = 0,0745$

$f_L := \frac{n \cdot L}{v_m} = 2,4941$ bevestiging dat n is n1,x ofwel eerste eigenfrequentie

$S_L := \frac{6,8 \cdot f_L}{\left(1 + 10,2 \cdot f_L \right)^{\left(\frac{5}{3} \right)}} = 0,0723$

$R := \sqrt{\frac{\pi^2}{2 \cdot \delta_{tot}} \cdot S_L \cdot K_s} = 0,6656$ spectrale dichtheidsfunctie

$v := n \cdot \sqrt{\frac{R^2}{B^2 + R^2}} = 0,4079$ verwachtingswaarde van de frequentie in een vlaag

$T := 600$ seconden

$k_p := \sqrt{2 \cdot \ln(v \cdot T)} + \frac{0,6}{\sqrt{2 \cdot \ln(v \cdot T)}} = 3,4976$ piekfactor maar groter dan 3

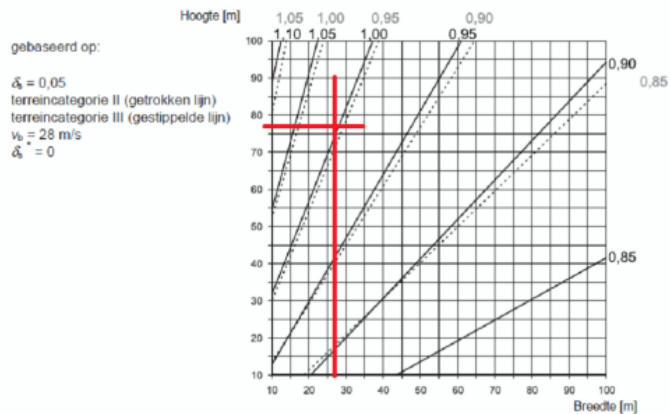
$c_s c_d$ -waarden voor verschillende constructietypen

$c_s := \frac{1 + 7 \cdot I_v \cdot B}{1 + 7 \cdot I_v} = 0,8277$ afmetingfact

$c_d := \frac{1 + 2 \cdot k_p \cdot I_v \cdot \sqrt{B^2 + R^2}}{1 + 7 \cdot I_v \cdot B} = 1,1856$

$C_s C_d := c_s \cdot c_d = 0,9813$

(1) De eigenfrequenties en trillingsvormen van de constructies in deze bijlage zijn afgeleid met lineaire analyse of geschat met de uitdrukkingen in bijlage F.



OPMERKING Voor waarden groter dan 1,1 mag de gedetailleerde procedure gegeven in 6.3 zijn toegepast (goedgekeurde minimumwaarde van $c_s c_d = 0,85$).

Figuur D.1 — $c_s c_d$ voor stalen gebouwen met meer verdiepingen met rechthoekige plattegrond en verticale gevels met een regelmatige verdeling van stijfheid en massa (frequentie volgens uitdrukking (F.2))

A3.3 Detail of the façade-floor connection

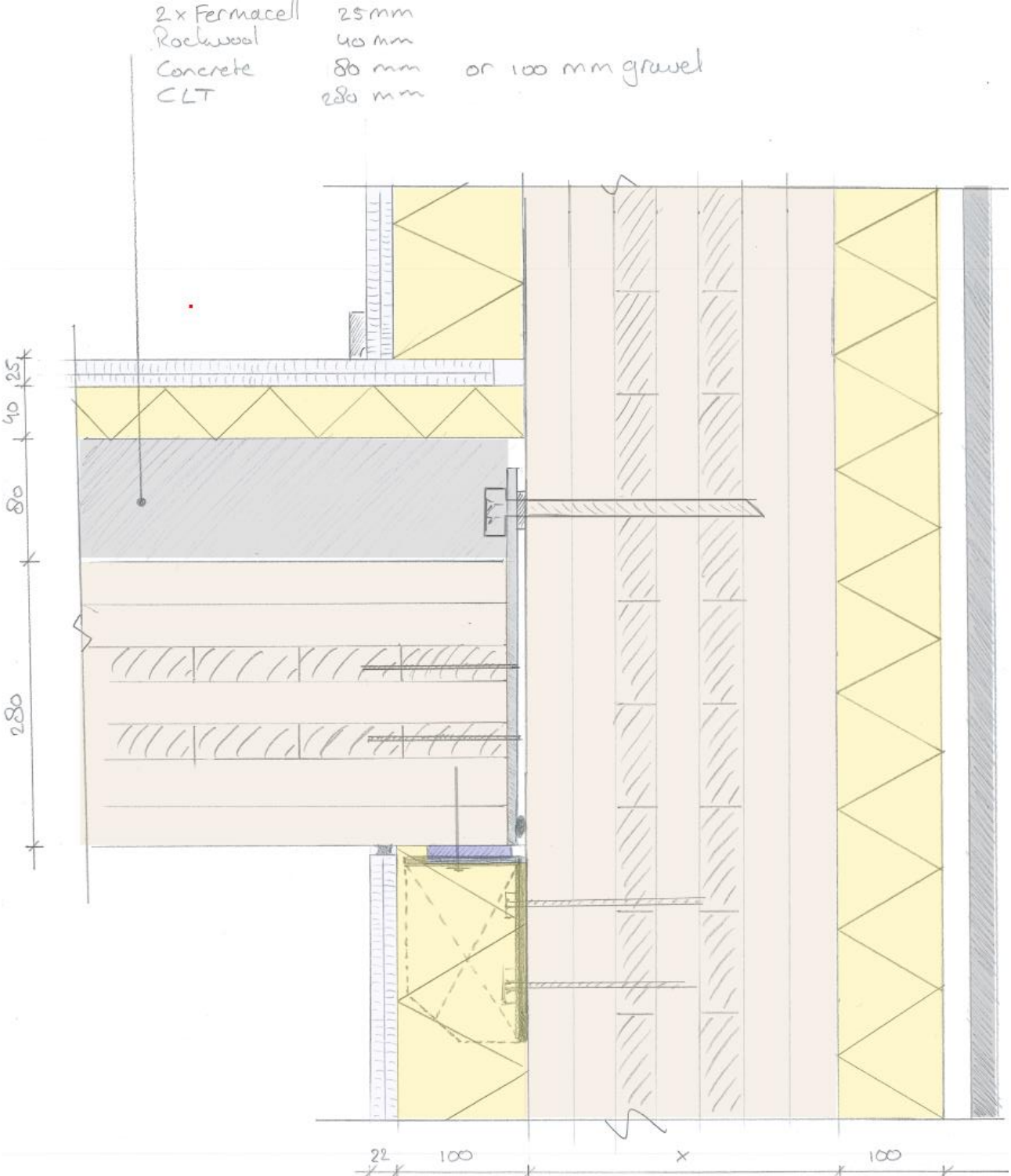


Figure 10, vertical detail of the CLT façade with a timber-concrete composite floor

A3.4 2nd order calculation for the structure

The second order contribution of the façade is calculated. There is no contribution of the foundation included. This makes that the result will be an underestimation of the second order effect.

Vertical load on the façade is calculated assuming half the vertical load is transferred to the façade and half the load is transferred to the inner load bearing structure. A top deformation of 229 mm was found in initial calculations, but might differ from the presented values slightly due to alterations after this calculation was performed. An equivalent bending stiffness EI_{eq} has been calculated based on a forget-me-not of a cantilevering beam with distributed load and the abovementioned top deformation.

This together leads to a vertical load on the stability element and a critical load. the calculated ratio n between these two loads is used to calculate the second order factor.

$$q_k := 27,1 \quad \text{kN/m}$$

$$a := \frac{27000}{2} = 13500 \quad \text{mm}$$

$$b := 20300 \quad \text{mm}$$

$$L := 77500 \quad \text{mm}$$

$$w := 229 \quad \text{mm} \quad \text{assumed top deflection based on first calculations of the top deformations}$$

$$n_{story} := 25$$

$$EI_{eq} := \frac{q_k \cdot L^4}{8 \cdot w} = 5,3364 \cdot 10^{17} \quad \text{Nmm}^2$$

a simplified calculation for the vertical load is made below

$$A_{floor} := 0,5 \cdot a \cdot b \cdot 10^{-6} = 137 \quad \text{m}^2 \quad \text{50\% of the floor load is assumed on the façade}$$

$$A_{façade} := (a + b) \cdot L \cdot 10^{-6} = 2619,5 \quad \text{m}^2$$

$$q_{floor,d} := 1,2 \cdot 14,82 + 1,5 \cdot 4,08 = 23,9 \quad \text{kN/m}^2$$

$$q_{façade,d} := 1,2 \cdot 0,4 \cdot 4,2 = 2,02 \quad \text{kN/m}^2$$

$$N_{v,Ed} := \frac{(n_{story} \cdot A_{floor} \cdot q_{floor,d} + A_{façade} \cdot q_{façade,d})}{2} = 43584 \quad \text{kN}$$

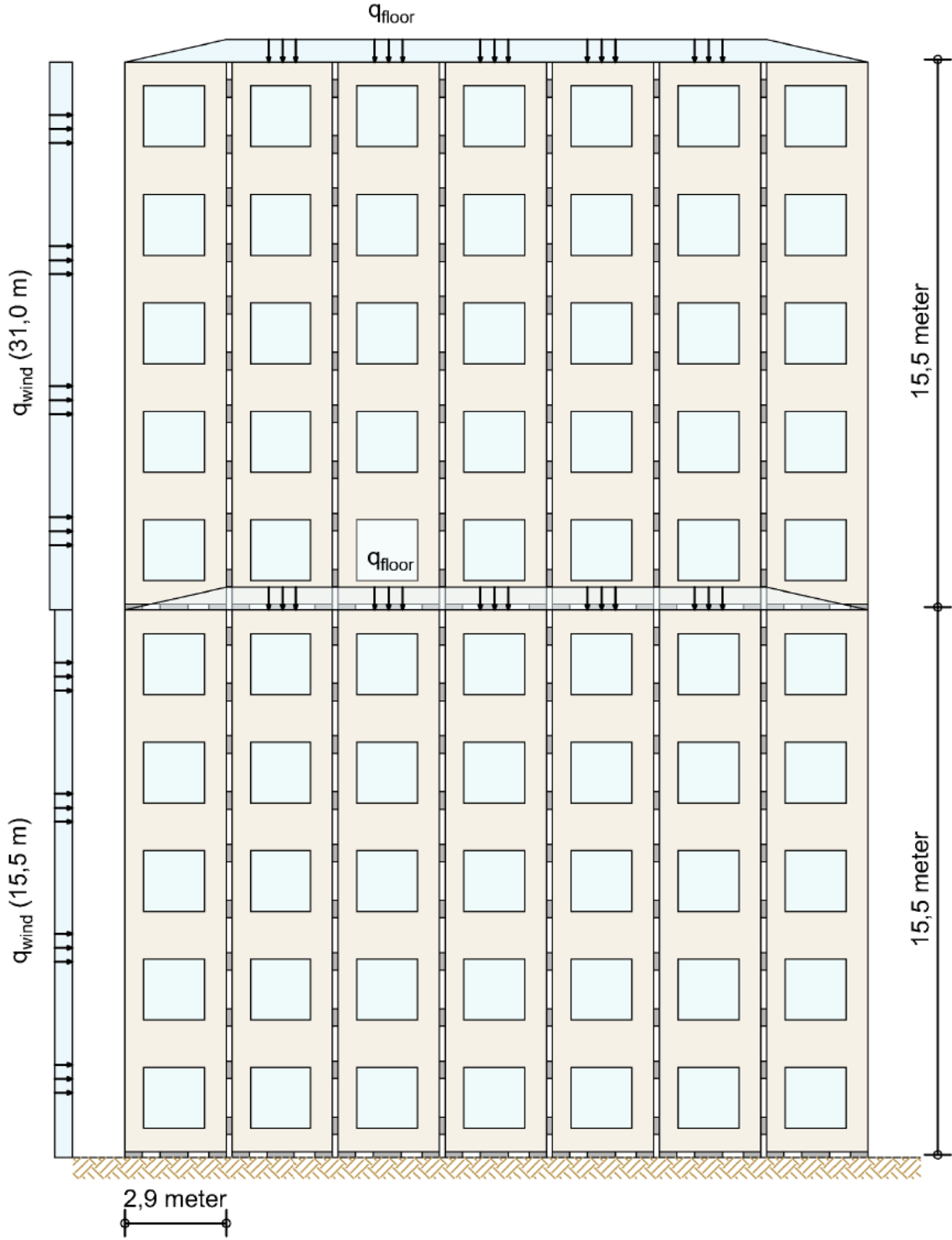
$$N_{cr,1} := \frac{\pi^2 \cdot EI_{eq}}{1000 \cdot ((1,12 \cdot L)^2)} = 699054,3 \quad \text{kN}$$

$$n_1 := \frac{N_{cr,1}}{N_{v,Ed}} = 16$$

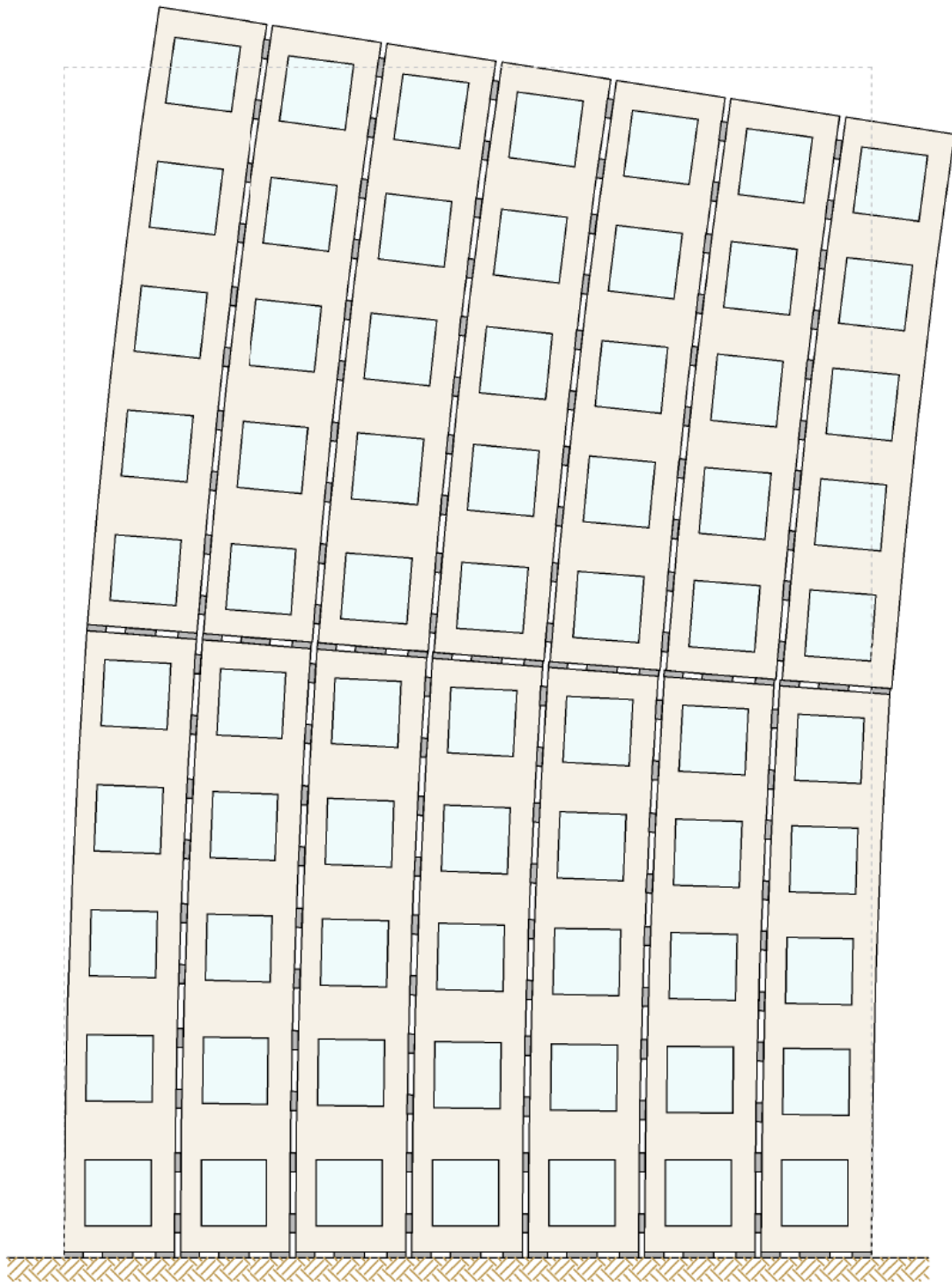
$$f_{2nd} := \frac{n_1}{n_1 - 1} = 1,066$$

A4 Chapter 4 appendices

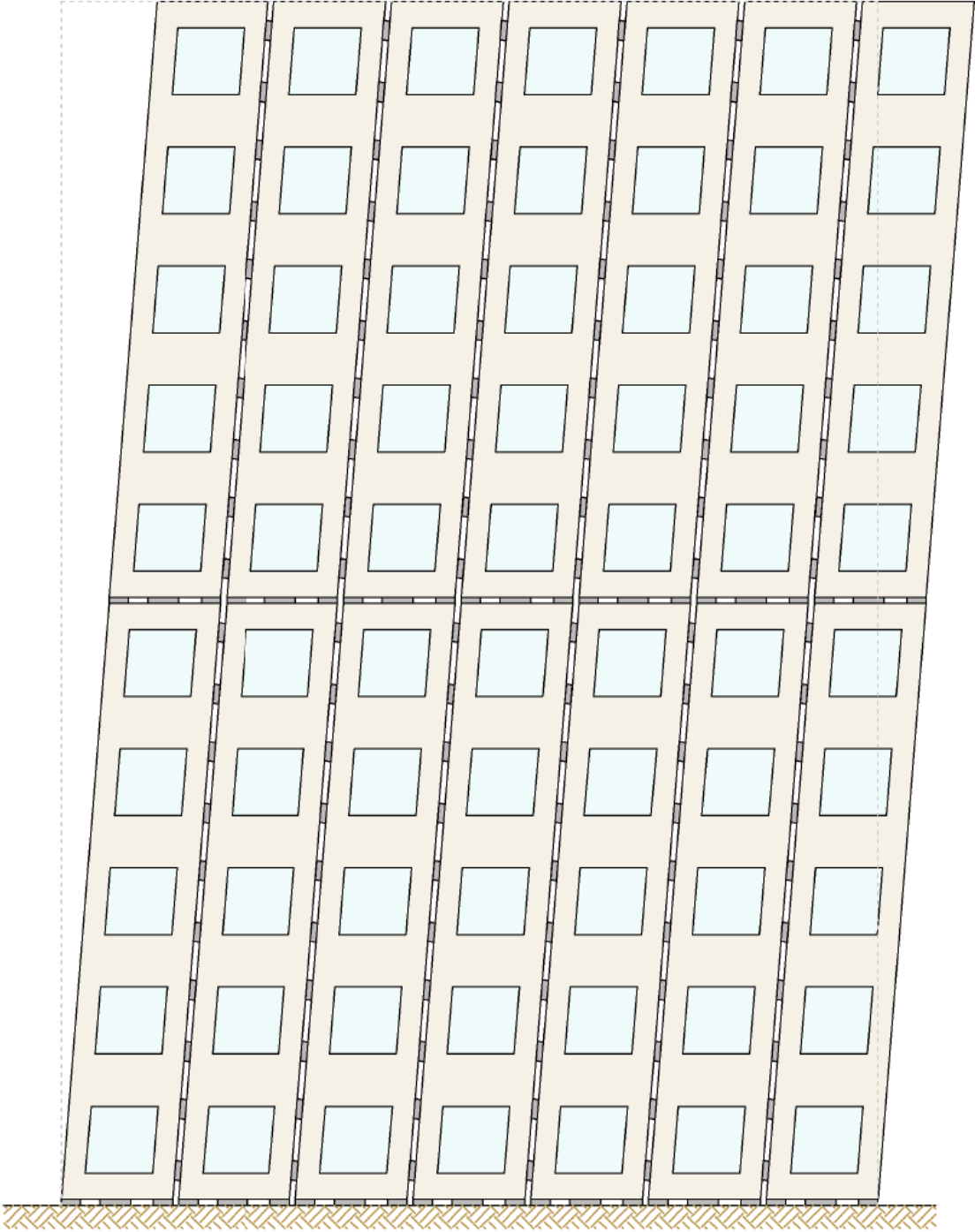
A4.1 Façade view and deflection components



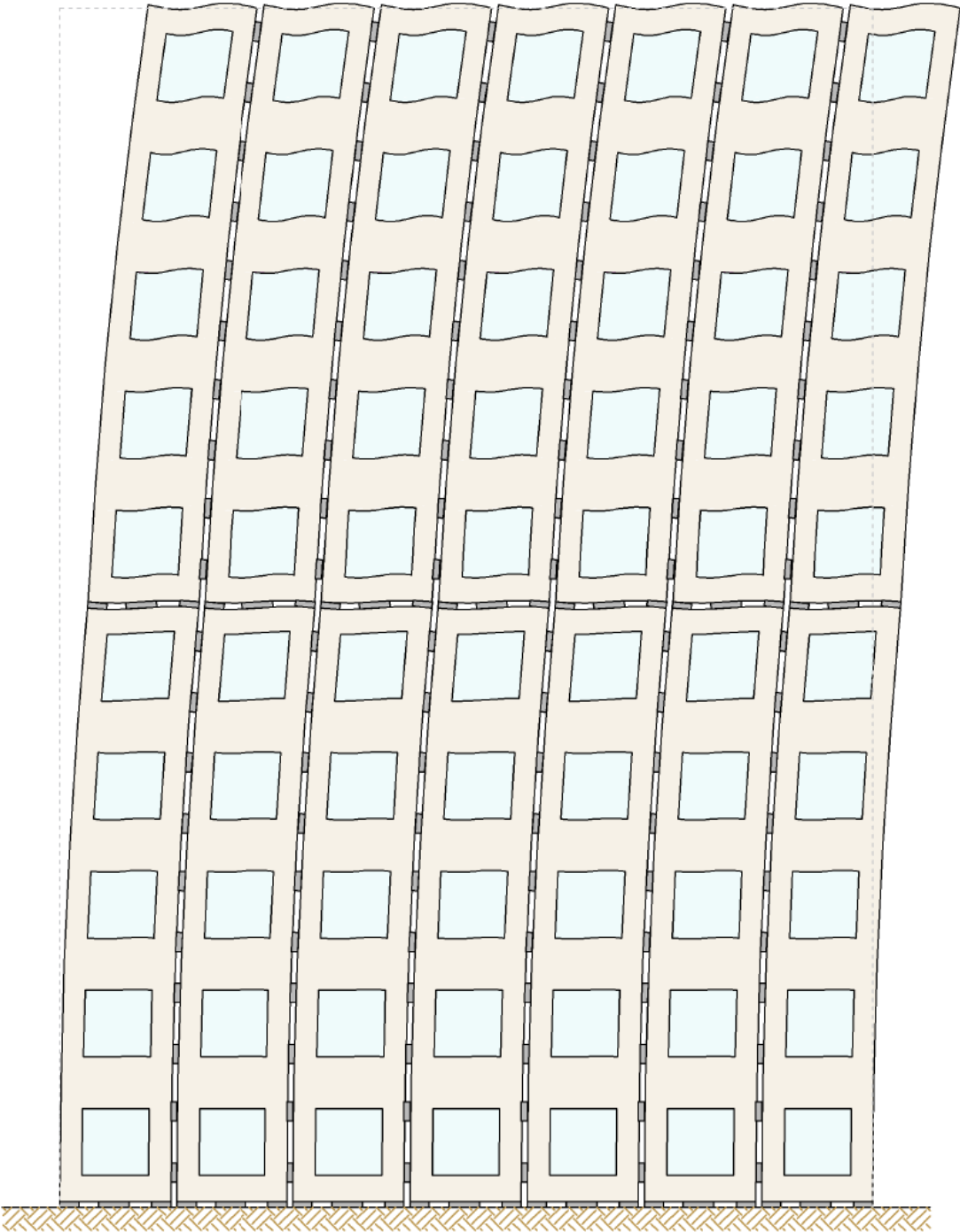
Bending of the façade



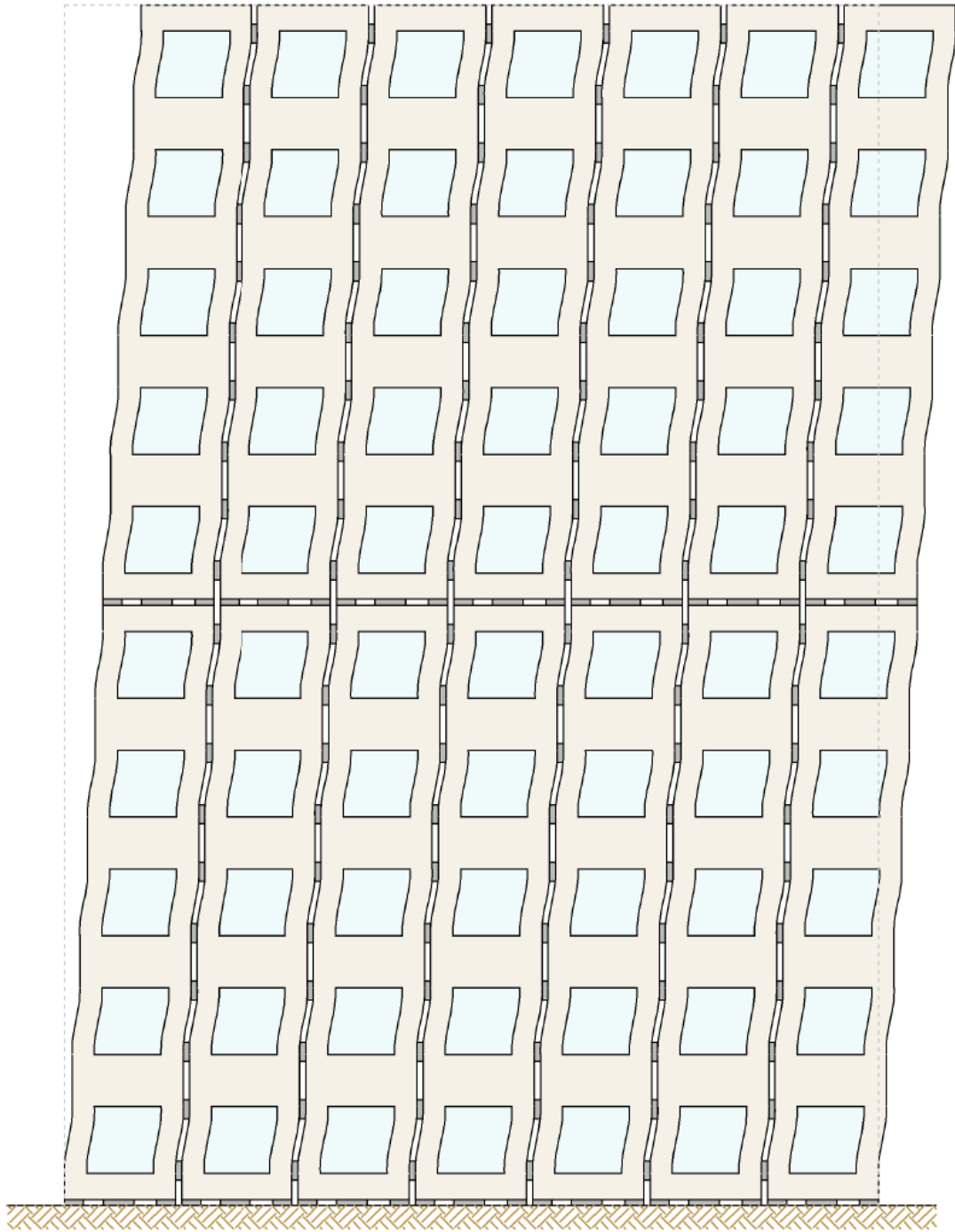
Shear of the façade



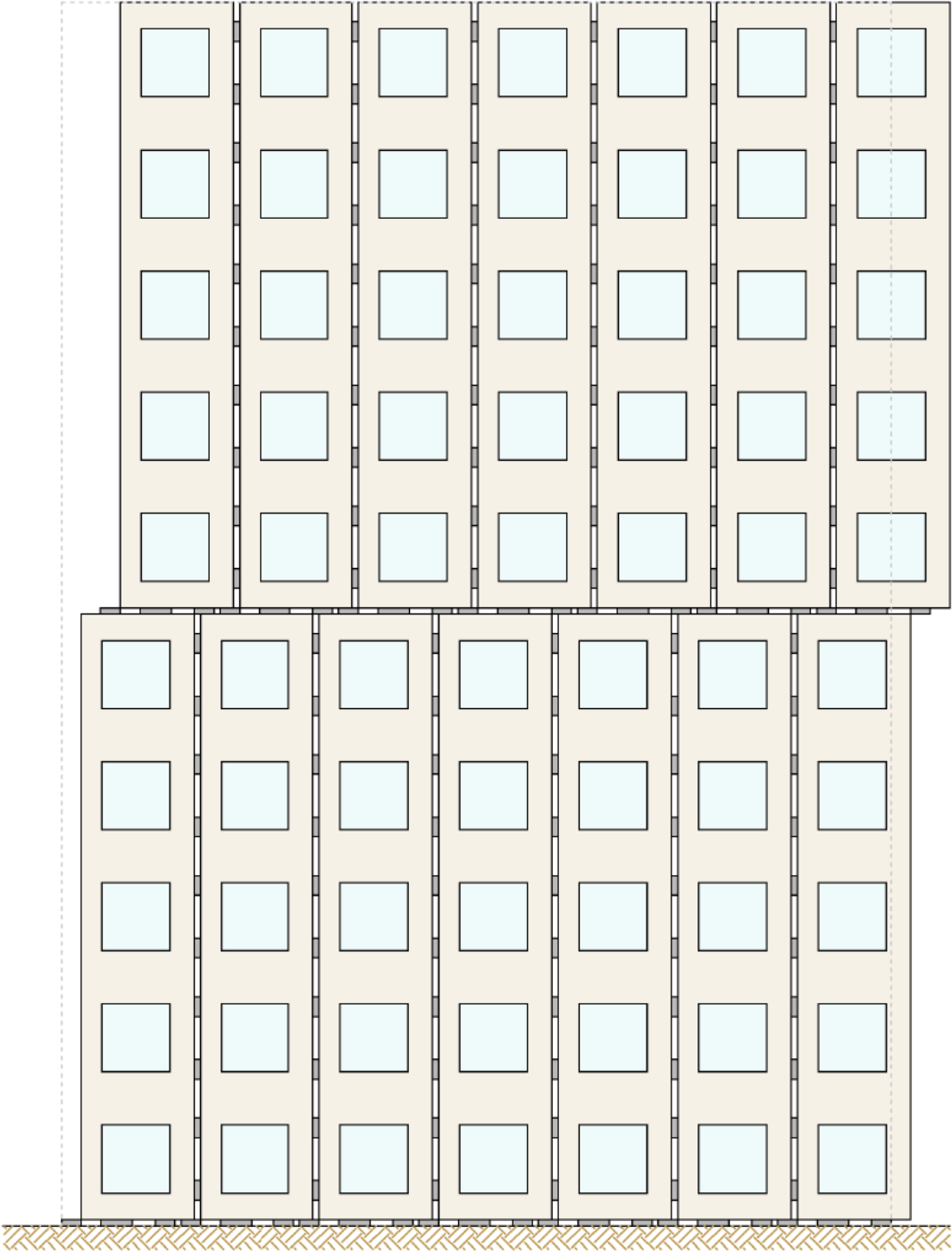
Bending of lintels



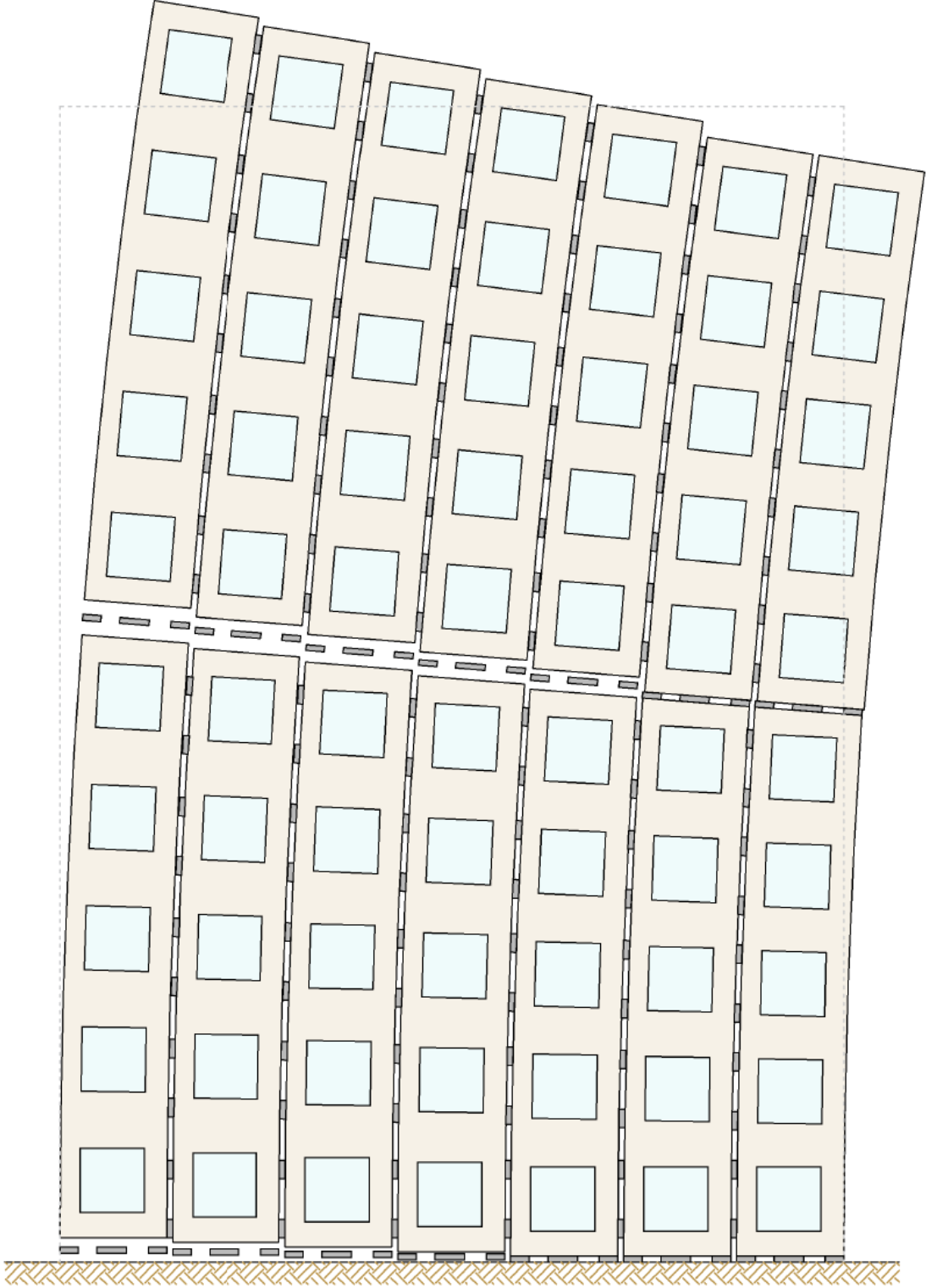
Bending of piers



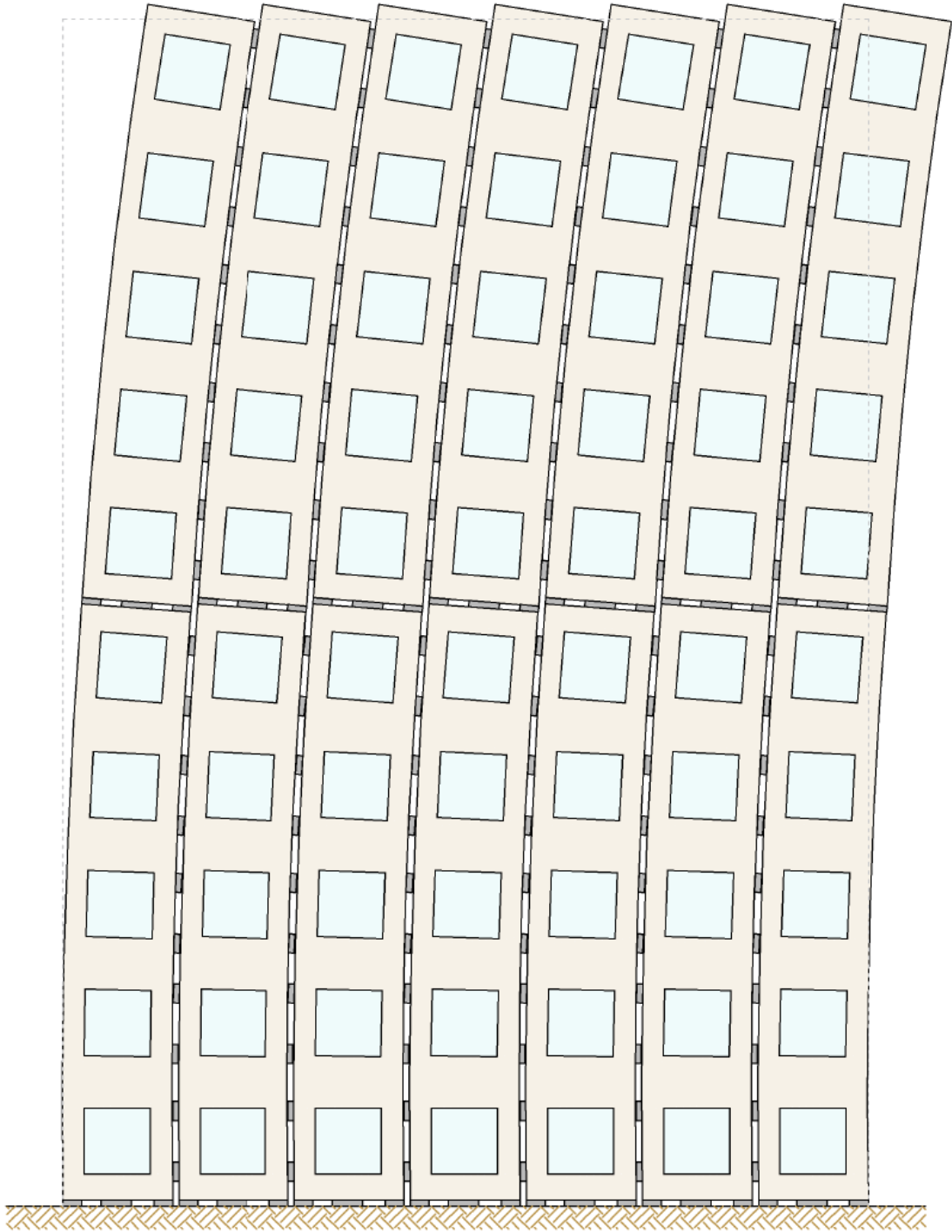
Sliding



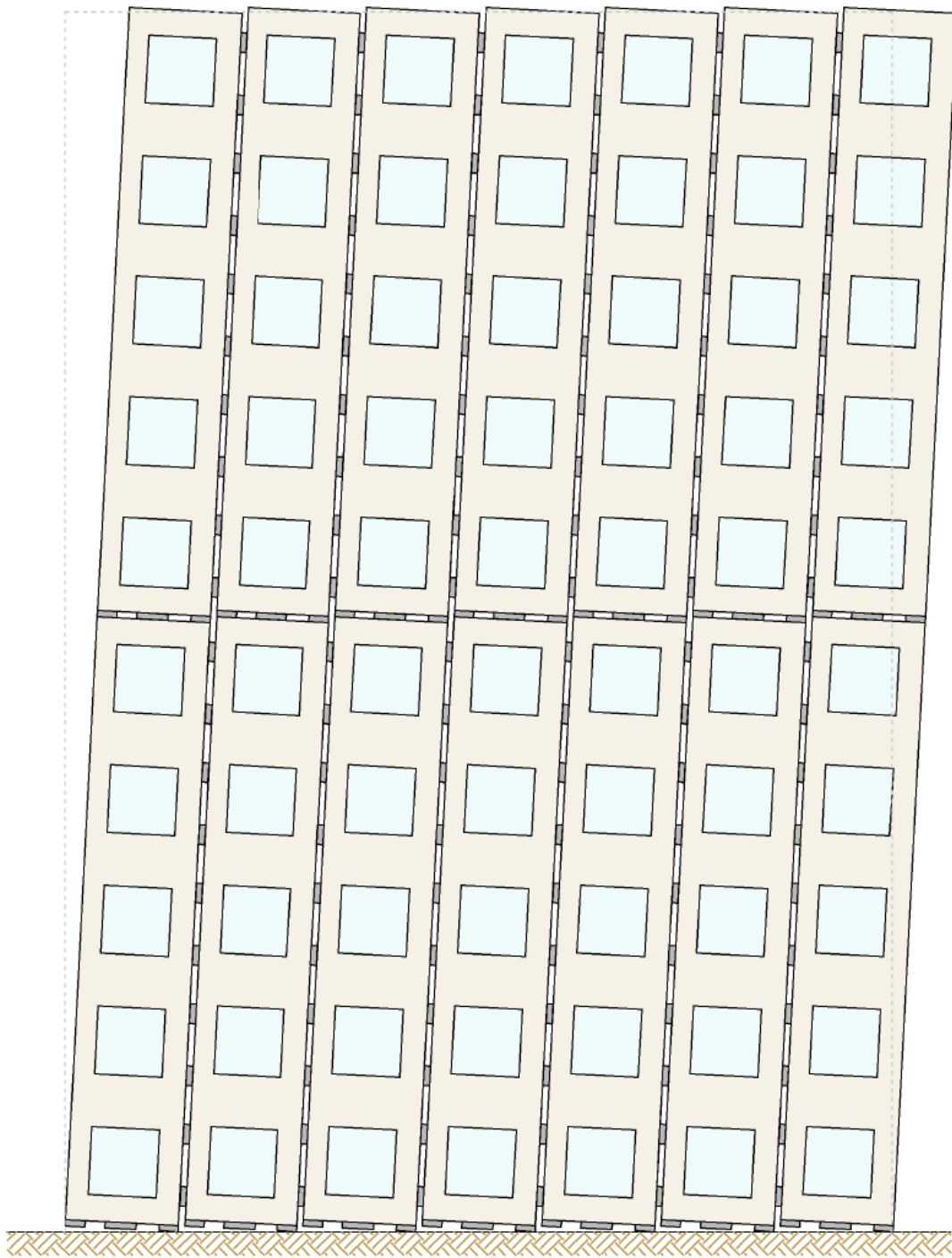
Rocking



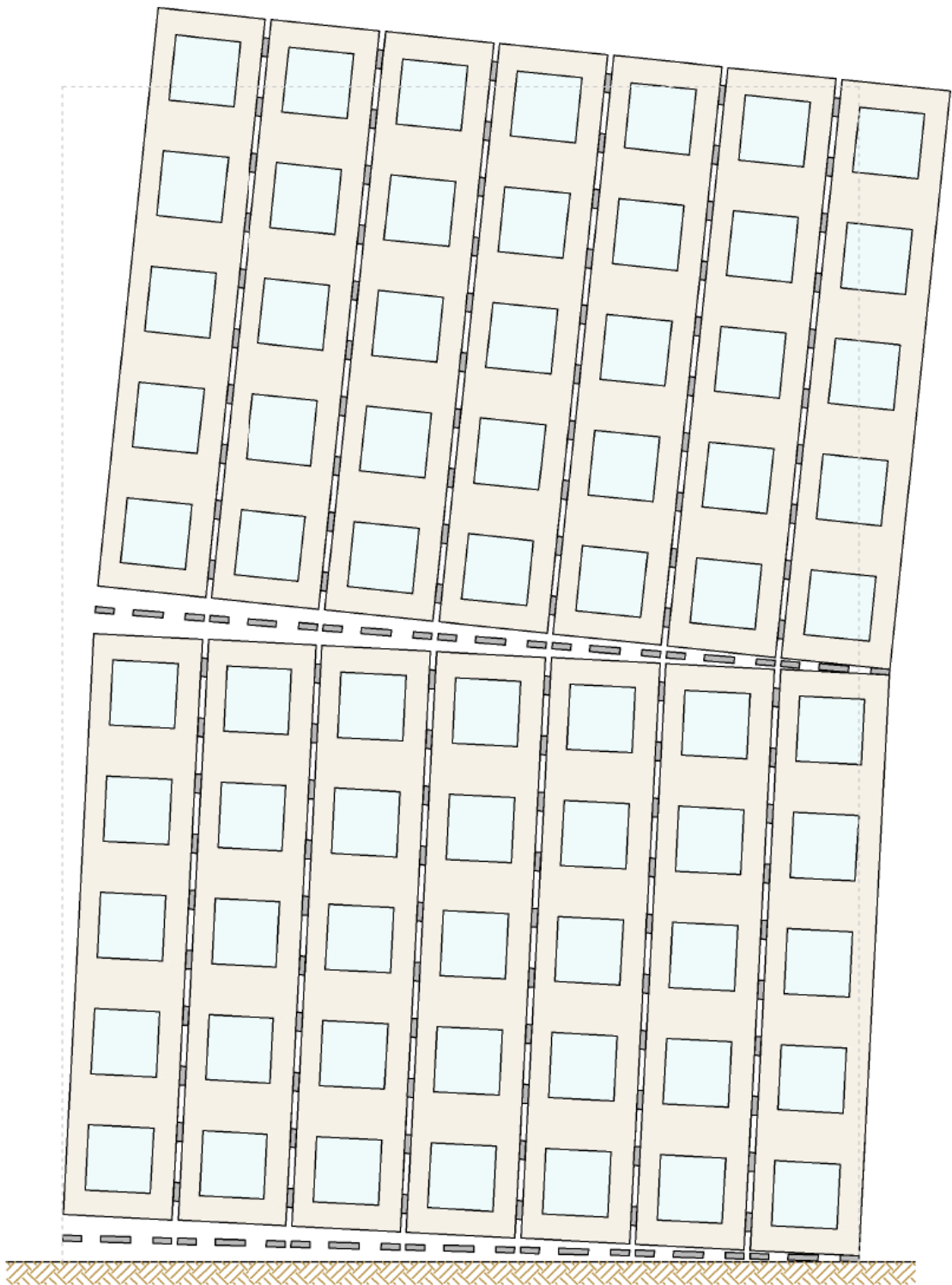
Additional bending deformation



Free bending deformation



Free rocking deformation



A4.2 Shear stiffness of fenestrated panels

Research has been done by Dujic et al. (2007) regarding the shear stiffness of fenestrated panels. Openings in a CLT panel result in a reduced shear stiffness which can be calculated using equations (55) and (56).

$$r = \frac{H \sum L_i}{H \sum L_i + \sum A_i} \quad (55)$$

$$K = \frac{r}{2 - r} \quad (56)$$

Where

H is the height of the panel
L_i is the width of full height wall segments
A_i is the sum of openings
K is the ratio of shear stiffness of fenestrated and non-fenestrated panels

For panels with a width of 2,9 meter; height of 15,5 meter and five openings of 1,74x1,74 meter, the reduction factor is 0,37. Or in other words, 37% of the shear stiffness of the full panel remains when the openings are included. This is only slightly less than the reduction of shear area at the height of the opening, which is 40% of the original area. Hence, this approach by Dujic et al. will not be included in the calculation of the shear deformation.

A4.3 Theoretical hand calculations

Calculations for the maximal compressive force for the model of 77,5 meter are presented below. The floor load has trapezoidal load distribution. That is why the vertical load is reduced by a factor 6/7. As six out of seven panels are effectively loaded and assuming that this load then distributes among all piers evenly.

Table 13, calculation of axial force in the piers of a CLT panel when unfavorable

	q		Factor		b		n_{story}		n_{piers}		γ		N_{Ed}
Self weight	3,44	x		x	20,3	x	25	/	14	x	1,20	=	150
Floor G	14,82	x	6/7	x	20,3	x	25	/	14	x	1,20	=	553
Façade	2,54	x		x	20,3	x	25	/	14	x	1,20	=	110
Floor Q	4,08	x	6/7	x	20,3	x	25	/	14	x	1,50	=	190
Total													1003 kN

Table 14, calculation of axial force in the piers of a CLT panel when favorable

	q		Factor		b		n_{story}		n_{piers}		γ		N_{Ed}
Self weight	3,44	x		x	20,3	x	25	/	14	x	0,90	=	112
Floor G	14,82	x	6/7	x	20,3	x	25	/	14	x	0,90	=	414
Façade	2,54	x		x	20,3	x	25	/	14	x	0,90	=	83
Floor Q	4,08	x	6/7	x	20,3	x	25	/	14	x	0,00	=	0
Total													609 kN

Calculation of shear force V_{Ek} and bending moment M_{Ek} on the façade acting at the foundation level. Wind load $q_{w,k}$ is translated into a horizontal force $F_{H,k}$ by multiplying it by 15,5 meter. The distance between the horizontal wind force and the foundation z is multiplied with the force to find the bending moment contribution of that force. The sum is the bending moment of 72.411 kNm on the foundation. Similarly, the sum of horizontal forces $F_{H,k}$ is the horizontal shear force on the foundation.

Table 15, calculation of M_{ek} due to wind load

Height	q_{w,k}	F_{H,k}	z	M
	<i>kN/m</i>	<i>kN</i>	<i>M</i>	
77,5 meter	27,1	420	69,8	29.295
62,0 meter	24,7	383	54,3	20.778
46,5 meter	22,3	346	38,8	13.408
31,0 meter	19,6	304	23,3	7.068
15,5 meter	15,7	243	7,8	1.883
Total V_{ek}		1696		
Total M_{Ek}				72.411

Similarly for other heights

Table 16, acting forces on the façade at half-way panel height of the bottom panels

Height	$M_{Ek,max}$ <i>kNm</i>	$V_{Ek,max}$ <i>kN</i>	M_{Ed} <i>kNm</i>	V_{Ed} <i>kN</i>
77,5 meter	72.411	1696	108.617	2544
62,0 meter	43.113	1276	64.669	1913
46,5 meter	22.343	893	33.515	1339
31,0 meter	8.949	547	13.424	821
15,5 meter	1.886	243	2829	365

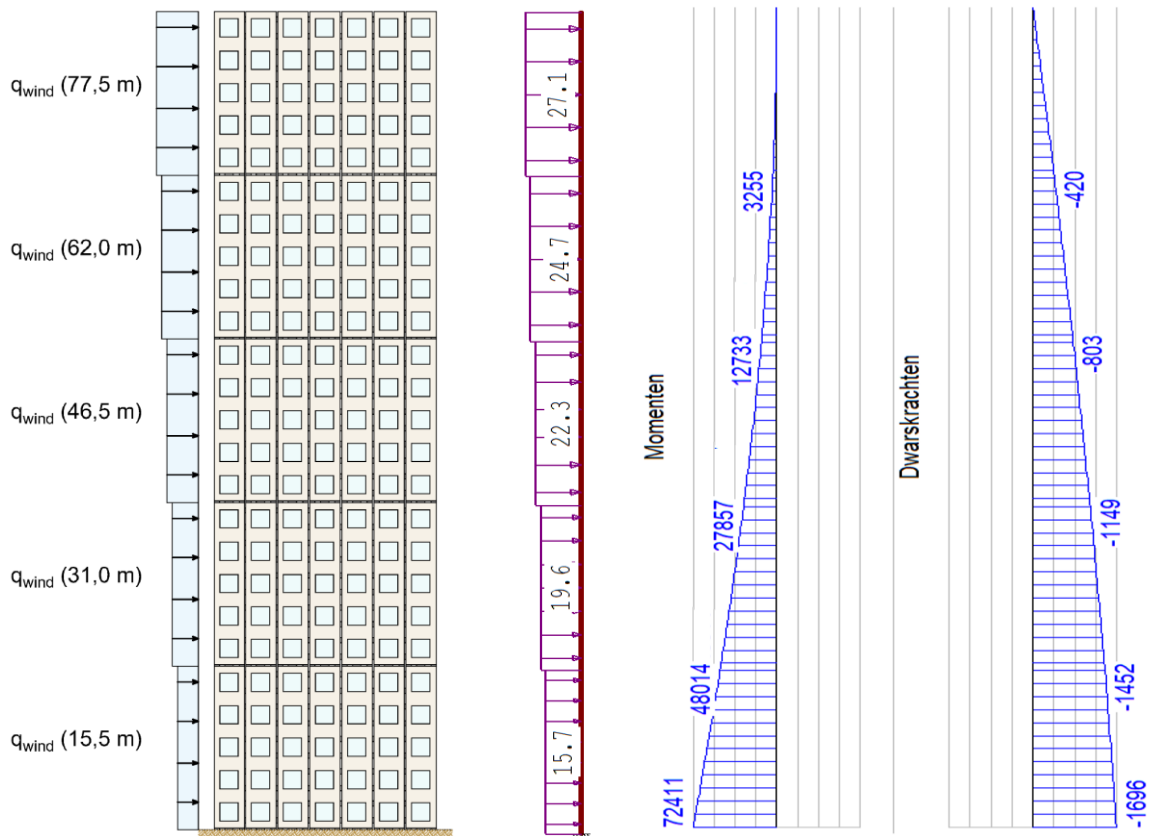


Figure 11, wind load on the façade

Calculation of axial force N_{Ed} in the outer pier due to wind for each model height

Table 17, axial force in outer piers

Wind	M_{Ed}		W		b_{pier}	t_{pier}		N_{Ed}		
	<i>kNm</i>		<i>mm³</i>		<i>m</i>	<i>m</i>		<i>kN</i>		
77,5 meter	108.617	* 10 ⁶	/	7,84*10 ⁹	x	0,58	x	0,28	=	2251
62,0 meter	64.669	* 10 ⁶	/	7,84*10 ⁹	x	0,58	x	0,28	=	1340
46,5 meter	33.515	* 10 ⁶	/	7,84*10 ⁹	x	0,58	x	0,28	=	694
31,0 meter	13.424	* 10 ⁶	/	5,60*10 ⁹	x	0,58	x	0,20	=	278
15,5 meter	2829	* 10 ⁶	/	4,20*10 ⁹	x	0,58	x	0,15	=	59

Calculation of the axial force in the hold-down connection. Where the maximum tension is the wind force reduced with the minimum weight and the maximum compression force is the wind force added to the maximum weight.

Table 18, results of maximum compressive and tensile forces in the outer connections at the foundation

Height	$N_{Ed,wind}$	$N_{Ed,weight,min}$	$N_{Ed,weight,max}$	$N_{t,d}$	$N_{c,d}$
	<i>kN</i>	<i>kN</i>	<i>kN</i>	<i>kN</i>	<i>kN</i>
77,5 meter	2251	-609	-1003	1642	-3254
62,0 meter	1340	-487	-802	853	-2142
46,5 meter	694	-365	-602	329	-1296
31,0 meter	278	-244	-401	34	-679
15,5 meter	59	-122	-201	0	-260

These theoretical results assume full cooperation between CLT panels. That is why these results are considered to be unfavorable. Actual tensile and compressive forces are expected to be higher. The actual magnitude of this deviation is to be found by comparing the theoretical results to the computer results.

A4.4 Theoretical top deformation without connection stiffness

The top deformation of a CLT façade of 77,5 meter is calculated. It includes the contribution of openings. It does not include the contribution of any stiffness of the fasteners in the connections. Four contributions to the top deformation are accounted for. These are bending and shear deformation of the façade with reduced stiffness due to openings and additional bending due to deformation of piers and lintels.

The contribution of the bending of lintels is calculated using the method of Schelling. The stiffness of the lintel is distributed over the height of the story. The piers are then considered as beam elements that are connected by the lintels. The length of the lintel is defined according to Hsiao (2014).

$$w_{bending} = \frac{q_{wind} * h^4}{8 * EI_{red}} = \frac{27,1 * 77500^4}{8 * 923 * 10^{15}} = 132 \text{ mm}$$

$$w_{shear} = \frac{q_{wind} * h^2}{2 * GA_{s,avg}} = \frac{27,1 * 77500^2}{2 * 2,019 * 10^9} = 40,3 \text{ mm}$$

$$w_{piers} = T_n * \frac{q_{wind} * h_{story} * h_{pier,eff}^3}{12 * \sum EI_{pier}} = 325 * \frac{27,1 * 3100 * 2420^3}{12 * 1,69 * 10^{15}} = 19,1 \text{ mm}$$

$$w_{Schelling} = \frac{1 - \gamma_{red}}{\gamma_{red}} w_b = \frac{0,165}{0,835} * 132 = 26,1 \text{ mm}$$

where

$\gamma_{red} = 0,835$ according to Maple script below

The total deformation of the top is the sum of the components

$$w_{top} = 218 \text{ mm}$$

A4.5 Maple script for the top deformation due to deformation of the lintels

```

> restart;
> qwind := 27.1;
> A := 2900·t0;
> t0 := 280;
> r90 := 120;
> E := 11600;
> Hlintel := 1360;
> Llintel := 2320;
> K :=  $\frac{12 \cdot E \cdot \left(\frac{1}{12}\right) \cdot r90 \cdot Hlintel^3}{Llintel^3} \cdot \frac{1}{3.1} \cdot 10^{-3}$ ;
90.45 (1)
> h := 77500;
> L := 2·h;
> a := 2900;
> Bpier := 580;
> a1 := 3.5·a - 280; a2 := 2.5·a; a3 := 1.5·a; a4 := 0.5·a; a5 := -0.5·a; a6 := -1.5·a;
a7 := -2.5·a; a8 := -3.5·a - 280;
> v11 :=  $\left(K + \frac{\text{Pi}^2}{L^2} \cdot E \cdot 0.5 \cdot A\right) \cdot a1$ ;
> v12 := -K·a2;
> v21 := -K·a1;
> v22 :=  $\left(K + K + \frac{\text{Pi}^2}{L^2} \cdot E \cdot A\right) \cdot a2$ ;
> v23 := -K·a3;
> v32 := -K·a2;
> v33 :=  $\left(K + K + \frac{\text{Pi}^2}{L^2} \cdot E \cdot A\right) \cdot a3$ ;
> v34 := -K·a4;
> v43 := -K·a3;
> v44 :=  $\left(K + K + \frac{\text{Pi}^2}{L^2} \cdot E \cdot A\right) \cdot a4$ ;
> v45 := -K·a5;
> v54 := -K·a4;
> v55 :=  $\left(K + K + \frac{\text{Pi}^2}{L^2} \cdot E \cdot A\right) \cdot a5$ ;
> v56 := -K·a6;
> v65 := -K·a5;
> v66 :=  $\left(K + K + \frac{\text{Pi}^2}{L^2} \cdot E \cdot A\right) \cdot a6$ ;
> v67 := -K·a7;
> v76 := -K·a6;
> v77 :=  $\left(K + K + \frac{\text{Pi}^2}{L^2} \cdot E \cdot A\right) \cdot a7$ ;
> v78 := -K·a8;
> v87 := -K·a7;
> v88 :=  $\left(K + \frac{\text{Pi}^2}{L^2} \cdot E \cdot 0.5 \cdot A\right) \cdot a8$ ;
> s1 := K·a;
> s2 := 0;
> s3 := 0;
> s4 := 0;
> s5 := 0;
> s6 := 0;
> s7 := 0;
> s8 := -K·a;
> with(linalg);
> Amatrix := matrix([[v11, v12, 0, 0, 0, 0, 0, 0], [v21, v22, v23, 0, 0, 0, 0, 0], [0, v32, v33, v34, 0, 0, 0, 0], [0, 0, v43, v44, v45, 0, 0, 0], [0, 0, 0, v54, v55, v56, 0, 0], [0, 0, 0, 0, v65, v66, v67, 0], [0, 0, 0, 0, 0, v76, v77, v78], [0, 0, 0, 0, 0, 0, v87, v88]]);
> S := vector([s1, s2, s3, s4, s5, s6, s7, s8]);
> b := evalf(linsolve(Amatrix, S));
[ 0.874 0.815 0.793 0.782 0.782 0.793 0.815 0.827 ] (2)
> Irigid :=  $\frac{2 \cdot t0 \cdot Bpier^3}{12} + \frac{5 \cdot t0 \cdot (2 \cdot Bpier)^3}{12} + 2 \cdot t0 \cdot Bpier \cdot a1^2 + 2 \cdot t0 \cdot (2 \cdot Bpier) \cdot a2^2 + 2 \cdot t0 \cdot (2 \cdot Bpier) \cdot a3^2 + 2 \cdot t0 \cdot (2 \cdot Bpier) \cdot a4^2$ ;
> Iopenings :=  $\frac{2 \cdot t0 \cdot Bpier^3}{12} + \frac{5 \cdot t0 \cdot (2 \cdot Bpier)^3}{12} + 2 \cdot b[1] \cdot t0 \cdot (Bpier) \cdot a1^2 + 2 \cdot b[2] \cdot t0 \cdot (Bpier) \cdot a2^2 + 2 \cdot b[3] \cdot t0 \cdot (2 \cdot Bpier) \cdot a3^2 + 2 \cdot b[4] \cdot t0 \cdot (2 \cdot Bpier) \cdot a4^2$ ;
> gamma_red :=  $\frac{Iopenings}{Irigid}$ ;
0.835 (3)
> additional_bending :=  $\frac{1 - \text{gamma\_red}}{\text{gamma\_red}} \cdot \frac{qwind \cdot h^4}{8 \cdot E \cdot Irigid}$ ;
26.14 (4)
> Alternative :=  $\frac{qwind \cdot h^4}{8 \cdot E \cdot Iopenings} - \frac{qwind \cdot h^4}{8 \cdot E \cdot Irigid}$ ;
26.14 (5)

```

A4.6 Theoretical top deformation - results

The results for all heights have been calculated in a similar way and shown before. The results in black are for the panels used in further calculations. The results in grey are for panels that will not be further researched.

Table 19, theoretical top deformation

Model	q_k <i>kN/m</i>	panel	t₀ <i>mm</i>	t <i>mm</i>	EI <i>x10¹⁵</i> <i>Nmm²</i>	GA_s <i>x10⁶</i> <i>N</i>	∑EI_p <i>x10¹⁵</i> <i>Nmm²</i>	γ_{red}	W_b <i>mm</i>	W_s <i>mm</i>	W_{pier} <i>mm</i>	W_{Schelling} <i>mm</i>	W_{tot} <i>mm</i>
15,5 meter	15,7	LL-190/7s	150	190	495	959	0,903	0,12	0,23	1,97	0,95	1,77	4,92
31,0 meter	19,6	LL-260/7s	200	260	660	1312	1,209	0,36	3,43	7,17	3,27	6,20	20,1
46,5 meter	22,3	LL-300/9s	240	300	792	1515	1,447	0,51	16,5	15,9	6,76	16,0	55,1
46,5 meter	22,3	LL-400/11s	280	400	923	2019	1,690	0,64	14,1	11,9	5,80	7,97	39,8
62,0 meter	24,7	LL-360/9s	240	360	792	1818	1,447	0,79	57,6	26,1	13,1	15,5	112
62,0 meter	24,7	LL-400/11s	280	400	923	2019	1,690	0,76	49,4	23,5	11,2	15,5	100
77,5 meter	27,1	LL-400/11s	280	400	923	2019	1,690	0,83	132	40,3	19,1	26,1	218

A4.7 Forces on the connections – additional bending moment

Chapter 4.5 already explained the forces acting on the connections. This appendix goes more into detail regarding the increase of forces due to additional bending moments as a result of eccentricities in the connection. The shear force in the connections is assumed to be resisted equally by all bolts.

$$F_v = \frac{V_{Ed}}{n * m} \quad (57)$$

The maximum force F_m as a result of the additional bending moment is located in the outer bolts. Meaning that one of the four outer bolts is by default the governing element. The maximum force F_{max} in one such bolt is calculated as the resulting vector of the two forces F_v and F_m . This maximum force should be below the resistance of the bolt $F_{v,Rd}$.

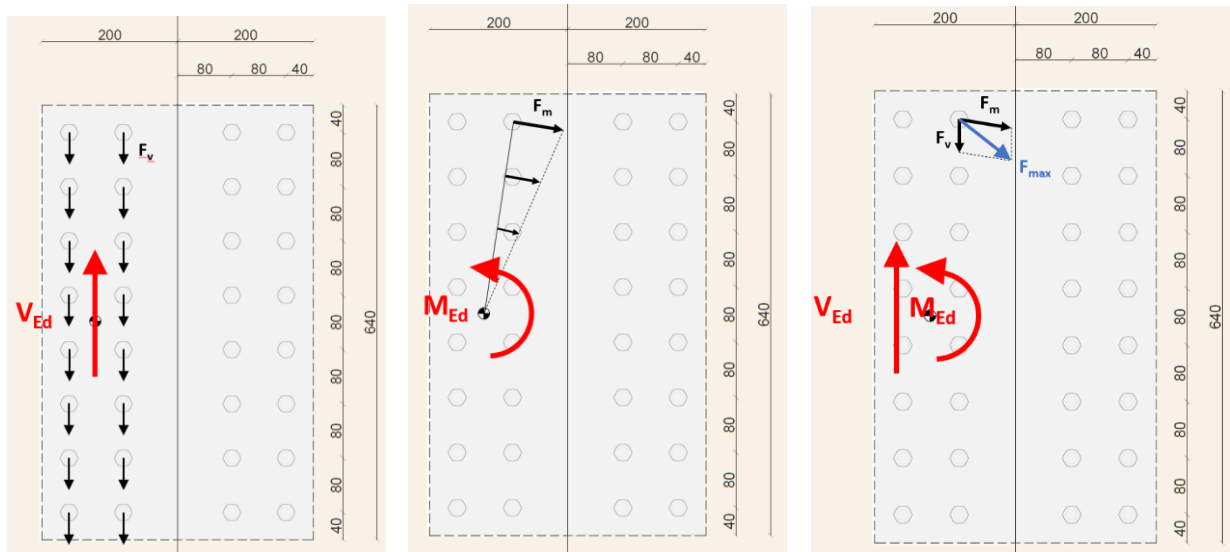


Figure 12, forces on the shear connection on the vertical edges of the panels

The force in the outer bolt due to bending is calculated using the equation below

$$M_{Ed} = \sum_{i=1}^n \frac{a_i^2}{a_{max}} * F_m \quad (58)$$

The force F_m is to be decomposed in a force vector in x- and y-direction.

$$F_{m,x} = \frac{3,5 * a}{a_{max}} * F_m \quad (59)$$

$$F_{m,y} = \frac{0,5 * a}{a_{max}} * F_m \quad (60)$$

The maximum force F_{max} is then calculated using the equation below

$$F_{max} = \sqrt{F_{m,x}^2 * (F_v + F_{m,y})^2} \quad (61)$$

A calculation is made for the shear key connection on the vertical edges of the CLT panels of the model of 77,5 meter.

$$M_{Ed} = V_{Ed} * \frac{e}{2} \quad (62)$$

$$V_{Ed} = 291 \text{ kN} \quad (63)$$

$$M_{Ed} = \sum_{i=1}^n \frac{a_i^2}{a_{max}} * F_m \quad (64)$$

$$M_{Ed} = 4 * \left[\frac{40^2}{283} + \frac{120^2}{283} + \frac{200^2}{283} + \frac{280^2}{283} \right] * F_m \quad (65)$$

$$M_{Ed} = 1900 * F_m \quad (66)$$

The force on the outer bolt due to bending on the connection is calculated and split into a horizontal component ($F_{m,x}$) and vertical component ($F_{m,y}$). These are added to the shear force per bolt (F_v).

$$F_m = \frac{M_{Ed}}{1900} \quad (67)$$

$$F_m = \frac{V_{Ed} * \frac{e}{2}}{1900} \quad (68)$$

$$F_m = \frac{291 * 0,12}{1900} = 18,4 \text{ kN} \quad (69)$$

$$F_{m,x} = \frac{280}{283} * 18,4 = 18,2 \text{ kN} \quad (70)$$

$$F_{m,y} = \frac{40}{283} * 18,4 = 2,6 \text{ kN} \quad (71)$$

$$F_v = \frac{291}{2 * 8} = 18,2 \text{ kN} \quad (72)$$

$$F_x = F_{m,x} = 18,2 \text{ kN} \quad (73)$$

$$F_y = F_{m,y} + F_v = 18,2 + 2,6 = 20,8 \text{ kN} \quad (74)$$

$$F_{max,d} = \sqrt{18,2^2 + 20,8^2} = 27,6 \text{ kN} \quad (75)$$

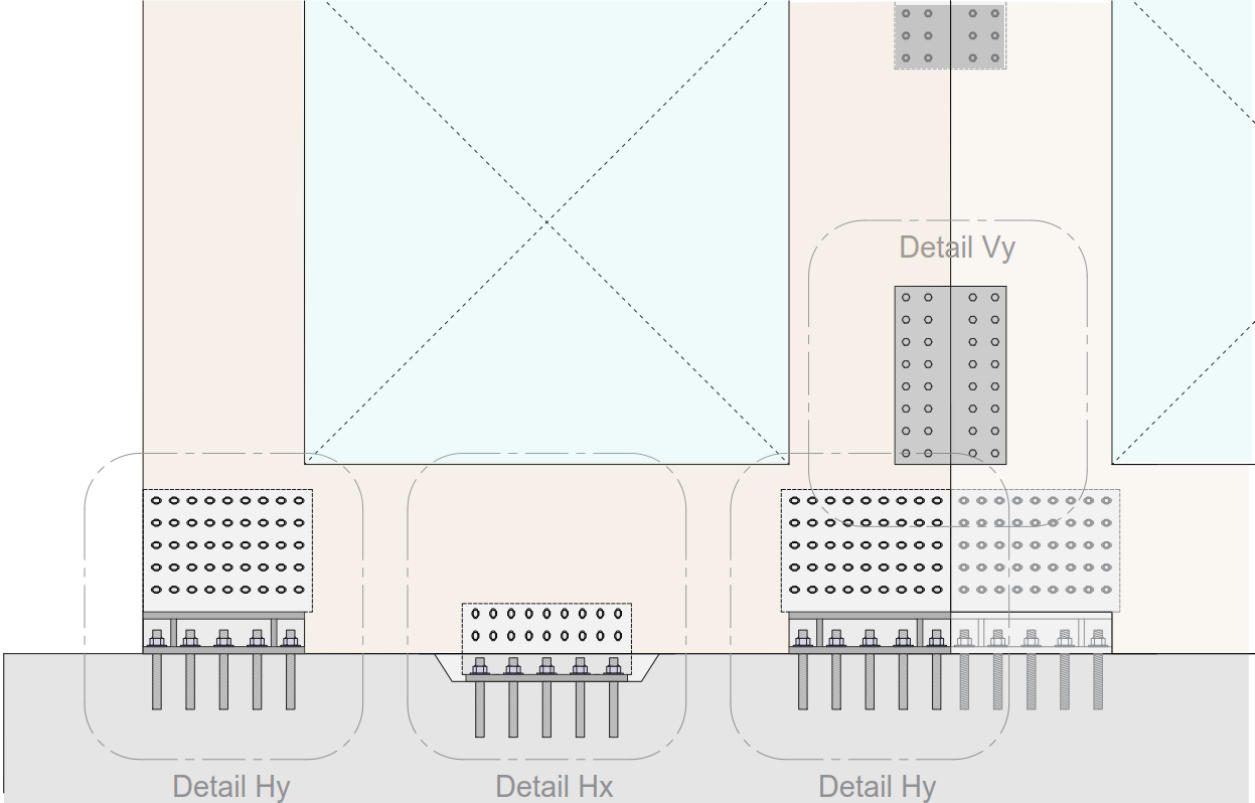
$$F_{v,Rd} = 40 \text{ kN} \quad (76)$$

The unity check was 0,46 (18,2 / 40) but increased to 0,69 (27,6 / 40). Which is an increase of 52%. This increase is independent of the value of V_{Ed} . It solely depends on the geometry of the connection.

A5 Chapter 5 appendices

A5.1 Detail drawings of the connections at the foundation

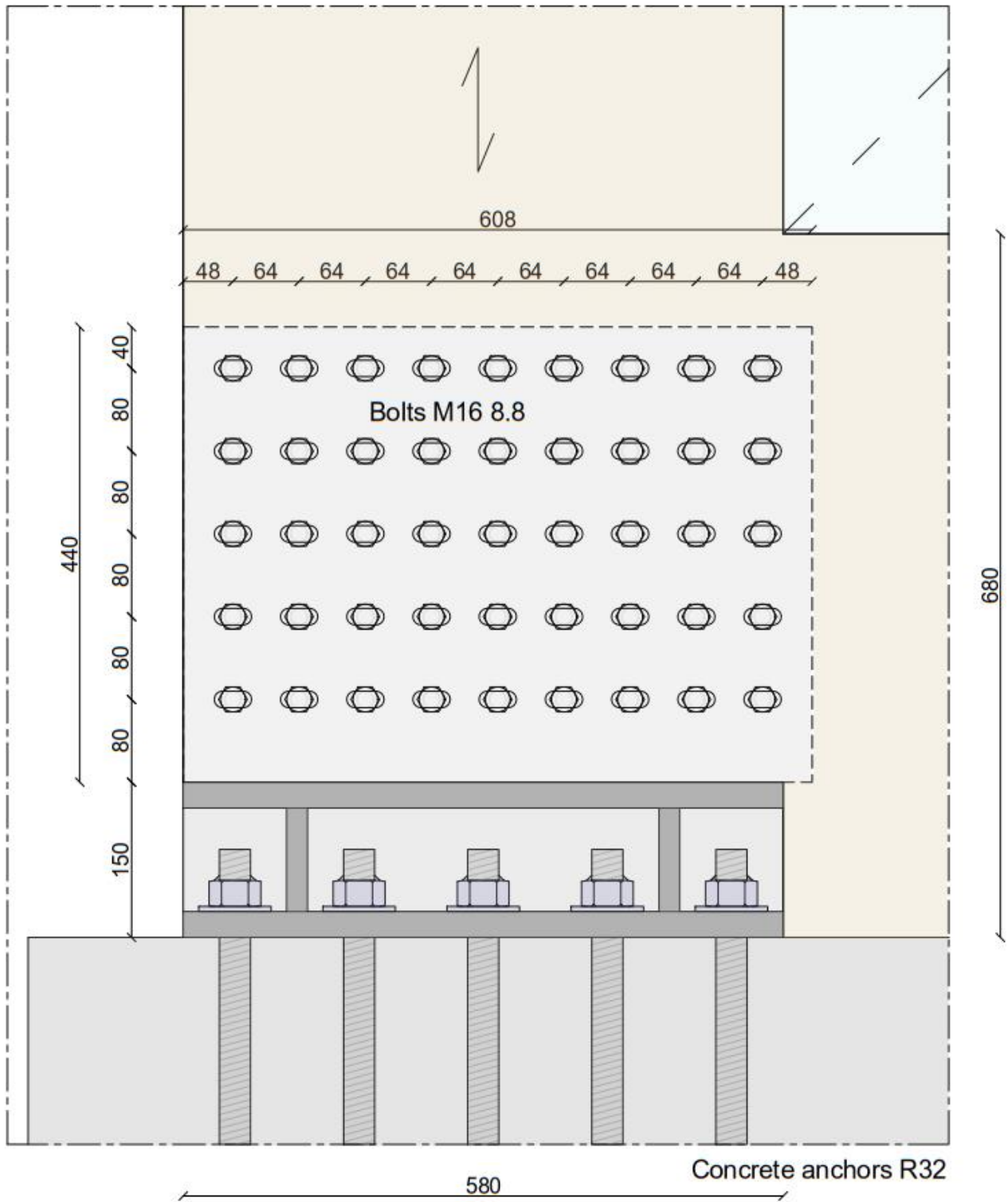
Details are presented for the model of 77,5 meter.



A5.1.1 Hold-down connection

horizontal edge

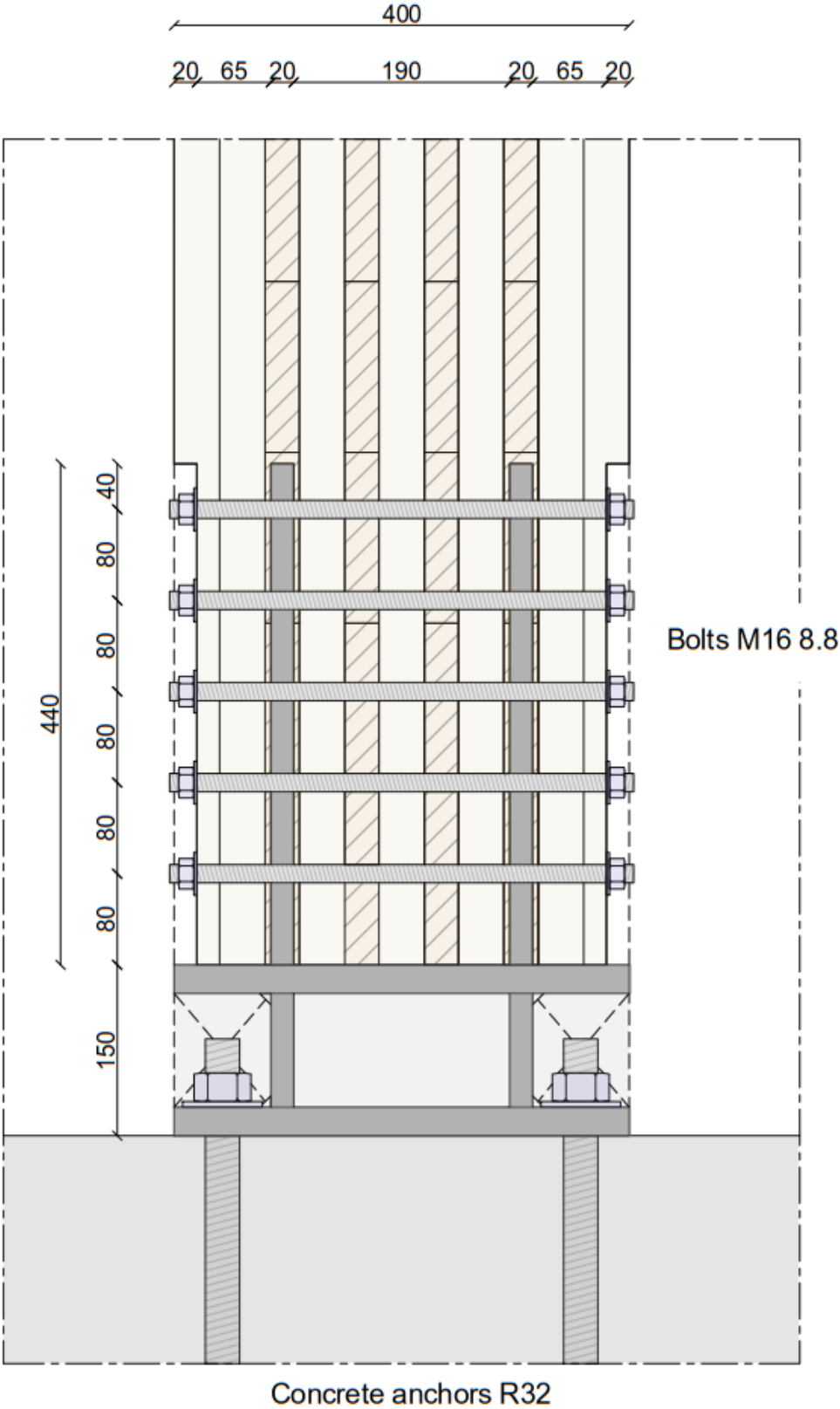
H_y front view



A5.1.2 Hold-down connection

horizontal edge

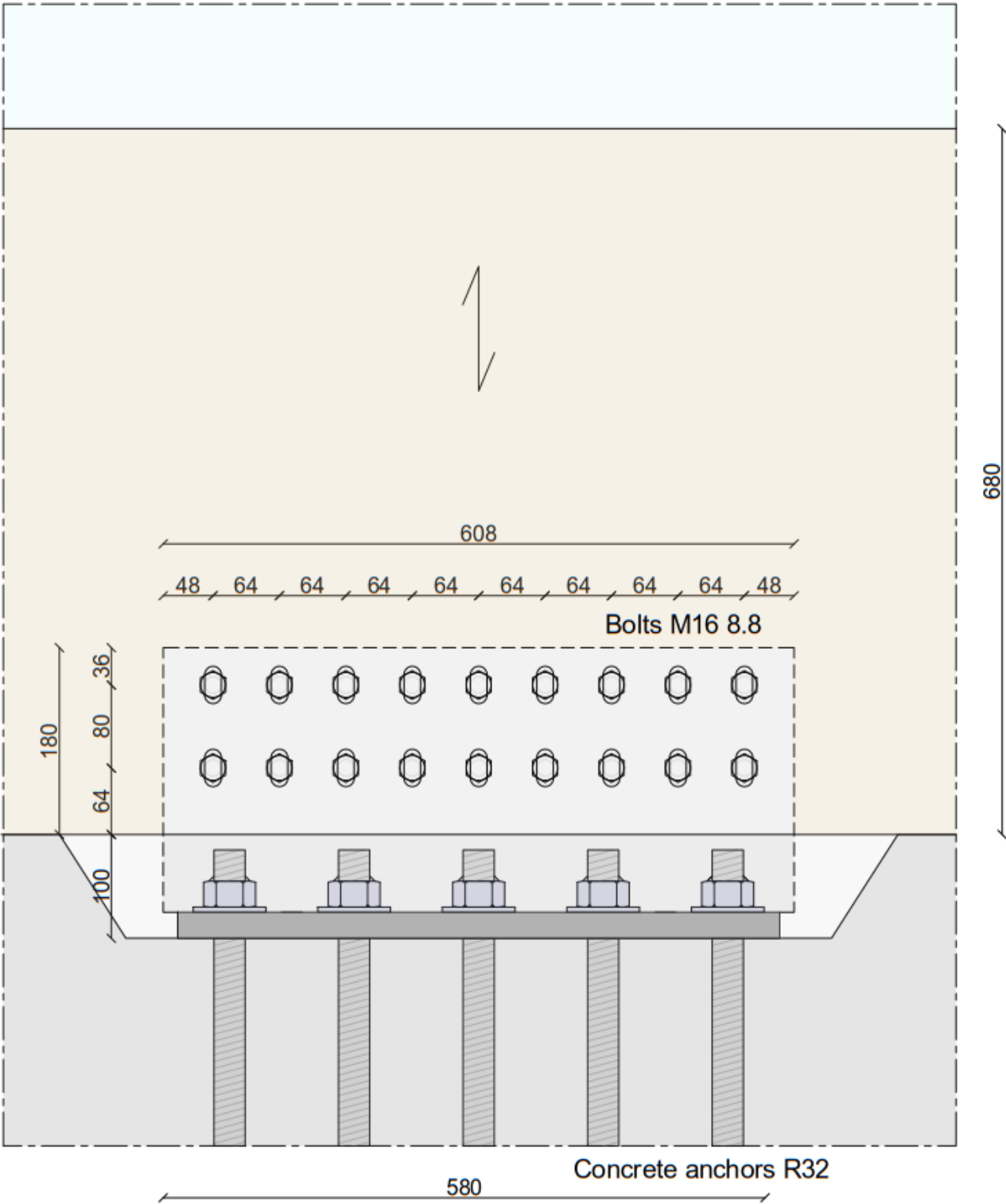
H_y cross-section



A5.1.3 Shear connection

horizontal edge

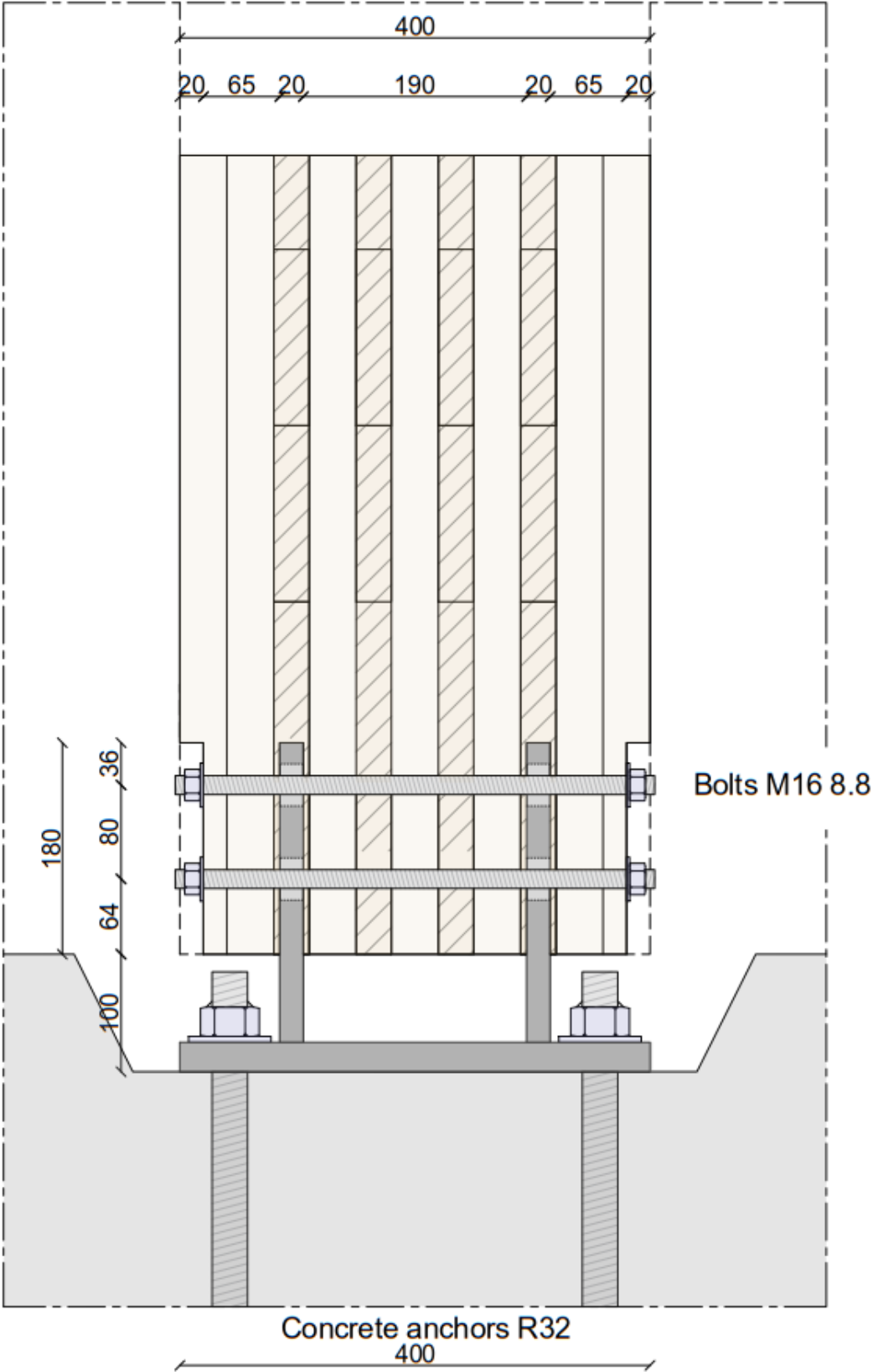
H_x front view



A5.1.4 Shear connection

horizontal edge

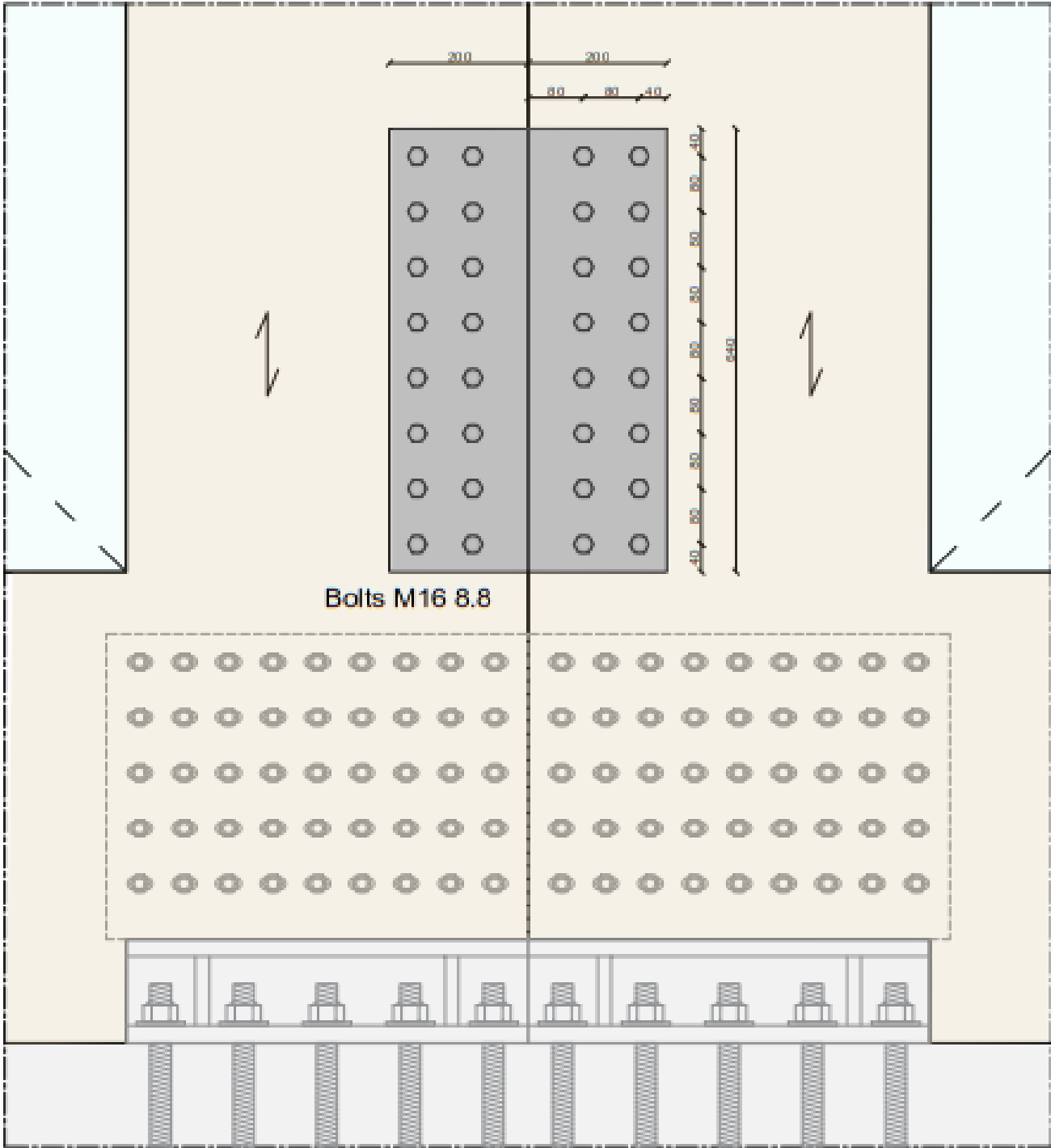
H_x cross-section



A5.1.5 Shear connection

vertical edge

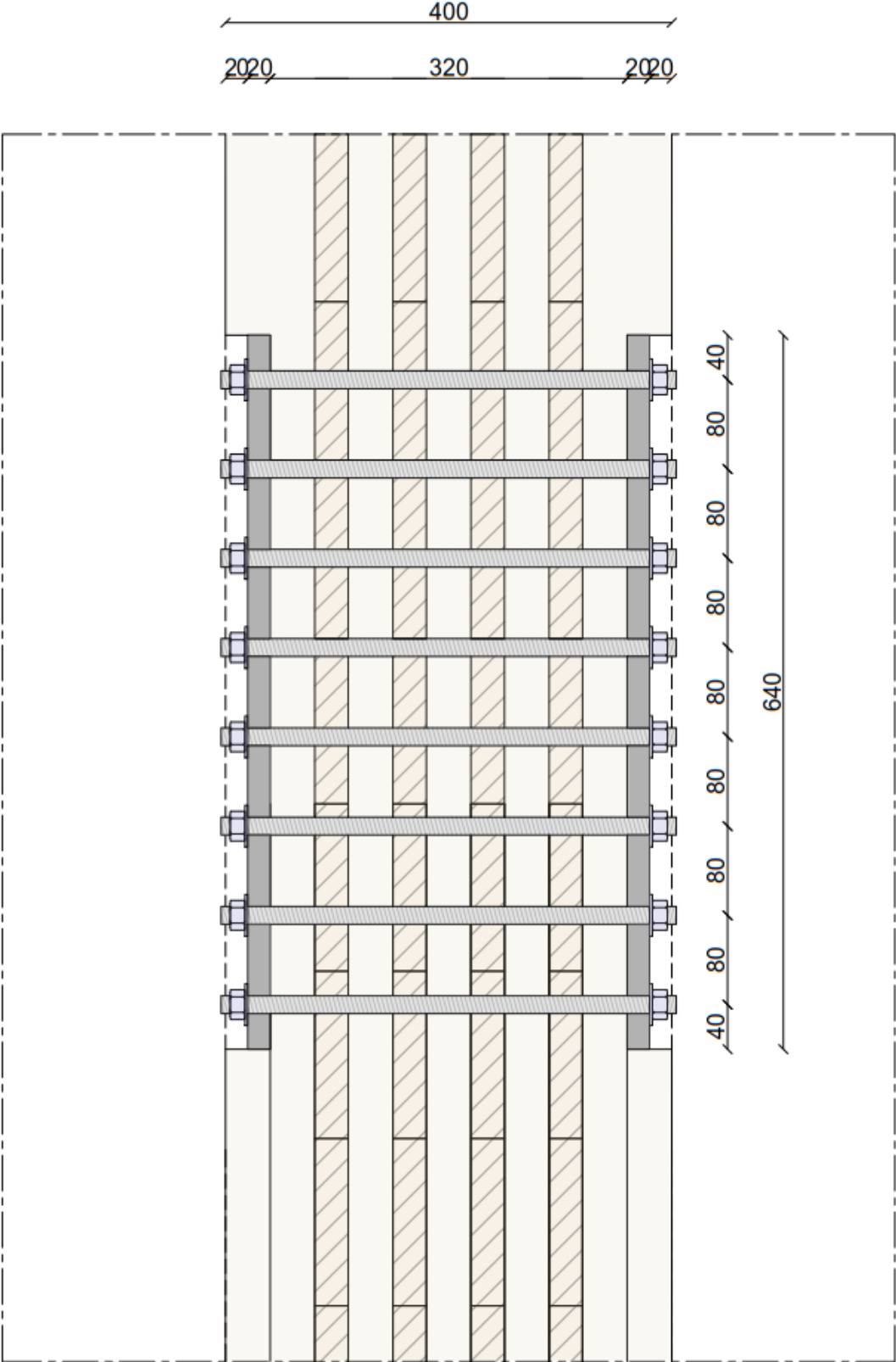
V_x front view



Shear connection

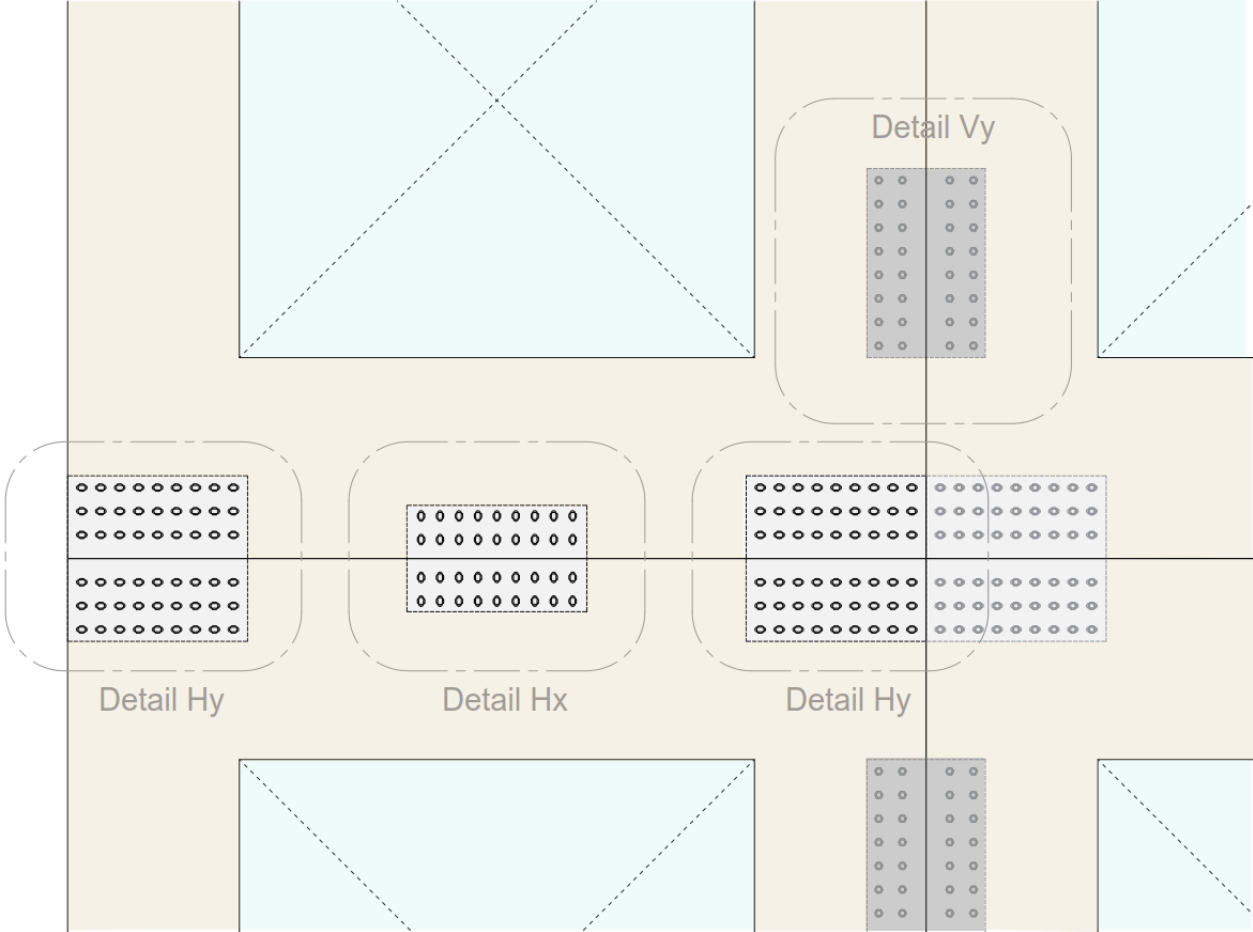
vertical edge

V_x cross-section



A5.2 Detail drawings of the connections at the fifth floor

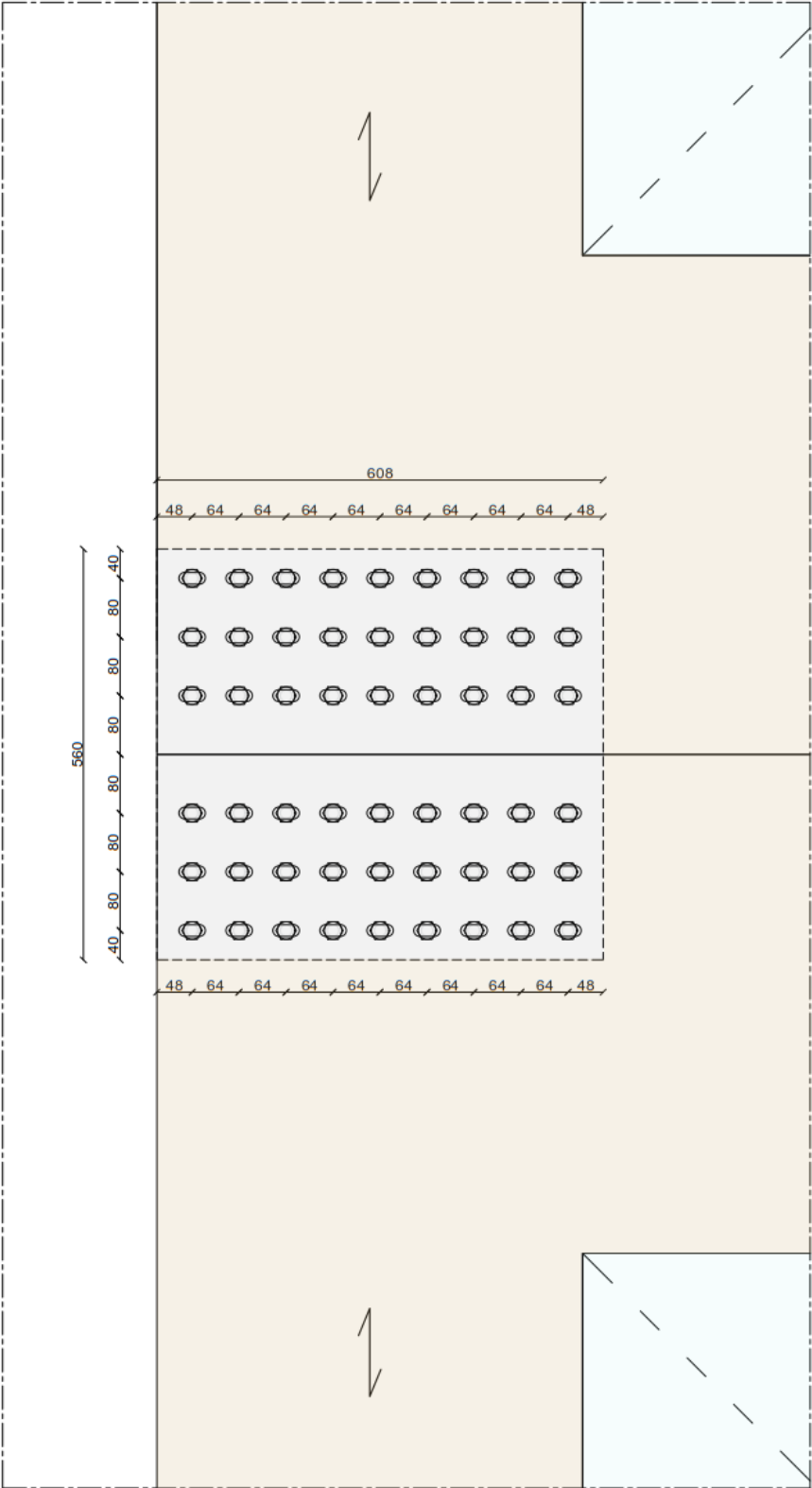
The shear connections on the vertical edge of the CLT panels are similar as those presented for the connections at the foundations for the model of 77,5 meter.



A5.2.1 Hold-down connection

horizontal edge

H_y front view

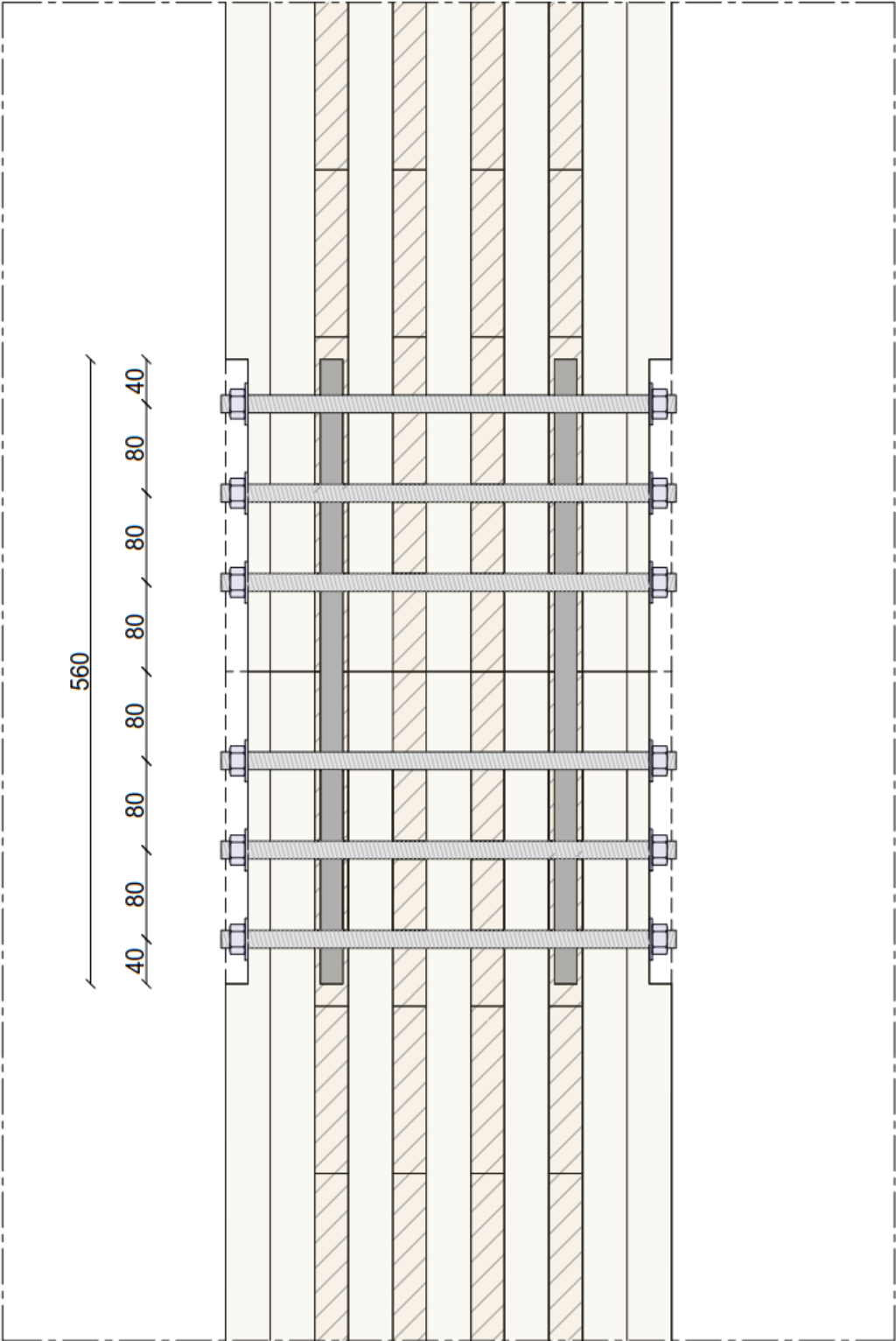


A5.2.2 Hold-down connection

horizontal edge

H_y cross-section

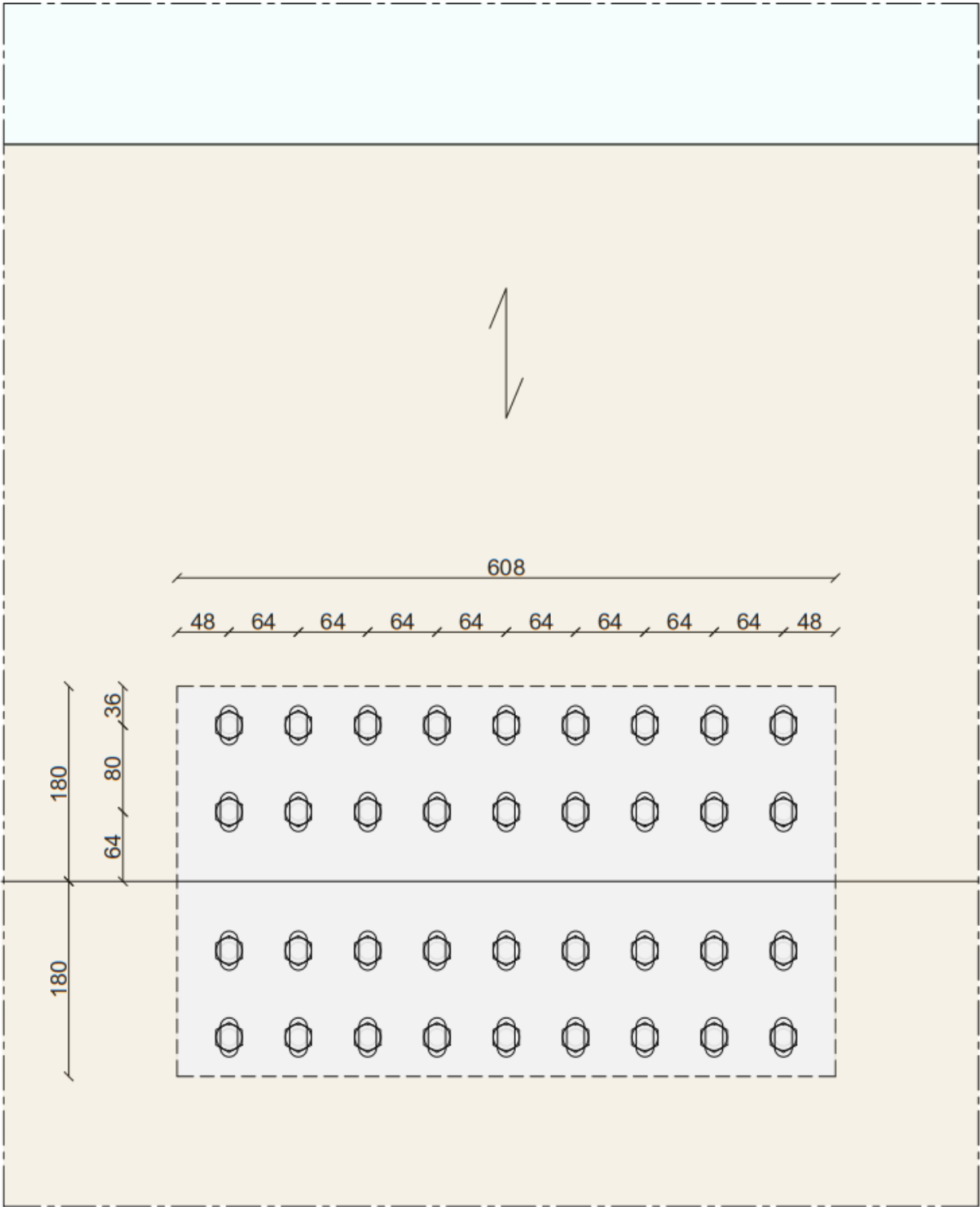
20, 65, 20, 190, 20, 65, 20



A5.2.3 Shear connection

horizontal edge

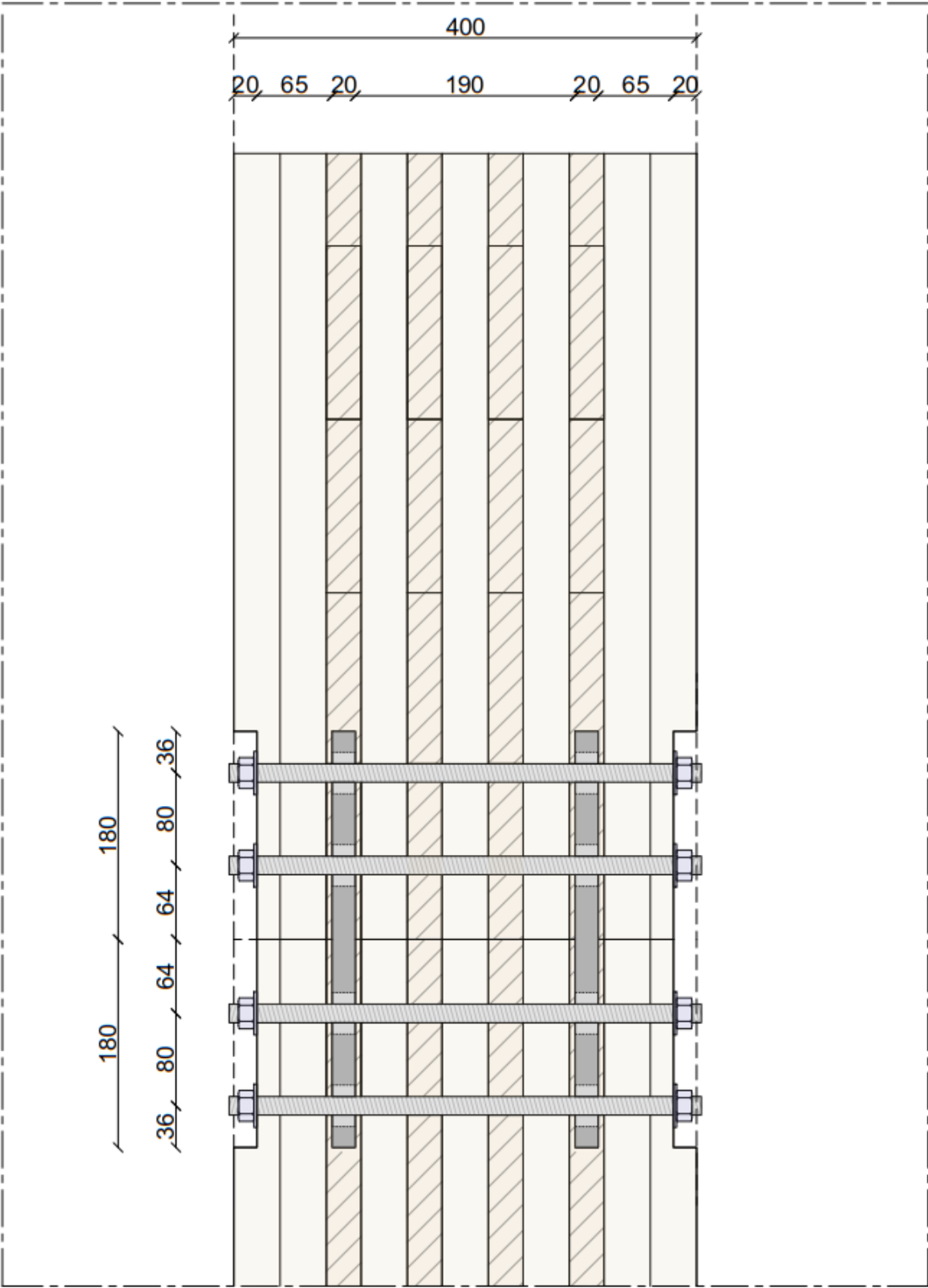
H_x front view



A5.2.4 Shear connection

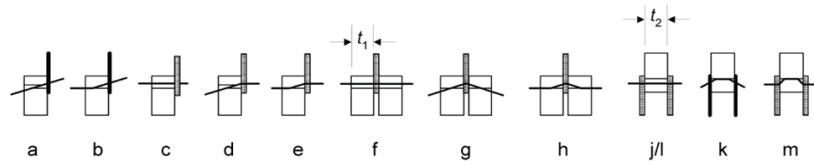
horizontal edge

H_x cross-section



A5.3 Calculation of the bolt resistance of a M16 bolt

$$\begin{aligned} d &:= 16 && \text{mm} \\ f_{u,k} &:= 800 && \text{N/mm}^2 \\ \rho_k &:= 385 && \text{kg/m}^3 \\ \alpha_{\text{degree}} &:= 90 \end{aligned}$$



$$\alpha_{\text{rad}} := \alpha_{\text{degree}} \cdot \frac{\pi}{180} = 1,5708$$

$$f_{h,CLT,k} := \frac{0,035 \cdot (1 - 0,015 \cdot d) \cdot \rho_k^{1,16}}{1,1 \cdot \sin(\alpha_{\text{rad}})^2 + \cos(\alpha_{\text{rad}})^2} = 24,13 \quad \text{N/mm}^2$$

$$M_{Y,k} := 0,3 \cdot f_{u,k} \cdot d^{2,6} = 3,2428 \cdot 10^5$$

$$t_1 := 65 \quad \text{mm}$$

$$t_2 := 190 \quad \text{mm}$$

Axial resistance of a washer M16

$$f_{c,90,k} := 2,5 \quad \text{N/mm}^2$$

$$D_{\text{ext}} := 50$$

$$D_{\text{int}} := 17$$

$$F_{ax,Rk} := \frac{\pi}{4} \cdot (D_{\text{ext}}^2 - D_{\text{int}}^2) \cdot 3 \cdot f_{c,90,k} \cdot 10^{-3} = 13,02 \quad \text{kN}$$

outer part

$$F_{V,Rk,f} := f_{h,CLT,k} \cdot t_1 \cdot d \cdot 10^{-3} = 25,1$$

$$F_{V,Rk,g} := f_{h,CLT,k} \cdot t_1 \cdot d \cdot \left(\sqrt{2 + \frac{4 \cdot M_{Y,k}}{f_{h,CLT,k} \cdot d \cdot t_1^2}} - 1 \right) \cdot 10^{-3} = 16,9$$

$$F_{V,Rk,h} := 2,3 \cdot \sqrt{M_{Y,k} \cdot f_{h,CLT,k} \cdot d} \cdot 10^{-3} = 25,7$$

$$Rope := \min \left(\left[\begin{array}{c} \frac{F_{ax,Rk}}{4} \\ 0,25 \cdot F_{V,Rk,g} \\ 0,25 \cdot F_{V,Rk,h} \end{array} \right] \right) = 3,26$$

$$F_{V,Rd} := \min \left(\left[\begin{array}{c} F_{V,Rk,f} \\ F_{V,Rk,g} + Rope \\ F_{V,Rk,h} + Rope \end{array} \right] \right) \cdot \frac{0,9}{1,3} = 13,93$$

inner part

$$F_{V,Rk,l} := 0,5 \cdot f_{h,CLT,k} \cdot t_2 \cdot d \cdot 10^{-3} = 36,7$$

$$F_{V,Rk,m} := 2,3 \cdot \sqrt{M_{Y,k} \cdot f_{h,CLT,k} \cdot d} \cdot 10^{-3} = 25,7$$

$$Rope_{\text{thick}} := \min \left(\left[\begin{array}{c} \frac{F_{ax,Rk}}{4} \\ 0,25 \cdot F_{V,Rk,m} \end{array} \right] \right) = 3,26$$

$$F_{V,Rd,thick} := \min \left(\left[\begin{array}{c} F_{V,Rk,l} \\ F_{V,Rk,m} + Rope_{\text{thick}} \end{array} \right] \right) \cdot \frac{0,9}{1,3} = 20,07$$

$$F_{V,Rd,tot} := 2 \cdot F_{V,Rd} + 2 \cdot F_{V,Rd,thick} = 68$$

Figure 13, example calculation for double internal steel plate

Table 20, resistance of a bolt in a connection with a single internal steel plate

Panel	t_1	M12		M16		M20	
	[mm]	[kN]		[kN]		[kN]	
LL-190/7s	65	18	Ductile	28	Ductile	38	Ductile
LL-260/7s	100	23	Ductile	33	Ductile	43	Ductile

Table 21, resistance of a bolt in a connection with two external steel plates

Panel	t	M12		M16		M20	
	[mm]	[kN]		[kN]		[kN]	
LL-190/7s	110	24	Brittle	29	Brittle		
LL-260/7s	180	25	Ductile	40	Ductile	55	Brittle
LL-300/9s	220	25	Ductile	40	Ductile	58	Ductile
LL-360/9s	280	25	Ductile	40	Ductile	58	Ductile
LL-400/11s	320	25	Ductile	40	Ductile	58	Ductile

Table 22, resistance of a bolt in a connection with two internal steel plates

Panel	t_1	t_2	M12		M16		M20	
	[mm]	[mm]	[kN]		[kN]		[kN]	
LL-260/7s	40	100	39	Brittle	48	Brittle	x	
LL-300/9s	45	130	41	Ductile	59	Brittle	x	
LL-360/9s	55	170	42	Ductile	67	Ductile	86	Brittle
LL-400/11s	65	190	42	Ductile	68	Ductile	96	Ductile

Table 23, internal stresses in a connection with two internal steel plates

Panel	t_1	t_2	M12		M16		M20	
			σ_{in}	σ_{out}	σ_{in}	σ_{out}	σ_{in}	σ_{out}
			N/mm ²					
	[mm]	[mm]						
LL-260/7s	40	100						
LL-300/9s	45	130	14,1	17,0	16,7	16,7		
LL-360/9s	55	170	12,4	12,8	15,3	16,0	15,4	15,4
LL-400/11s	65	190			13,4	13,2	14,8	15,1

A5.4 Maximum force on bolts of shear key connections on vertical edges of the panels

The maximum force on the bolts of the shear key connections on the vertical edges of the panels is the result of the shear force acting on the connection and the bending moment acting on the connection. The equations to calculate F_{\max} have been presented in the main report and chapter A4.7.

The table below shows the forces acting on the bolts and ultimately the maximum force F_{\max} on the outer bolts. The last column indicates the increase of the force on the bolt due to the additional bending moment. It can be seen that for the connection with two columns of bolts, the forces increase by 52%. Whereas for the connections with one column of bolts, the forces only increase by 12%. This is due to the fact that the bending moment is smaller due to less eccentricity, as well as the lack of a vertical component of the force vector from the bending moment.

The increase of 52% and 12% is constant for all connections of one and two columns of bolts. The increased force on the bolts can also be calculated using a multiplication factor depending on the geometry of the bolts.

Table 24, maximum force on bolt - shear connection vertical edges

Model height	Location	V_{Ed}	e	M_{Ed}	F_m	$F_{m,x}$	$F_{m,y}$	F_v	F_{\max}	$F_{v,Rd}$	F_{\max} / F_v
		<i>kN</i>	<i>m</i>	<i>kNm</i>	<i>kN</i>	<i>kN</i>	<i>kN</i>	<i>kN</i>	<i>kN</i>	<i>kN</i>	
77,5 meter	Foundation	291	0,24	34,9	18,38	18,18	2,60	18,19	27,6	40	1,52
77,5 meter	Fifth floor	250	0,24	30,0	15,79	15,62	2,23	15,63	23,7	40	1,52
62,0 meter	Foundation	219	0,24	26,3	13,83	13,68	1,95	13,69	20,8	40	1,52
62,0 meter	Fifth floor	177	0,12	10,6	11,06	11,06	0	22,13	24,7	40	1,12
46,5 meter	Foundation	153	0,12	9,18	9,56	9,56	0	19,13	21,4	40	1,12
46,5 meter	Fifth floor	112	0,12	6,72	7,00	7,00	0	14,00	15,7	40	1,12
31,0 meter	Foundation	94	0,12	5,64	5,88	5,88	0	11,75	13,1	40	1,12
31,0 meter	Fifth floor	59	0,12	3,54	3,69	3,69	0	7,38	8,2	40	1,12
15,5 meter	Foundation	42	0,12	2,52	2,63	2,63	0	5,25	5,9	29	1,12

A6 Chapter 6 appendices

A6.1 Validation of the model

In order to get a better understanding of the validity of the model, several verifications have been performed. First the structural behavior of the panels has been verified. The top deformation and maximum forces at the foundation are considered for a simplified version of the computer models. The simplified models have their openings removed. All other properties remain the same. The results of the models are then compared to the expected results from theoretical hand calculations.

First the bending and shear deformation at the top are calculated by hand and compared to the computer results. Then the forces in the bottom CLT panels are compared (at half the height of the panels).

The calculations in SCIA for the validation is performed as linear elastic calculations.

A6.1.1 Deformations of the panels

The values used for the calculation are presented below.

Table 25, values for the calculation of the top deflection

Model	Panel	t	t₀	t₉₀	GA_{s,avg}	EI	W
	<i>Type</i>	<i>mm</i>	<i>mm</i>	<i>mm</i>	<i>kN</i>	<i>kNm²</i>	<i>m³</i>
77,5 meter	LL-400/11s	400	280	120	3.045.000	2.264*10 ⁶	19,23

$$GA_s = \frac{5}{6} * 450 * 400 * 20.300 = 3.045.000 \text{ kN} \quad (77)$$

$$EI = 11.600 * \frac{1}{12} * 280 * 20300^3 = 2.264 * 10^6 \text{ kNm}^2 \quad (78)$$

$$W = \frac{1}{6} * 280 * 20300^2 = 19,23 \text{ m}^3 \quad (79)$$

$$w_b = \frac{q_{wind} * h^4}{8 * EI} = \frac{27,1 * 77.500^4}{8 * 2.264 * 10^6} = 54,0 \text{ mm} \quad (80)$$

$$w_s = \frac{q_{wind} * h^2}{2 * GA_s} = \frac{27,1 * 77.500^2}{2 * 3.045.000} = 26,7 \text{ mm} \quad (81)$$

A6.1.2 Forces at the foundation

Not only the top deformation is considered, but also the forces at the foundation are calculated. The theoretical forces are calculated as:

$$n_y = \frac{M_{Ed}}{W} \pm \frac{N_{Ed}}{A} \quad (82)$$

The bending moment on the façade is given in Table 16. Vertical loads for calculating the normal force is the sum of loads from the floor and the self-weight of the façade. These loads are per story height. Depending on whether the maximum compression or tensile forces are calculated, the vertical load has to be calculated with the corresponding safety factors. The values for the model with a height of 77,5 meter are calculated in the equations below. The forces at half the height of the first panel are considered (h=7,75 m) since the connections at the location of the foundation influence the results significantly.

Vertical load on the façade per story is calculated below for maximum compression forces and maximum tensile forces.

$$q_{v,ULS,1} = 1,20 * (14,82 + 2,54 + 0,4 * 4,2) + 1,5 * 4,08 = 28,6 \text{ kN/m}$$

$$q_{v,ULS,2} = 0,9 * (14,82 + 2,54 + 0,4 * 4,2) + 0 * 4,08 = 17,1 \text{ kN/m}$$

$M_{Ed} = 72.411 \text{ kNm}$ at the foundation, but the check is performed at a height of 7,75 m from the foundation, or 69,75 meter from the top. The bending moment at that location is calculated below.

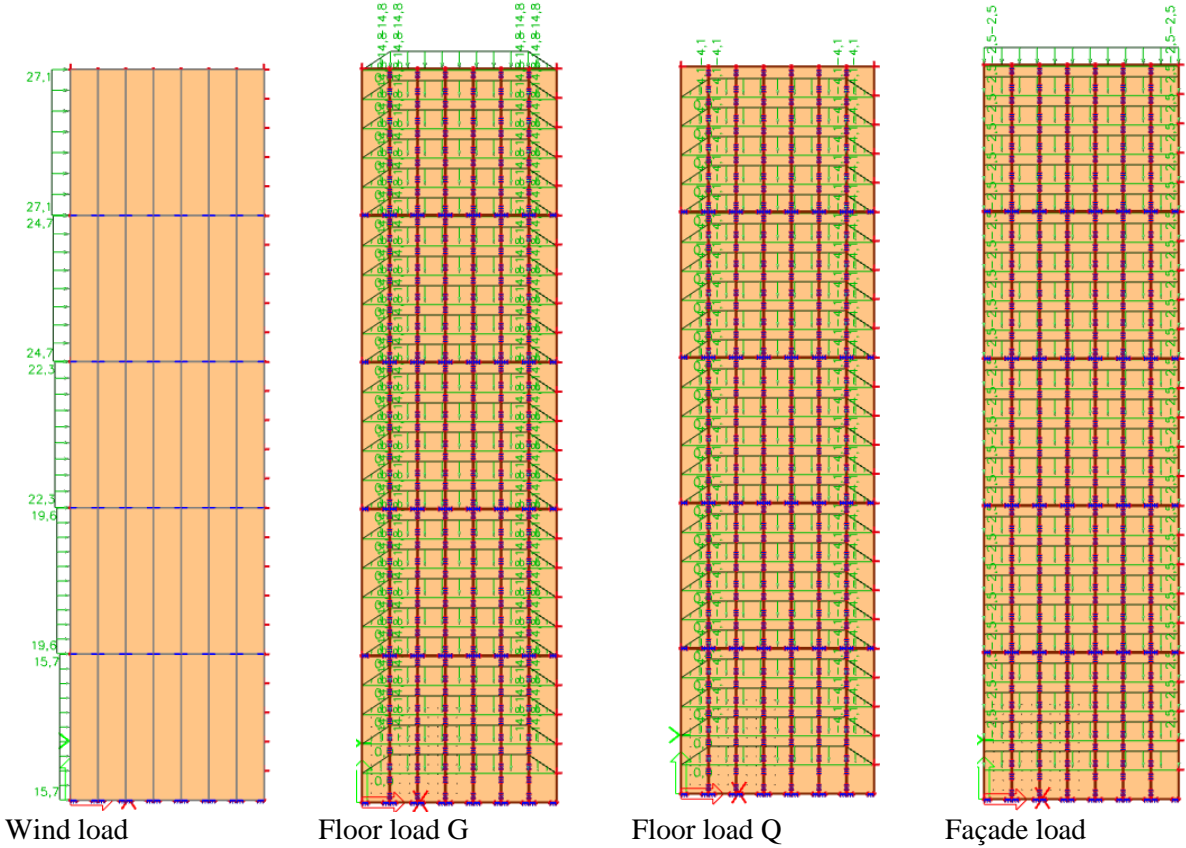
$$M_{Ed} \cong \frac{69,75^2}{77,5^2} * 72.411 = 59.720 \text{ kNm} \quad (83)$$

The force per meter in both compression ($n_{y,c}$) and tension ($n_{y,t}$) can then be calculated. There are 22 stories that introduce loads from the floor and façade. This is then multiplied by a factor of 6/7 to account for the triangular load distribution near the corners.

$$n_{y,c} = \frac{1,5 * 59.720}{\frac{19,23}{0,28}} + 22 * 28,6 * \frac{6}{7} = -1281 + -539 = -1820 \frac{\text{kN}}{\text{m}} \quad (84)$$

$$n_{y,t} = \frac{1,5 * 59.720}{\frac{19,23}{0,28}} - 22 * 17,1 * \frac{6}{7} = 1281 - 294 = 987 \frac{\text{kN}}{\text{m}} \quad (85)$$

The figures below show the loads on the façade.



Wind load

Floor load G

Floor load Q

Façade load

Figure 14, loads on the façade

A6.1.3 Verification conclusions

The calculated deformation is 81 mm by hand whereas the observed deformation in SCIA is 89 mm, as can be seen in Figure 15. The resulting forces per meter in SCIA are -2166 kN/m in compression and +1041 kN/m in tension. Theoretical hand calculations were -1820 kN/m in compression and +987 kN/m in tension.

The compression forces per meter deviate 346 kN/m which is 19%

The tension forces per meter deviate 54 kN/m which is 6%

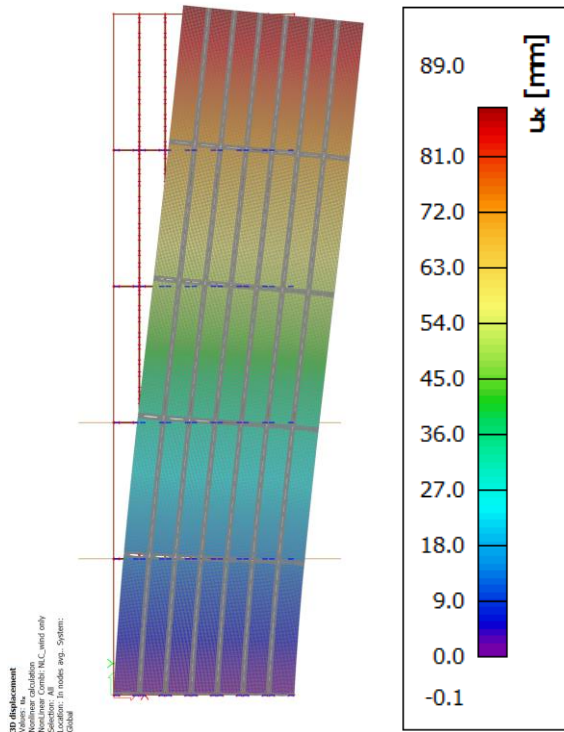


Figure 15, top deformation of the simplified model

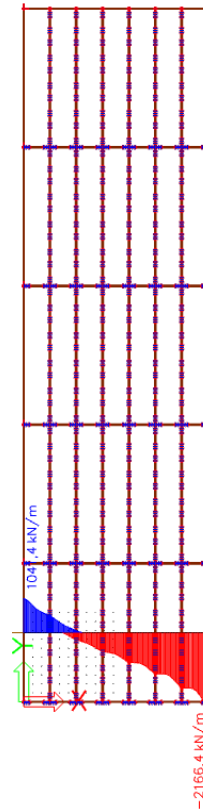


Figure 16, forces on the façade panels

It can be concluded that the computer model gives predictable results for this simplified setup. Adding openings to the panels will increase the complexity of the verification, but the model will still remain functional. It is to be noted that the computer model shows higher forces per meter in both tension and compression. In other words the theoretical hand calculations are an underestimation, both for the forces in the structure as well as the deflection at the top.

The deviations can be explained by the fact that the panels are separated from one another with the steel connection plates already modelled in between the panels. Only the fastener stiffness is missing in the models. This separation makes that there are two factors contributing to the deviations between hand calculations and computer results

- Load introduction from one panel to the panel below is through one such connection plate. This causes peaks in the load introduction in the lower panel.
- Separation of the panels makes that there can be a slight reduction in the cooperation. This causes a reduction of the bending stiffness and moment of resistance. Which in turn increases forces per meter as a result of wind load.

A6.2 Validation of connections (with linear stiffness)

The previous chapter showed that the model yields predictable results when the openings are not included. The behavior of the connections on the horizontal and vertical edges of the CLT panels is the next verification that has been made. Verification of the connections on the horizontal edges is split for sliding and rocking behavior of the connections. Deformation due to rocking was manually calculated as the rigid body rotation of each layer of CLT panels due to elongation of the connections in tension and deformation of the CLT panels in compression. Verification of the connections on the vertical edges is based on the method of Schelling.

The modelled stiffness that is used for the interface between the steel plate and the CLT panels is a linear stiffness (100 kN/mm per meter). This is done in order to make the comparison to the theoretical results simpler. Hold-down connections on the horizontal edge have a rigid behavior in compression. Connections on the vertical edge of the panel result in deformation due to a reduction of bending stiffness. This bending slip is calculated using the method of Schelling. The stiffness of the fasteners is smeared over the height of one story in the theoretical hand calculation.

A6.2.1 Connections on the vertical edge

In order to verify the functioning of the connections on the vertical edges of the panels a linear spring stiffness is added to the model. A connection in the computer model is defined as a steel plate in between the two CLT panels. This was already present in the previous verification. But for this verification, the interfaces between the steel plate and the CLT panels on either side are given a linear spring behavior. In compression it will behave rigid. In tension it will have a tensile stiffness.

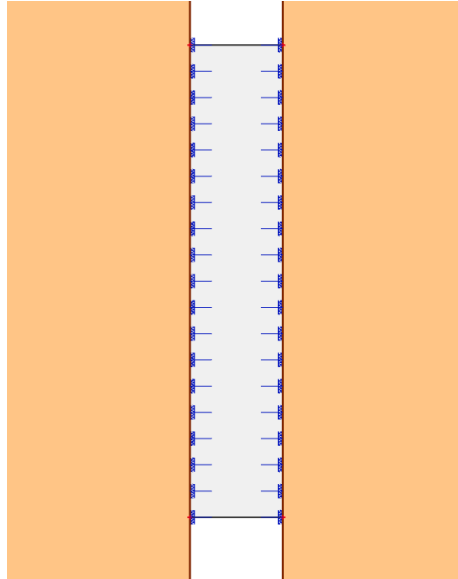


Figure 17, connection as modelled in SCIA (right)

The façade is a cantilever structure which means that the height used in the method of Schelling is twice the height of the façade. Local connections have been modelled, but the method of Schelling assumes a distributed connection. The theoretical hand calculation results are shown in Table 26. One example is presented in chapter A6.2.2.

Table 26, gamma values and top deflection calculated with the method of Schelling

K <i>kN/mm/m</i>	γ_{red} <i>mm</i>	W_{b,slip,theory} <i>mm</i>
1	0,071	708
3	0,155	293
10	0,357	97
30	0,617	33,5
100	0,841	10,2
300	0,941	3,4

In order to compare the spring stiffness in SCIA with a hand calculation, the spring stiffness in SCIA has to be recalculated into an effective stiffness. If the stiffness of the interface between the left CLT panel and the steel plate is 200 kN/mm per meter, the stiffness of the connection is 100 kN/mm per meter (assuming the steel plate is rigid). The connection stiffness is then distributed over the height of one story to get an average stiffness per meter panel. The height of the connection per story is 1,0 meter (2 x 0,5 meter) for this verification. One story has a height of 3,1 meter. So the average stiffness per meter panel is (100 / 3,1 =) 30 kN/mm per meter. Table 27 shows the resulting top deformations for several stiffnesses. The observed top deformation is then reduced by the top deformation of the façade without connection

stiffness (89,0 mm as was found in the previous chapter). This deformation is the additional deformation due to the connections at the vertical edges of the façade.

Table 27, SCIA results; top deflection including bending slip for various stiffness values

K_{ef}	W_{top}	$W_{b,slip,SCIA}$
$kN/mm/m$	mm	mm
1	882,9	794
3	401,3	312
10	209,8	121
30	128,6	39,6
100	102,5	13,5
300	92,8	3,8

Comparing the results from the theoretical hand calculations with the computer results it can be concluded that there is a good correlation between the two methods.

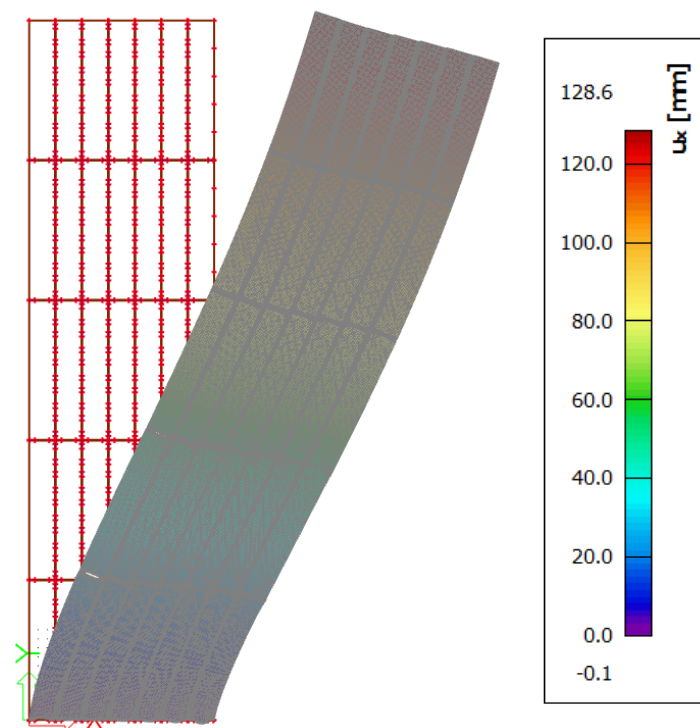


Figure 18, top deformation of the façade for $k_{ef} = 30 \text{ kN/mm}$

A6.2.2 Theoretical hand calculation of bending slip

The equations below show the calculation performed to assess the bending slip deformation for a smeared stiffness $K_{ef} = 30 \text{ kN/mm}$ using the method of Schelling.

$$\begin{aligned} t &:= 280 \\ b &:= 2900 \\ A &:= b \cdot t = 8,12 \cdot 10^5 \\ E &:= 11600 \\ k &:= 30 \\ h &:= 77500 \\ L &:= 2 \cdot h \\ a_1 &:= 3,0 \cdot b = 8700 \\ a_2 &:= 2,0 \cdot b = 5800 \\ a_3 &:= 1,0 \cdot b = 2900 \\ a_4 &:= 0 \end{aligned}$$

$$Y_1 := Y_7$$

$$Y_7 := \frac{(A^2 \cdot E^2 \cdot \mathbf{n}^4 + 4 \cdot A \cdot k \cdot E \cdot L^2 \cdot \mathbf{n}^2 + 3 \cdot k^2 \cdot L^4) \cdot k \cdot L^2}{3 \cdot (A^3 \cdot E^3 \cdot \mathbf{n}^6 + 5 \cdot A^2 \cdot k \cdot E^2 \cdot L^2 \cdot \mathbf{n}^4 + 6 \cdot A \cdot k^2 \cdot E \cdot L^4 \cdot \mathbf{n}^2 + k^3 \cdot L^6)}$$

$$Y_2 := Y_6$$

$$Y_6 := \frac{(A \cdot E \cdot \mathbf{n}^2 + 2 \cdot k \cdot L^2) \cdot k^2 \cdot L^4}{2 \cdot (A^3 \cdot E^3 \cdot \mathbf{n}^6 + 5 \cdot A^2 \cdot k \cdot E^2 \cdot L^2 \cdot \mathbf{n}^4 + 6 \cdot A \cdot k^2 \cdot E \cdot L^4 \cdot \mathbf{n}^2 + k^3 \cdot L^6)}$$

$$Y_3 := Y_5$$

$$Y_5 := \frac{k^3 \cdot L^6}{1 \cdot (A^3 \cdot E^3 \cdot \mathbf{n}^6 + 5 \cdot A^2 \cdot k \cdot E^2 \cdot L^2 \cdot \mathbf{n}^4 + 6 \cdot A \cdot k^2 \cdot E \cdot L^4 \cdot \mathbf{n}^2 + k^3 \cdot L^6)}$$

$$Y_1 = 0,6333$$

$$Y_2 = 0,5725$$

$$Y_3 = 0,5379$$

$$Y_4 := 1$$

$$I_{ef} := \frac{7 \cdot t \cdot b^3}{12} + 2 \cdot Y_1 \cdot t \cdot b \cdot a_1^2 + 2 \cdot Y_2 \cdot t \cdot b \cdot a_2^2 + 2 \cdot Y_3 \cdot t \cdot b \cdot a_3^2 = 1,2046 \cdot 10^{14}$$

$$I := \frac{7 \cdot t \cdot b^3}{12} + 2 \cdot t \cdot b \cdot a_1^2 + 2 \cdot t \cdot b \cdot a_2^2 + 2 \cdot t \cdot b \cdot a_3^2 = 1,9519 \cdot 10^{14}$$

$$Y_{red} := \frac{I_{ef}}{I} = 0,617$$

$$EI_{ef} := E \cdot I_{ef} = 1,3973 \cdot 10^{18} \quad \text{Nmm}^2$$

$$q := 27,1$$

$$\frac{(1 - Y_{red})}{Y_{red}} \cdot \frac{q \cdot h^4}{8 \cdot E \cdot I} = 33,5$$

$$M := 59720 \cdot 10^6 \quad \text{mm}$$

$$N_1 := \frac{Y_1 \cdot E \cdot a_1 \cdot M \cdot t \cdot b}{EI_{ef}} \cdot 10^{-3} = 2218$$

$$N_2 := \frac{Y_2 \cdot E \cdot a_2 \cdot M \cdot t \cdot b}{EI_{ef}} \cdot 10^{-3} = 1337$$

$$N_3 := \frac{Y_3 \cdot E \cdot a_3 \cdot M \cdot t \cdot b}{EI_{ef}} \cdot 10^{-3} = 628$$

Where,

N_1 , N_2 and N_3 are axial forces in the panels 1, 2 and 3.

A6.2.3 Force distribution in the panels

Not only the top deflection is used to verify the connection on the vertical edge. Also the forces on the panels are verified. Forces as a result of wind on the façade have been calculated.

$$n_i = \frac{\gamma * E * a_i * M * t}{EI_{ef}} \quad (86)$$

Where

- n_i is the force per meter width in tension or compression
- γ is the gamma reduction factor of the façade
- E_i is the modulus of elasticity for the considered panel
- a_i is the distance from the center of the panel to the center of the façade
- M is the bending moment on the façade
- EI_{ef} is the bending stiffness of the façade

As already described in chapter A2.2, the method of Schelling does not account for additional bending forces on the individual elements, thus leading to an underestimation of the forces in the elements. A correction based on section force equilibrium has been applied.

Section force equilibrium

The bending moment on the façade is equal to the sum of all bending moments on the panels and the normal forces in each panel multiplied with its distance to the center of the façade.

$$M = \sum_{i=1}^n M_i(x) + \sum_{i=1}^n N_i(x) * a_i \quad (87)$$

M_i is the bending moment on the panel

In case the bending moment on each panel is considered to be equal, the value of this bending moment per panel can be calculated. The axial forces per panel are calculated using equation (89). These are then multiplied with their respective distance to the center in equation (90).

The bending moment due to wind has been calculated at the half-way point of the bottom CLT panel and was found to be 59.270 kNm. The axial force in a panel is calculated as the average force per meter multiplied by the width. The average force per meter is calculated using the equation below from the method of Schelling.

$$M = 59.270 \text{ kNm} \quad (88)$$

$$N_i(x) = n_i * b \quad (89)$$

b is the width of the panel

Writing out equation (87) the bending moment on a single panel $M_i(69,75)$ can be calculated

$$59.270 = 7 * M_i(69,75) + 2 * 2218 * 3 * 2,9 + 2 * 1337 * 2 * 2,9 + 2 * 628 * 2,9 \quad (90)$$

$$59.270 = 7 * M_i(69,75) + 57.745 \quad (91)$$

$$M_i(69,75) = 218 \text{ kNm} \quad (92)$$

The axial forces per meter width can be calculated with equations (93)

$$\Delta n_1 = \frac{M_i}{W_p} = \frac{218}{\frac{1}{6} * 2,9^2} = 155 \text{ kN/m} \quad (93)$$

W_p is the moment of resistance of the panel

n is the number of elements

Conclusions and comparissons

Due to local disturbances at the foundation, forces have been calculated at half the height of the bottom panels. On the left, the normal forces are given for a rigid structure. On the right, the normal forces are given for the structure with a smeared stiffness of 30 kN/mm. Forces presented in the figures below are characteristic forces as a result of wind load on the façade.

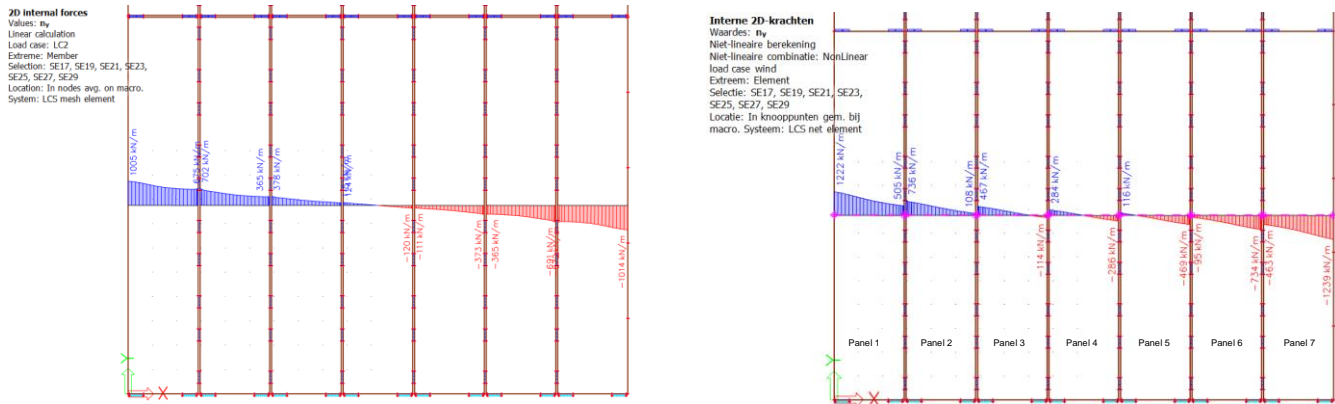


Figure 19, forces in the panels for rigid connections (left) and for connections with stiffness $k_{ef} = 30$ kN/mm (right)

The forces at the panel edges are shown in Table 28 (panels numbered from left to right, for the first four panels). The forces are shown for the model without connection stiffness modelled (rigid, left figure) and the model with a stiffness of $K_{ef} = 30$ kN/mm modelled.

Table 28, average normal forces in the panels

	$N_{1,max}$	$N_{1,min}$	$N_{2,max}$	$N_{2,min}$	$N_{3,max}$	$N_{3,min}$	$N_{4,max}$	$N_{4,min}$
SCIA rigid	1005	675	702	365	378	115	124	-120
SCIA springs $K_{ef}=30$	1222	505	736	108	467	-114	284	-286
Schelling theory Original	943	557	648	266	420	34	193	-193
Schelling theory Adjusted - Member equilibrium	1098	402	803	111	575	-121	348	-348

The computer results for rigid connections are the forces that occur without fastener stiffness included. Which is basically similar to the forces expected on standard beam theory. The results for SCIA springs $k_{ef}=30$ are the results as indicated in the figure. The results of the method of Schelling and the adjusted results are also shown in the figure in dashed lines.

The additional bending moment results in forces in the panels that do indeed more closely resemble the results from the computer model.

The forces in the panels for all four cases have been summarized in the graph below. In yellow, the forces are shown in case no connection stiffness is applied. All other curves indicate forces due to connection stiffnesses. The blue line is the actual force in each panel based on computer results.

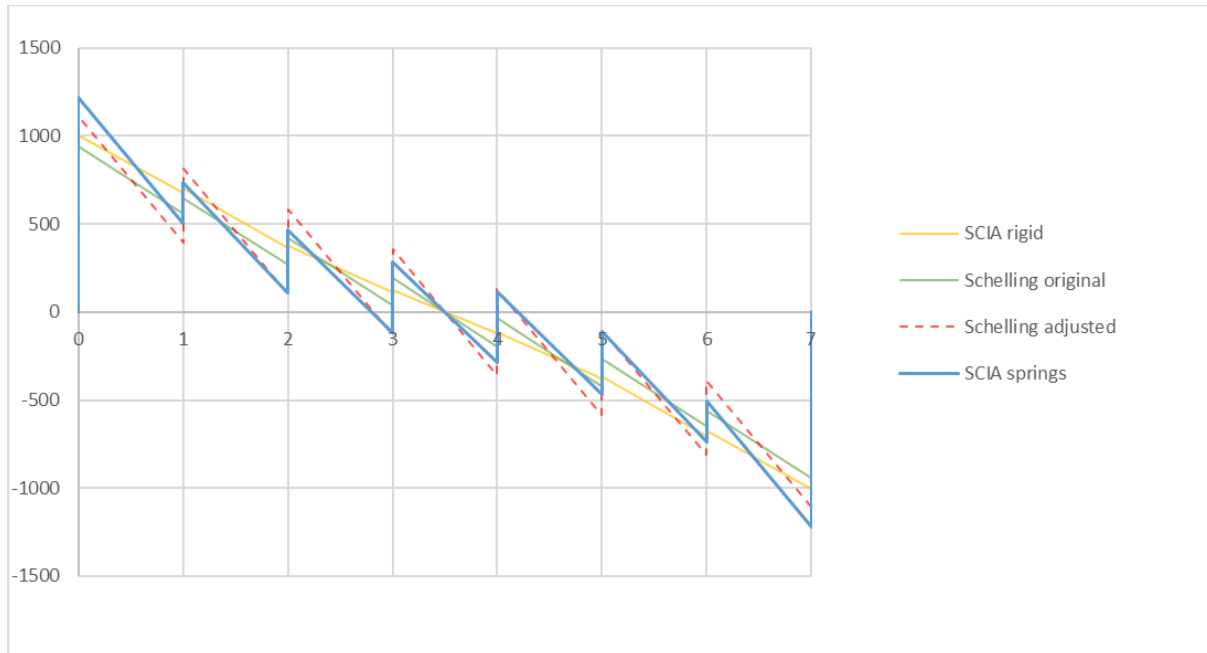


Figure 20, forces in the panels for the method of Schelling

In conclusion

It can be concluded that the adjustment of the method of Schelling leads to a better correlation to the computer results. A good correlation is found for both stiffness and strength behavior of the façade under the influence of connection stiffnesses of connections on the vertical edges of the façade.

A6.2.4 Connections on the horizontal edge - rocking

Rocking deformation is the result of elongation of the connections in tension and decompression of the CLT panels due to compressive forces (Chen and Popovski, 2014). It is assumed that the panels rotate as rigid bodies and that at least half of the width of the façade is in compression.

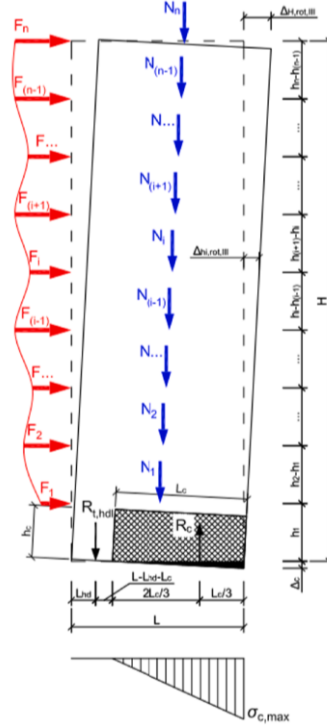


Figure 21, rocking of a CLT panel

The following equations are defined in order to calculate rocking deformation

Vertical equilibrium
$$R_c = R_t + \sum q_v \quad (94)$$

Moment equilibrium
$$M_{Ed} = e_t * R_t + e_v * \sum q_v \quad (95)$$

Where

e_t eccentricity between the resultant tension force and the resultant compression force

e_v eccentricity between the resultant vertical load and the resultant compression force

Compression force
$$R_c = \frac{1}{2} * \sigma_{c,max} * L_c * t \quad (96)$$

$$\sigma_{c,max} = E_{eff} \frac{u_c}{k * L_c} \quad (97)$$

Assuming that the angle caused by tensile forces is equal to the angle caused by compressive forces yields the following equation

$$\tan(\theta_{rock}) = \frac{u_c}{L_c} * \frac{R_t/k_t}{e_t} \quad (98)$$

The presented equations can be solved using iterative procedures (Chen and Popovski, 2014).

Rocking is calculated based on rigid body rotation of the panels. The elongation of the connection and the compression of the timber are calculated. The contribution to the rocking deformation of each level is then this total vertical deformation multiplied by the height to the top, divided by the width of the façade.

$$u_t = \frac{R_t}{k_t} \quad (99)$$

$$u_c = \frac{k * R_c}{t * E} \quad (100)$$

$$\theta_{rocking} = \frac{u_{t,i} + u_{c,i}}{b} \quad (101)$$

$$w_{rocking} = \sum_{i=1}^n \theta_{rocking} * h_i \quad (102)$$

Where

u_t is the elongation of the hold-down connection in tension
 u_c is the compression of the CLT panel under compression forces

There are no tensile forces in the connections at the 15th and 20th floor level. This makes that the rotation of those panels is identical independent of the connection stiffness. Only the connections at the ground floor, 5th floor and 10th floor will elongate under tensile forces. Furthermore, all compressive deformations can be calculated beforehand due to the assumption that the forces do not change under different stiffness values.

The forces in the connections due to wind and vertical load are presented in the table below. These forces are calculated in SLS.

Table 29, forces in the connections (SLS)

	$R_{y,t,0}$	$R_{y,t,5th}$	$R_{y,t,10th}$	$R_{y,t,15th}$	$R_{y,t,20th}$	$R_{y,c,0}$	$R_{y,c,5th}$	$R_{y,c,10th}$	$R_{y,c,15th}$	$R_{y,c,20th}$
	<i>kN</i>	<i>kN</i>	<i>kN</i>	<i>kN</i>	<i>kN</i>	<i>kN</i>	<i>kN</i>	<i>kN</i>	<i>kN</i>	<i>kN</i>
N_{wind}	1054	675	380	169	42	1054	675	380	169	42
$N_{weight,min}$	578	462	347	231	116					
$N_{weight,max}$						578	462	347	231	116
N_{tot}	476	213	33	0	0	1632	1137	727	400	158

Using these values together with the potential elongation of the fasteners per level, the rotation of each row of CLT panels is found.

The compression deformation of the CLT panel can be calculated using equation (100).

$$u_{c,5th} = \frac{k * R_c}{t * E} = \frac{2 * 1137}{280 * 11.600} = 0,70 \text{ mm} \quad (103)$$

This is done at all heights of the connections in the table below.

Table 30, compression deformation at the connection

u_c	Description	Value	
$u_{c,0}$	Compression deformation at foundation level	1,00	mm
$u_{c,5th}$	Compression deformation at 5 th floor	0,70	mm
$u_{c,10th}$	Compression deformation at 10 th floor	0,45	mm
$u_{c,15th}$	Compression deformation at 15 th floor	0,25	mm
$u_{c,20th}$	Compression deformation at 20 th floor	0,10	mm

The tensile elongation of the connections is calculated using equation (99). The stiffness of the connection is half that of the stiffness of the modelled stiffness of the interface. This is similar to the approach for the connections at the vertical edges of the CLT panels. The stiffness of the interface between the steel plate and the CLT panel is 100 kN/mm. Hence the stiffness of the connection is 50 kN/mm. Results are shown in the table below. The resulting rotations of the rigid bodies are also presented in this table.

Table 31, tensile elongation of the connection

K	K_{con}	u_{t,10th}	u_{t,5th}	u_{t,0}	θ_{20th}	θ_{15th}	θ_{10th}	θ_{5th}	θ₀	W_{rocking}
<i>kN/mm per m</i>	<i>kN/mm per m</i>	<i>mm</i>	<i>mm</i>	<i>mm</i>	<i>mrad</i>	<i>mrad</i>	<i>mrad</i>	<i>mrad</i>	<i>mrad</i>	<i>mm</i>
k = 10	k = 5	6,6	42,6	95,2	0,005	0,012	0,347	2,133	4,739	516
k = 100	k = 50	0,66	4,26	9,52	0,005	0,012	0,055	0,244	0,518	58,3
k = 1000	k = 500	0,07	0,43	0,95	0,005	0,012	0,025	0,055	0,096	12,5
k = 10.000	k = 5.000	0,01	0,04	0,10	0,005	0,012	0,022	0,037	0,054	8,0
k = infinite	k = infinite	0	0	0	0,005	0,012	0,022	0,034	0,049	7,4

Computer results have been shown in the table below. The rocking deformation is the increase in deformation at the top due to the connection stiffness. Forces in the connections have been presented as well for the bottom three panels. Based on these values, it can be observed that the tension force in the connection decreases for lower stiffness values. Similarly, the compression force increases.

Table 32, computer results for rocking deformation of various connection stiffnesses

K	u_x	W_{rocking}	R_{y,t,0}	R_{y,t,5th}	R_{y,t,10th}	R_{y,c,0}	R_{y,c,5th}	R_{y,c,10th}
<i>kN/mm per m</i>	<i>mm</i>	<i>mm</i>	<i>kN</i>	<i>kN</i>	<i>kN</i>	<i>kN</i>	<i>kN</i>	<i>kN</i>
k = 10	144,5	54,9	63	9	0	-2152	-1185	-683
k = 100	119,9	30,3	303	83	4	-1889	-1118	-667
k = 1000	101,0	11,4	781	273	47	-1698	-1041	-645
k = 10.000	95,9	6,3	1045	371	84	-1646	-1018	-636
k = infinite	89,6	0	1022	377	82	-1589	-1028	-640

The results for the top deformation have been gathered in the table above. It can be seen that the rocking deformation from computer results does not match that of the theory. This is due to the assumption that

loads on the connections do not change. The force in the connection at the ground floor is only 6% of the assumed force, hence only 6% of the elongation will occur.

When the elongation of the connection is corrected for the observed tensile forces in the computer model an adjusted rocking deformation can be calculated. The elongation of the connections and compression of the CLT panels has been calculated based on the forces found in SCIA from Table 32. Results are presented in the tables below. The resulting rigid body rotation and rocking deformation at the top is also presented.

Table 33, elongation of the connections and compression of the CLT panels based on forces from SCIA

	$U_{t,10th}$	$U_{t,5th}$	$U_{t,0}$	$U_{c,20th}$	$U_{c,15th}$	$U_{c,10th}$	$U_{c,5th}$	$U_{c,0}$
	<i>mm</i>	<i>mm</i>	<i>mm</i>	<i>mm</i>	<i>mm</i>	<i>mm</i>	<i>mm</i>	<i>mm</i>
k = 10	12,6	1,8	0	0,10	0,25	0,42	0,73	1,33
k = 100	6,06	1,66	0,08	0,10	0,25	0,41	0,69	1,16
k = 1000	1,56	0,55	0,09	0,10	0,25	0,40	0,64	1,05
k = 10.000	0,21	0,07	0,02	0,10	0,25	0,39	0,63	1,01
k = infinite	0	0	0	0,10	0,25	0,39	0,63	0,98

Table 34, rotation of rigid bodies and resulting rocking deformation at the top

	θ_{20th}	θ_{15th}	θ_{10th}	θ_{5th}	θ_0	$W_{rocking}$
	<i>mrاد</i>	<i>mrاد</i>	<i>mrاد</i>	<i>mrاد</i>	<i>mrاد</i>	<i>mm</i>
k = 10	0,005	0,012	0,641	0,125	0,065	43,1
k = 100	0,005	0,012	0,319	0,118	0,069	28,0
k = 1000	0,005	0,012	0,098	0,063	0,070	14,3
k = 10.000	0,005	0,012	0,031	0,040	0,066	9,5
k = infinite	0,005	0,012	0,021	0,036	0,065	8,7

This adjusted rocking deformation is a better estimate of the actual rocking deformation in SCIA.

In conclusion

It is found that the tensile forces in the connections highly depend on the stiffness of the connections. This implies that a simplified theoretical hand calculation can only be performed for connections with a relative large stiffness. Otherwise the forces calculated in the connections will be a significant overestimation of the actual forces, leading to an overestimation of the elongation of that connection. This in turn results in large rocking deformations that have not been observed in the computer model.

Calculating the rocking deformation by hand with the use of forces from the computer model shows that the method can predict rocking deformations reasonably accurate, but that there is a need to use the actual tensile forces in the connection.

A6.2.5 Connections on the horizontal edge – sliding

The sliding deformation is calculated by the equation below

$$w_{sl} = \frac{(q_{wind} - \mu_F * q_{weight}) * h * n}{2 * b * K_{ser}} \quad (104)$$

Where

h	is the total height of the structure	m
n	is the number of sliding surfaces along the height	-
b	is the total width of the structure	m
k _{ser}	is the stiffness of the fastener group	kN/mm

A single connection has two surfaces or interfaces that have a stiffness to model the bolt stiffnesses of one side of the connection. Each with an assumed stiffness of 100 kN/mm. Except at the foundation, where only one surface with a stiffness is modelled. A total of 9 surfaces of 100 kN/mm are modelled over the height. Over the width of the façade 14 connections each with a width of 0,58 meter have been modelled. This in total leads to a slip deformation of 11,6 mm.

$$w_{sl} = \frac{(27,1 - 0) * 77,5 * 9}{2 * 14 * 0,58 * 100} = 11,6 \text{ mm} \quad (105)$$

This is compared to results from SCIA. Here a top deformation was found of 102,4 mm, whereas the top deformation without sliding connection stiffness was found to be 89,0 mm. This difference of 13,4 mm is the result of sliding deformation. Hence the sliding behavior is acceptable.

3D displacement
 Values: u_x
 Nonlinear calculation
 NonLinear Combi: NCq_SLS
 Selection: All
 Location: In nodes avg.. System:
 Global

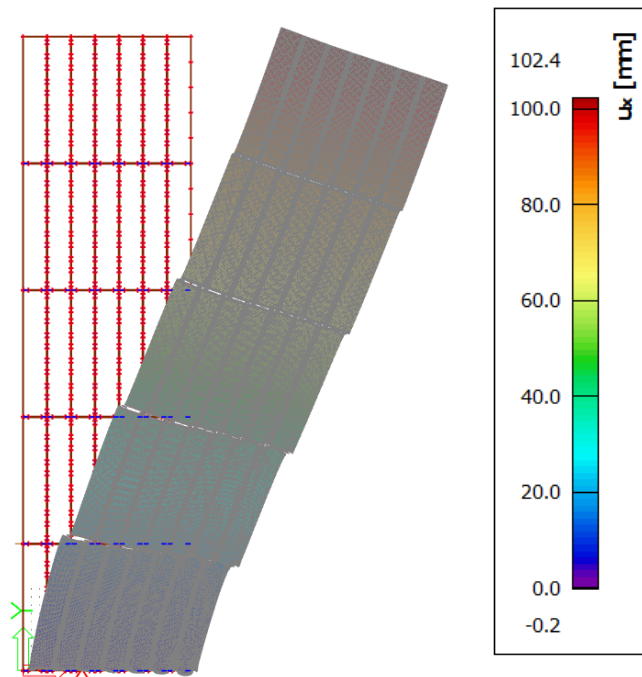


Figure 22, top displacement in SCIA for a model with only connections deforming under sliding

A6.3 Modelling of the transversal façade

The effective width has been calculated using an equation presented by Chiewanichakorn et al. (2004).

$$b_{eff} = \frac{\int_{\frac{1}{2}b}^b n_y}{n_{y,max}} = \frac{0,5 * R_y}{n_{y,max}} \quad (106)$$

A simplified model was made of the transversal façade consisting of nine CLT panels next to one another. On the edge panels a distributed vertical load of 100 kN/m has been applied. The figure below shows the maximum force per meter on the CLT façade at a height of 3,1 meter from the foundation, which is 1483 kN/m. A total force of 3100 kN acts on the structure. Which results in an effective width of 1,0 meter. Values for other heights are presented in Table 35.

Interne 2D-krachten

Waardes: n_y
 Lineaire berekening
 Belastingsgeval: LC8
 Extreem: Element
 Selectie: SE183, SE184, SE187,
 SE188, SE191, SE192, SE195..SE197
 Locatie: In knooppunten gem. bij
 macro. Systeem: LCS net element

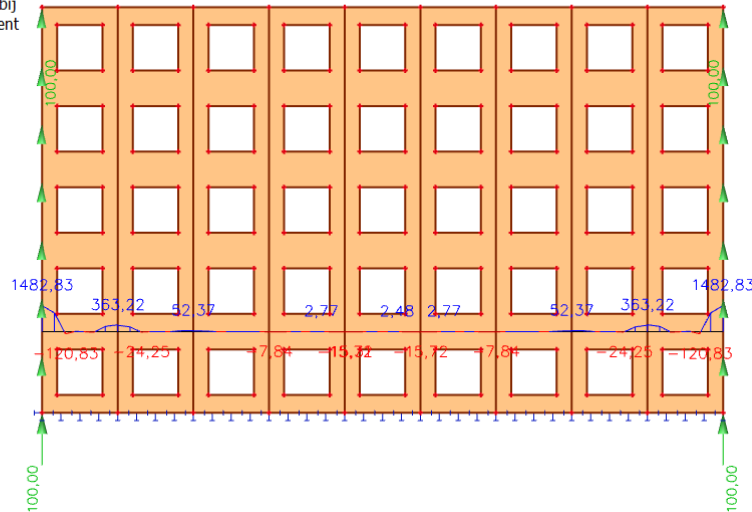


Figure 23, force n_y per meter on the façade

Table 35, effective width of the transversal façade

Model	R_y <i>kN</i>	$n_{y,max}$ <i>kN/m</i>	b_{eff} <i>m</i>	Percentage	b_{eff} applied <i>m</i>
15,5 meter	3100	1483	1,0	20%	1,1
31,0 meter	6200	2143	1,4	28%	1,3
46,5 meter	9300	2533	1,8	35%	2,0
62,0 meter	12.400	2864	2,2	41%	2,7
77,5 meter	15.500	3185	2,4	47%	3,4

The applied effective width deviates from the calculated effective width. This is due to the fact that initially a different force on the structure was applied in an earlier calculation. This resulted in a different effective width, which was then modelled in SCIA. In hindsight this approach was deemed unsuitable and was adjusted to be more accurate. However, this was not altered in the model due to time constraints.

A7 Chapter 7 appendices

A7.1 Theoretical top deformation including connection stiffness

The computer results will be compared to theoretical results. To do so, the top deformation of the model of 77,5 meter is calculated in this chapter. The contribution of each deformation component is calculated for the actual applied connection that has been presented in the previous chapters.

The deformation of the façade structure without connections was calculated in chapter A4 and found to be 218 mm.

The connection stiffness for the theoretical deformation is calculated using table 14 from chapter 5.4. The k_{ser} value used for hand calculations cannot equal the multi-linear load-displacement curve used in the computer model. Hence the multi-linear curve has to be simplified by taking an average stiffness. This stiffness is 60% of k_{ser} as indicated with the red line in the figure below, without including the initial slip.

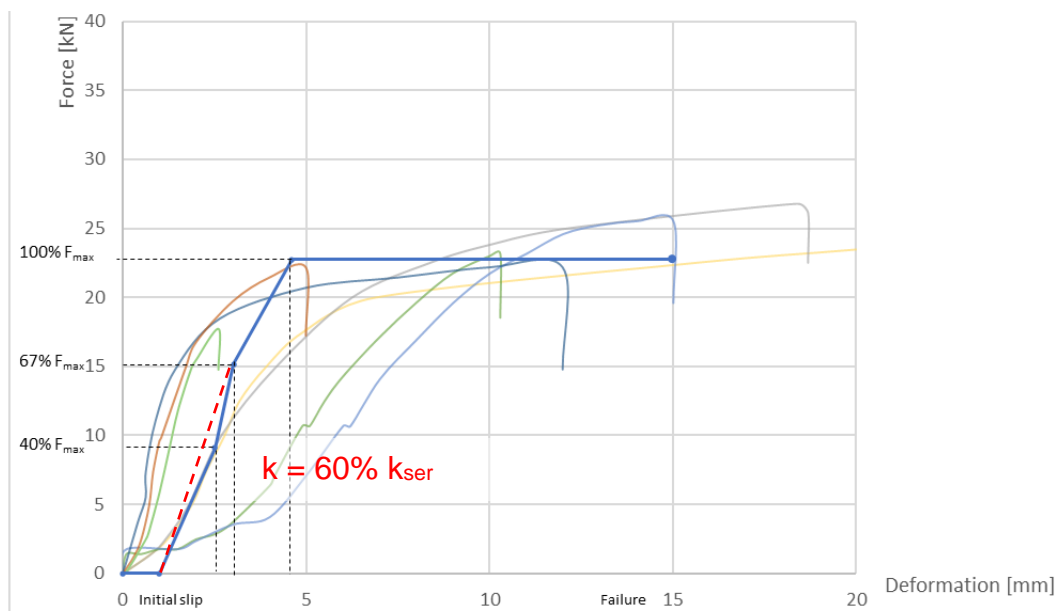


Figure 24, non-linear load-deformation curve for a multiple fastener connection

Sliding

The sliding deformation is calculated below. The number of sliding surfaces for the model of 77,5 meter is 9. There are seven connections that each have a stiffness of 768 kN/mm.

$$w_{sliding} = \frac{q_{wind} * h * n}{2 * n_{con} * K_{ser}} = \frac{27,1 * 77,5 * 9}{2 * 7 * 514} = 2,6 \text{ mm}$$

Rocking

The rocking deformation is calculated below. The stiffness of the hold-down connection is 2215 kN/mm at the foundation and 665 kN/mm for all other hold-down connections at higher levels (which is half of the $k_{ser,ef}$ value found above of 1329 kN/mm as this is the stiffness per side of the connection.)

It is expected that the forces on the connections will reduce due to the stiffness of the connections. This effect will not be included in the calculation of the rocking deformation.

$$q_{wind} = 27,1 \text{ kN/m}$$

$$q_{weight} = 14,82 + 2,54 + 3,44 = 20,8 \text{ kN/m per story}$$

Table 36, calculation of the rocking deformation

Connection location	M_{Ek}	N_{Ek}	$n_{y,wind}$	$n_{y,c}$	$n_{y,t}$	b_t	b_c	ΔL	u_c	θ	a_{top}	w_r
	kNm	kN/m	kN/m			m	m	mm	mm	mrad	m	mm
Twentieth floor	<i>No tension, so no rocking contribution</i>										15,5	
Fifteenth floor	12.733	208	455	663	247	5,5	14,8	0,64	0,24	0,04	31,0	1,34
Tenth floor	27.857	312	995	1307	683	7,0	13,3	1,77	0,47	0,11	46,5	5,13
Fifth floor	48.014	416	1715	2131	1299	7,7	12,6	3,37	0,76	0,20	62,0	12,6
Foundation	72.411	520	2586	3106	2066	8,1	12,2	1,61	1,11	0,13	77,5	10,4
											Total	29,5

The rocking deformation is found to be

$$w_{rocking} = 29,5 \text{ mm}$$

Additional bending deformation - Schelling

Reduction of the bending stiffness results in additional bending deformation that is calculated using the method of Schelling. The stiffness value is a smeared value of the connection stiffness. This value is halved since it is the bolt stiffness on both sides of the steel plate. There are two connections per story.

$$k_{ser} = 2 * \frac{128}{3,10} = 82,8 \frac{kN}{mm} \text{ per story}$$

The additional deformation due to reduced bending stiffness is an additional deformation that can be considered as a percentage of the calculated bending deformation. The calculation of the γ_{red} value is presented on the next page.

$$w_{schelling} = \frac{1 - \gamma_{red}}{\gamma_{red}} * w_{bending} = 0,23 * 132 = 30,0 \text{ mm}$$

The total contribution of the connection stiffness to the deformation is the sum of the components

$$w_{stiffness} = w_{sliding} + w_{rocking} + w_{schelling} = 2,6 + 29,5 + 30,0 = 62 \text{ mm}$$

Adding this to the deformation of the structure, the total theoretical deformation is found to be

$$w_{top} = 218 + 62 = 280 \text{ mm}$$

Calculation of the additional bending deformation

$$t := 280$$

$$b := 2900$$

$$A := b \cdot t = 8,12 \cdot 10^5$$

$$E := 11600$$

$$k := 82,9$$

$$h := 77500$$

$$L := 2 \cdot h$$

$$a_1 := 3,0 \cdot b = 8700$$

$$a_2 := 2,0 \cdot b = 5800$$

$$a_3 := 1,0 \cdot b = 2900$$

$$a_4 := 0$$

$$Y_1 := Y_7$$

$$Y_7 := \frac{\left(A^2 \cdot E^2 \cdot \pi^4 + 4 \cdot A \cdot k \cdot E \cdot L^2 \cdot \pi^2 + 3 \cdot k^2 \cdot L^4 \right) \cdot k \cdot L^2}{3 \cdot \left(A^3 \cdot E^3 \cdot \pi^6 + 5 \cdot A^2 \cdot k \cdot E^2 \cdot L^2 \cdot \pi^4 + 6 \cdot A \cdot k^2 \cdot E \cdot L^4 \cdot \pi^2 + k^3 \cdot L^6 \right)}$$

$$Y_2 := Y_6$$

$$Y_6 := \frac{\left(A \cdot E \cdot \pi^2 + 2 \cdot k \cdot L^2 \right) \cdot k^2 \cdot L^4}{2 \cdot \left(A^3 \cdot E^3 \cdot \pi^6 + 5 \cdot A^2 \cdot k \cdot E^2 \cdot L^2 \cdot \pi^4 + 6 \cdot A \cdot k^2 \cdot E \cdot L^4 \cdot \pi^2 + k^3 \cdot L^6 \right)}$$

$$Y_3 := Y_5$$

$$Y_5 := \frac{k^3 \cdot L^6}{1 \cdot \left(A^3 \cdot E^3 \cdot \pi^6 + 5 \cdot A^2 \cdot k \cdot E^2 \cdot L^2 \cdot \pi^4 + 6 \cdot A \cdot k^2 \cdot E \cdot L^4 \cdot \pi^2 + k^3 \cdot L^6 \right)}$$

$$Y_1 = 0,8233$$

$$Y_2 = 0,7926$$

$$Y_3 = 0,7746$$

$$Y_4 := 1$$

$$I_{ef} := \frac{7 \cdot t \cdot b^3}{12} + 2 \cdot Y_1 \cdot t \cdot b \cdot a_1^2 + 2 \cdot Y_2 \cdot t \cdot b \cdot a_2^2 + 2 \cdot Y_3 \cdot t \cdot b \cdot a_3^2 = 1,5907 \cdot 10^{14}$$

$$I := \frac{7 \cdot t \cdot b^3}{12} + 2 \cdot t \cdot b \cdot a_1^2 + 2 \cdot t \cdot b \cdot a_2^2 + 2 \cdot t \cdot b \cdot a_3^2 = 1,9519 \cdot 10^{14}$$

$$Y_{red} := \frac{I_{ef}}{I} = 0,815$$

$$EI_{ef} := E \cdot I_{ef} = 1,8452 \cdot 10^{18} \quad \text{Nmm}^2$$

$$w_b := 132$$

$$w_{Schelling} := \frac{(1 - Y_{red})}{Y_{red}} \cdot w_b = 30$$

Theoretical top deformation including connection stiffness - results

The results for all heights have been calculated in a similar way and shown below.

Table 37, theoretical top deformation for the different heights of the façade

Model	h	q_k	panel	t₀	t	EI	GA_s	∑EI_p	w_{façade}	w_{sl}	w_r	w_{b,slip}	w_{tot}
	<i>m</i>	<i>kN/m</i>		<i>mm</i>	<i>mm</i>	<i>x10¹⁵</i> <i>Nmm²</i>	<i>x10⁶</i> <i>N</i>	<i>x10¹⁵</i> <i>Nmm²</i>	<i>mm</i>	<i>mm</i>	<i>mm</i>	<i>mm</i>	<i>mm</i>
15,5 meter	15,5	15,7	LL-190/7s	150	190	495	959	0,903	4,92	0,1	0,1	1,2	6
31,0 meter	31	19,6	LL-260/7s	200	260	660	1312	1,209	20,1	0,5	0,7	6,6	28
46,5 meter	46,5	22,3	LL-400/11s	280	400	923	2019	1,690	39,8	1,3	5,2	17,3	64
62,0 meter	62	24,7	LL-400/11s	280	400	923	2019	1,690	100	2,5	13,2	34,6	150
77,5 meter	77,5	27,1	LL-400/11s	280	400	923	2019	1,690	218	2,6	29,5	30,0	280

A7.2 Theoretical top deformation including connection stiffness and slip

Adding an additional slip to the non-linear load-displacement curve results in additional deformations of the top that have to be calculated differently than the theory presented before.

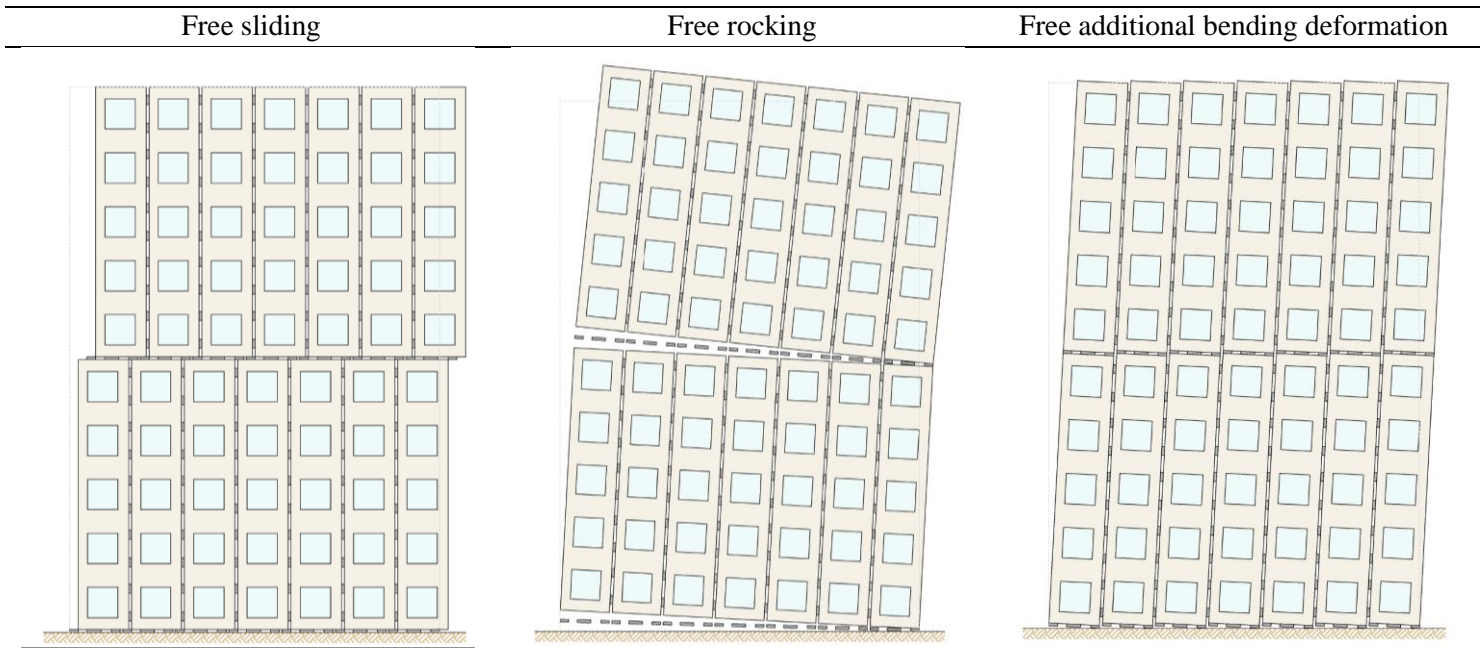


Figure 25, overview of deflection components due to free initial slip in the connections

Sliding slip

Sliding slip deformation is the sum of the initial slip of each shear plane. The model of 77,5 meter has 9 shear planes, which makes that the deformation is

$$w_{sliding,slip} = n * slip = 9 * 1,0 = 9,0 \text{ mm}$$

Rocking slip

Rocking slip is the sum of the top deflection contributions of rigid body rotation of each layer of the façade. This rigid body rotation of a single layer is the result of the elongation of the connection (in this case free slip) multiplied by the ration width over distance to the top. Provided that the connection is in tension. Otherwise, no slip will occur.

$$w_{rocking,slip} = \frac{h_i}{b} * slip$$

Table 38, rocking deformation (rigid body rotation) as a result of free slip

Connection location	b	Distance to top	ΔL_{con}	w_r
	m	m	mm	mm
Twentieth floor				0
Fifteenth floor	20,3	31,0	2,0	3,1
Tenth floor	20,3	46,5	2,0	4,6
Fifth floor	20,3	62,0	2,0	6,1
Foundation	20,3	77,5	1,0	3,8
Total				17,6

$$w_{rocking,slip} = 17,6 \text{ mm}$$

Additional bending deformation - Schelling

Top deformation due to slip in the shear keys on the vertical edges of the panels is the result of rigid body rotation.

$$w_{Schelling,slip} = 2 * slip * \frac{h}{b_{panel}} = 2 * 1,0 * \frac{77,5}{2,9} = 53,4 \text{ mm}$$

Total deformation

The total contribution of the connection slip to the deformation is the sum of the components

$$w_{slip} = w_{sliding,slip} + w_{rocking,slip} + w_{Schelling,slip} = 9,0 + 17,6 + 53,4 = 80 \text{ mm}$$

Adding this to the deformation of the structure, the total theoretical deformation is found to be

$$w_{top} = 280 + 80 = 360 \text{ mm}$$

A similar calculation for the other modelled heights gives the following overview.

Table 39, top deformations of the individual slip components

Model	$k_{sliding}$	$k_{holddown}$	$k_{Schelling}$	$W_{sliding}$	$W_{rocking}$	$W_{schelling}$	$W_{sliding,sl}$	$W_{rocking,sl}$	$W_{schelling,sl}$
	<i>kN/mm</i>	<i>kN/mm</i>	<i>kN/mm</i>	<i>mm</i>	<i>mm</i>	<i>mm</i>	<i>mm</i>	<i>mm</i>	<i>mm</i>
15,5 meter	128	128	128	0,1	0,1	1,2	1,0	0,8	10,7
31,0 meter	128	128	128	0,5	0,7	6,6	3,0	3,1	21,4
46,5 meter	514 257	514 257	128	1,3	5,2	17,3	5,0	6,9	32,1
62,0 meter	514 257	771 514	257 128	2,5	13,2	34,6	7,0	12,2	42,8
77,5 meter	514	1285 771	257	2,6	29,5	30,0	9,0	17,6	53,4

The stiffness values for the models of 46,5 meter and 62,0 meter differ for the bottom panels and the panels starting from the 5th floor and onwards. That is why there are two values in the table. Where the highest value is the stiffness value of the connection at the foundation level and the lowest value is the stiffness of the other connections.

Table 40, top deformations of the façade with and without connection stiffnesses

Model	W_{rigid}	$W_{springs}$	$W_{springs+slip}$
	<i>mm</i>	<i>mm</i>	<i>mm</i>
15,5 meter	4,92	6,32	18,8
31,0 meter	20,1	27,9	55,4
46,5 meter	39,8	63,6	108
62,0 meter	99,6	150	212
77,5 meter	218	280	360

In conclusion

The theoretical top deformations indicate an increase of the top deformation according to the values in Table 40. The increase of the top deformation when connection stiffness is included without initial slip shows an even increase for all heights. The deformation increase of the model of 62,0 meter is relatively larger than that of the model of 77,5 meter. Which is explained by the fact that the model of 77,5 meter has larger connections which have a higher stiffness.

The additional top deformation of the façades including initial slip of the connection shown that for all heights the top deformation increases significantly. The relative increase of the top deformation of the model of 15,5 meter is a factor 3, which is very high. This increase is primarily the result of the additional bending deformation.

A7.3 Addition of a concrete core

The addition of a concrete core (modelled as a concrete wall of 300 mm with cracked concrete properties) will have a beneficial influence on the strength and stiffness behavior of the CLT façade.

- The deformation of the structure is reduced
- The forces on the façade are reduced

A7.3.1 Reduced deformation of the structure

The deformation of the structure is reduced as the concrete core has a bending stiffness and shear stiffness that resist lateral deformation. Especially the shear deformation is reduced given the fact that the shear stiffness of concrete is significantly higher than that of CLT (4167 vs 450 N/mm²).

For the model of 77,5 meter

EI_{CLT}	923	$\cdot 10^{15}$	Nmm ²	(88%)
EI_{core}	128	$\cdot 10^{15}$	Nmm ²	(12%)
$EI_{combined}$	1051	$\cdot 10^{15}$	Nmm ²	
$GA_{s,CLT}$	2019	$\cdot 10^3$	kN	(27%)
$GA_{s,core}$	5556	$\cdot 10^3$	kN	(73%)
$GA_{s,combined}$	7575	$\cdot 10^3$	kN	

It is assumed that the bending deformation and deformation due to bending slip (method of Schelling) is reduced by 12% as the bending stiffness of the structure is increased by that same amount. Shear deformation and deformation of the piers is reduced by 73%. The overall reduction of the top deformation is found to be 29%. The table below shows one example of the calculation of the top deformation for the model of 77,5 meter with an additional core. Chapter A7.5 contains a complete overview.

Table 41, exemplary calculation for the façade of 77,5 meter with an additional concrete wall

Model	$W_{bending}$ $\frac{q_{wind} * h^4}{8 * EI_{red}}$	W_{shear} $\frac{q_{wind} * h^2}{2 * GA_s}$	W_{piers} $T_n * \frac{q_{wind} * h_{story} * h_{pier,eff}^3}{12 * \sum EI_{pier}}$	$W_{Schelling}$ <i>Method of Schelling</i>	W_{tot}
CLT	132	40,3	19,1	26,1	218
CLT+core	116	10,8	5,1	23,0	155

A7.3.2 Reduced forces of the façade

The forces on the structure are reduced due to the additional concrete core that has been added to the structure. Bending forces on the façade can be reduced by 12%.

The shear forces on the façade can be reduced by 73% by adding a concrete stability element to the structure. This is an important design option given the fact that the panel dimensions for the models of 15,5; 31,0 and 46,5 meter were governed by the shear forces. When 27% of the shear forces in the corners is calculated, it is found that the thickness of the CLT panels can significantly be reduced.

When different type (smaller thickness) of CLT panels are used, the shear force on the panel will be lower as the contribution of the shear stiffness of that panel to the total shear stiffness of the structure is lower. This makes that the smaller the thickness of the CLT panels, the lower the actual shear force on the panel, as the core will resist more shear force.

Table 42, required CLT panels and corresponding unity checks, adjusted for concrete core

Model	Panel <i>type</i>	Unity checks					
		$n_{y,t}$	$n_{y,c}$	n_{xy}	$n_{xy,corner}$	$n_{xy,reduced}$	$n_{xy,corner,red}$
15,5 meter	LL-190/7s	0,00	0,20	0,42	0,63	0,10	0,15
31,0 meter	LL-190/7s	0,08	0,50	0,95	1,43	0,23	0,35
31,0 meter	LL-260/7s	0,06	0,33	0,64	0,96	0,20	0,30
46,5 meter	LL-190/7s	0,36	0,92	1,56	2,34	0,38	0,57
46,5 meter	LL-260/7s	0,27	0,62	1,04	1,56	0,32	0,48
46,5 meter	LL-300/9s	0,22	0,52	1,04	1,56	0,34	0,51
46,5 meter	LL-400/11s	0,19	0,43	0,52	0,78	0,21	0,32
62,0 meter	LL-300/9s	0,52	0,83	1,48	2,22	0,49	0,74
62,0 meter	LL-360/9s	0,52	0,83	0,74	1,11	0,28	0,42
62,0 meter	LL-400/11s	0,45	0,70	0,74	1,11	0,30	0,45
77,5 meter	LL-400/11s	0,85	1,06	0,99	1,49	0,40	0,60

A7.4 Theoretical contribution of the effective width

The transversal walls can have a contribution on the strength and stiffness behavior of the CLT façade as well. Research has been done on the potential contribution of these walls. The effective width of the transversal walls itself is fully researched, only the effect that a certain effective width may have on the structure.

- The deformation of the structure is reduced
- The forces on the façade are different, not necessarily reduced

A7.4.1 Reduced deformation of the structure

The transversal façades will increase the bending stiffness of the overall structure. It will not have a significant influence on the shear stiffness, nor the deformation of the lintels and piers.

The bending stiffness of the overall structure is reduced by the connection stiffness according to the method of Schelling. This method was previously derived for 7 elements. With the addition of transversal walls, this method is to be derived for a structure of 9 elements as well. This derivation is shown in chapter A7.4.3. Special attention is required for the outer elements as they have a different distance a_i . Subsequently the boundary conditions have been adjusted.

A comparison of the effective gamma-factor for a façade with and without a transversal panel (width of 2,9 meter) has been made. The graph below on the left shows that the effective gamma-factor for the façade with effective width is slightly less than the values that would be found for the façade without the influence of the transversal walls.

Looking at the bending stiffness of the façade including effective width a significant increase can be found. An increase of $1,94 \cdot 10^{18} \text{ Nmm}^2$ is calculated with equation (107). The bending stiffness then becomes $2,86 \cdot 10^{18} \text{ Nmm}^2$. The graph in Figure 27 shows that for high stiffnesses of the connections, the bending stiffness indeed approaches $2,86 \cdot 10^{18} \text{ Nmm}^2$.

$$\Delta EI = E * \sum A * a^2 = 11.600 * 2 * 280 * 2900 * 10.150^2 = 1,94 * 10^{18} \quad (107)$$

$$EI_{CLT} = 0,92 * 10^{18} + 1,94 * 10^{18} = 2,86 * 10^{18} \quad (108)$$

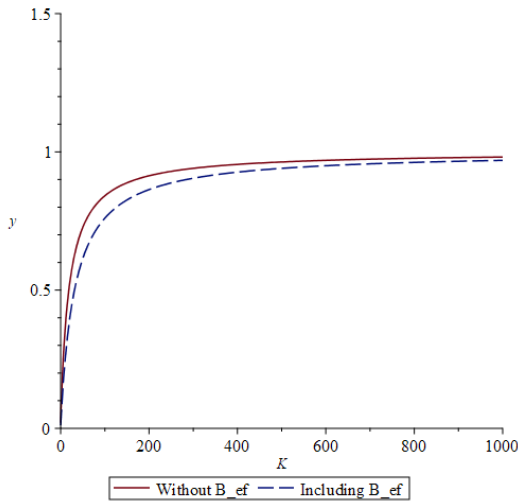


Figure 26, gamma factor of the façade with and without transversal walls

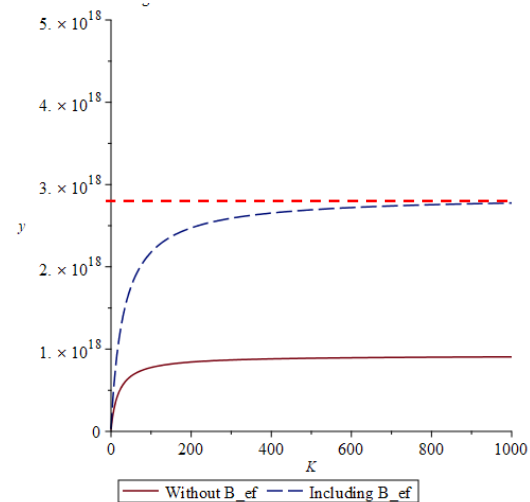


Figure 27, bending stiffness of the façade with and without transversal walls

The increased bending stiffness has a direct relation to the bending deformation. This bending deformation was found to be 132 mm for the façade of 77,5 meter. The increased bending stiffness results in a bending deformation of 43 mm, which is a reduction of 89 mm. This shows that there is a large potential contribution of the transversal façade on the bending stiffness.

A7.4.2 Forces on the transversal façade

The transversal façades have the potential to contribute largely to the bending stiffness. By doing so, the force transfer in the façade will also change significantly. The moment of resistance W is related to the moment of inertia I as shown below. This makes that the moment of resistance also increases by a factor 3 in case transversal walls are included.

The force in the transversal wall can be calculated by first calculating the maximum stress in the outer panel for the new found bending stiffness. This stress is then multiplied by the area of the transversal wall. The maximum increment of the bending moment for a single story ΔM is taken from the table in chapter 4 of the main report.

$$\sigma_y = \frac{\Delta M * b}{2 * I} = \frac{7885 * 10^6 * 20,3}{2 * \frac{2,86 * 10^{18}}{11.600}} = 0,325 \text{ N/mm}^2 \quad (109)$$

$$F_d = \sigma_y * t * b_{ef} = n_y * b_{ef} \quad (110)$$

$$F_d = 0,325 * 280 * 2900 = 264 \text{ kN} \quad (111)$$

This force of 264 kN is 68% of the acting bending moment ΔM ($264 * 20,3 = 5350$ kNm). 32% of the bending moment is resisted by the façade itself. In other words, the additional transversal walls reduce the forces in the façade by 68%.

This force of 264 kN is to be transferred to the transversal walls by the connections in the corners. The connections on the vertical edges of the façade panels have been designed for a force of 291 kN according to the table in chapter 4.5. This shows that the connections required for connecting the façade to the transversal panels can be similar to the connections used for the façade panels on the vertical edges. Although additional bending moments due to eccentricities do have to be included.

A7.4.3 Maple script for the effective bending stiffness of the façade with an effective width

```

> restart;
>
Calculation of the bending stiffness of a façade including the effective width of the transversal façade
the height is multiplied by 2 as the method of Schelling is derived for a beam on two supports, whereas
the
façade is schematized as a cantilever.

The equation of Schelling has previously been used to calculate the façade without the effective width
of the transversal façade.
this equation used 7 elements.

The following equation is derived for 9 elements, where the first and last element have the area of the
effective width of the façade.

the boundary conditions of the matrix denoted by s_i have been adjusted for the 9 element structure. the
fact that the transversal
façade panels contribute to the stiffness influences these boundary conditions as s1 (first), s2, s8 and s9
(last) have a value; wherea for the 7 element structure
only s1 and s7 (first and last) boundary conditions were non-zero.

it is assumed that the connections to the transversal façade have the same stiffness as the other
connections
>
> A := b·t :
> A_eff := b_eff·t :
> t := 280 :
> E := 11600 :
> K := 100
                                     K := 100                                (1)
> L := 2·77500 :
> b := 2900 :
> b_eff := 2900;
                                     b_eff := 2900                                (2)
> EIfaçade := 923·1015 + E·2·b_eff·t· $\left(\frac{20300}{2}\right)^2$ ;
                                     2.86 × 1018                                (3)
>
> a1 := 3.5·b : a2 := 3·b : a3 := 2·b : a4 := b : a6 := -b : a7 := -2·b : a8 := -3·b : a9 :=
-3.5·b : a5 := 0 :
>
> v11 :=  $\left(K + \frac{\text{Pi}^2}{L^2} \cdot E \cdot A\_eff\right) \cdot a1$  : v12 := -K·a2 :

```

```

> v21 := -K·a1 : v22 :=  $\left( K + K + \frac{\text{Pi}^2}{L^2} \cdot E \cdot A \right) \cdot a2$  : v23 := -K·a3 :
> v32 := -K·a2 : v33 :=  $\left( K + K + \frac{\text{Pi}^2}{L^2} \cdot E \cdot A \right) \cdot a3$  : v34 := -K·a4 :
> v43 := -K·a3 : v44 :=  $\left( K + K + \frac{\text{Pi}^2}{L^2} \cdot E \cdot A \right) \cdot a4$  : v45 := -K·a5 :
> v54 := -K·a4 : v55 :=  $\left( K + K + \frac{\text{Pi}^2}{L^2} \cdot E \cdot A \right) \cdot a5$  : v56 := -K·a6 :
> v65 := -K·a5 : v66 :=  $\left( K + K + \frac{\text{Pi}^2}{L^2} \cdot E \cdot A \right) \cdot a6$  : v67 := -K·a7 :
> v76 := -K·a6 : v77 :=  $\left( K + K + \frac{\text{Pi}^2}{L^2} \cdot E \cdot A \right) \cdot a7$  : v78 := -K·a8 :
> v87 := -K·a7 : v88 :=  $\left( K + K + \frac{\text{Pi}^2}{L^2} \cdot E \cdot A \right) \cdot a8$  : v89 := -K·a9 :
> v98 := -K·a8 : v99 :=  $\left( K + \frac{\text{Pi}^2}{L^2} \cdot E \cdot A_{\text{eff}} \right) \cdot a9$  :
>
> s1 := 0.5·K·b :
> s2 := 0.5·K·b :
> s3 := 0 :
> s4 := 0 :
> s5 := 0 :
> s6 := 0 :
> s7 := 0 :
> s8 := -0.5·K·b :
> s9 := -0.5·K·b :
>
> with(linalg) :
> Amatrix := matrix([ [v11, v12, 0, 0, 0, 0, 0, 0, 0], [v21, v22, v23, 0, 0, 0, 0, 0, 0], [0, v32, v33,
v34, 0, 0, 0, 0, 0], [0, 0, v43, v44, v45, 0, 0, 0, 0], [0, 0, 0, v54, v55, v56, 0, 0, 0], [0, 0, 0, 0,
v65, v66, v67, 0, 0], [0, 0, 0, 0, 0, v76, v77, v78, 0], [0, 0, 0, 0, 0, 0, v87, v88, v89], [0, 0, 0,
0, 0, 0, 0, v98, v99]]) :
> S := vector([s1, s2, s3, s4, s5, s6, s7, s8, s9]) :
>
> sol := linsolve(Amatrix, S);
      [ 0.765  0.761  0.737  0.723  -t1,000  0.723  0.737  0.761  0.765 ]
>

```

The solution holds the gamma-factors for each element.

(4)

sol[1] is the first gamma-factor and-so-on.

the moment of inertia is calculated for the façade without openings.

First the I-value including stiffness is calculated, then the I-value without stiffness is calculated.

This gives a reduction factor for the façade.

This factor is then multiplied with the moment of inertia for the façade with openings to find the bending stiffness of the façade including the effective width.

>

$$\begin{aligned} > I_{ef} := & \frac{7 \cdot t \cdot b^3}{12} + 2 \cdot sol[1] \cdot t \cdot b_{eff} \cdot a l^2 + 2 \cdot sol[2] \cdot t \cdot b \cdot a 2^2 + 2 \cdot sol[3] \cdot t \cdot b \cdot a 3^2 + 2 \cdot sol[4] \cdot t \cdot b \\ & \cdot a 4^2; \\ & 275.67 \times 10^{12} \end{aligned} \quad (5)$$

$$\begin{aligned} > I_{full} := & \frac{7 \cdot t \cdot b^3}{12} + 2 \cdot t \cdot b_{eff} \cdot a l^2 + 2 \cdot t \cdot b \cdot a 2^2 + 2 \cdot t \cdot b \cdot a 3^2 + 2 \cdot t \cdot b \cdot a 4^2; \\ & 362.50 \times 10^{12} \end{aligned} \quad (6)$$

>

$$\begin{aligned} > gamma_{red} := & \frac{I_{ef}}{I_{full}} \\ & 0.760 \end{aligned} \quad (7)$$

$$\begin{aligned} > El_{schelling} := & gamma_{red} \cdot E I_{façade} \\ & 2.18 \times 10^{18} \end{aligned} \quad (8)$$

>

A7.5 Reduced top deformation – theoretical calculation without connection stiffnesses

The theoretical top deformation of the models with an additional core and/or effective width has been calculated for all heights, using the equations presented in the previous chapters. First the top deformation of the façade is calculated without connections (Table 43). Then the increased top deformations due to connection deformation is calculated in Table 44. Finally the initial slip of the connections is also included in the top deformation (Table 45).

Table 43, theoretical top deformations for façades with additional stability elements – without connection stiffnesses

Model	Height	Wbending		Wshear		Wpiers		WSchelling		Wtot
CLT	77,5 meter	132	100%	40,3	100%	19,1		26,1		218
CLT+core	77,5 meter	116	88%	10,8	27%	5,1	27%	23,0	88%	155
CLT+b_{eff}	77,5 meter	38,1	29%	40,3	100%	19,1	100%	26,1	100%	124
Both	77,5 meter	33,7	25%	10,8	27%	5,1	27%	23,0	88%	72,6
CLT	62,0 meter	49,4	100%	23,5	100%	11,2		15,5		100
CLT+core	62,0 meter	43,5	88%	6,35	27%	3,02	27%	13,6	88%	66,5
CLT+b_{eff}	62,0 meter	16,7	34%	23,5	100%	11,2	100%	15,5	100%	66,9
Both	62,0 meter	14,8	30%	6,35	27%	3,02	27%	13,6	88%	37,8
CLT	46,5 meter	14,1	100%	11,9	100%	5,80		7,97		39,8
CLT+core	46,5 meter	12,4	88%	3,21	27%	1,57	27%	7,01	88%	24,2
CLT+b_{eff}	46,5 meter	5,7	41%	11,9	100%	5,80	100%	7,97	100%	31,4
Both	46,5 meter	5,1	36%	3,21	27%	1,57	27%	7,01	88%	16,9
CLT	31,0 meter	3,43	100%	7,17	100%	3,27		6,20		20,1
CLT+core	31,0 meter	2,88	84%	1,36	19%	0,62	19%	5,21	84%	10,1
CLT+b_{eff}	31,0 meter	1,81	53%	7,17	100%	3,27	100%	6,20	100%	18,5
Both	31,0 meter	1,53	45%	1,36	19%	0,62	19%	5,21	84%	8,7
CLT	15,5 meter	0,23	100%	1,97	100%	0,95		1,77		4,92
CLT+core	15,5 meter	0,18	79%	0,24	12%	0,11	12%	1,40	79%	1,90
CLT+b_{eff}	15,5 meter	0,15	67%	1,97	100%	0,95	100%	1,77	100%	4,84
Both	15,5 meter	0,12	53%	0,24	12%	0,11	12%	1,40	79%	1,87

Table 44, theoretical top deformations for façades with additional stability elements –connection stiffnesses without slip

Model	Height	W_{tot}	W_{slip}		W_{rock}		W_{b,slip}		W_{tot}
CLT	77,5 meter	218	2,6	100%	29,5	100%	30,0	100%	280
CLT+core	77,5 meter	155	0,7	27%	26,0	88%	26,4	88%	208
CLT+b_{eff}	77,5 meter	124	2,6	100%	8,56	29%	8,7	29%	144
Both	77,5 meter	72,6	0,7	27%	7,38	25%	7,5	25%	88
CLT	62,0 meter	100	2,5	100%	13,2	100%	34,6	100%	150
CLT+core	62,0 meter	66,5	0,7	27%	11,6	88%	30,4	88%	109
CLT+b_{eff}	62,0 meter	66,9	2,5	100%	4,49	34%	11,8	34%	86
Both	62,0 meter	37,8	0,7	27%	3,96	30%	10,4	30%	53
CLT	46,5 meter	39,8	1,3	100%	5,2	100%	17,3	100%	64
CLT+core	46,5 meter	24,2	0,4	27%	4,58	88%	15,2	88%	44
CLT+b_{eff}	46,5 meter	31,4	1,3	100%	2,13	41%	7,09	41%	42
Both	46,5 meter	16,9	0,4	27%	1,87	36%	6,23	36%	25
CLT	31,0 meter	20,1	0,5	100%	0,7	100%	6,6	100%	28
CLT+core	31,0 meter	10,1	0,1	19%	0,59	84%	5,54	84%	16
CLT+b_{eff}	31,0 meter	18,5	0,5	100%	0,37	53%	3,50	53%	23
Both	31,0 meter	8,7	0,1	19%	0,32	45%	2,97	45%	12
CLT	15,5 meter	4,92	0,1	100%	0,1	100%	1,2	100%	6,3
CLT+core	15,5 meter	1,90	0,0	12%	0,08	79%	0,95	79%	2,9
CLT+b_{eff}	15,5 meter	4,84	0,1	100%	0,07	67%	0,80	67%	5,8
Both	15,5 meter	1,87	0,0	12%	0,05	53%	0,64	53%	2,6

Table 45, theoretical top deformations for façades with additional stability elements –connection stiffnesses including slip

Model	Height	W_{tot}	W_{sliding,sl}		W_{rock,sl}		W_{schelling,sl}		W_{tot}
CLT	77,5 meter	280	9	100%	17,6	100%	53,4	100%	360
CLT+core	77,5 meter	208	2,43	27%	15,5	88%	47	88%	273
CLT+b_{eff}	77,5 meter	144	9	100%	17,6	100%	53,4	100%	266
Both	77,5 meter	88	2,43	27%	15,5	88%	47	88%	191
CLT	62,0 meter	150	7	100%	12,2	100%	42,8	100%	212
CLT+core	62,0 meter	109	1,89	27%	10,7	88%	37,7	88%	159
CLT+b_{eff}	62,0 meter	86	7	100%	12,2	100%	42,8	100%	145
Both	62,0 meter	53	1,89	27%	10,7	88%	37,7	88%	100
CLT	46,5 meter	64	5	100%	6,9	100%	32,1	100%	108
CLT+core	46,5 meter	44	1,35	27%	6,07	88%	28,2	88%	80,0
CLT+b_{eff}	46,5 meter	42	5	100%	6,9	100%	32,1	100%	81,9
Both	46,5 meter	25	1,35	27%	6,07	88%	28,2	88%	57,5
CLT	31,0 meter	28	3	100%	3,1	100%	21,4	100%	55,4
CLT+core	31,0 meter	16	0,57	19%	2,6	84%	18	84%	37,5
CLT+b_{eff}	31,0 meter	23	3	100%	3,1	100%	21,4	100%	47,2
Both	31,0 meter	12	0,57	19%	2,6	84%	18	84%	30,6
CLT	15,5 meter	6,3	1	100%	0,8	100%	10,7	100%	18,8
CLT+core	15,5 meter	2,9	0,12	12%	0,63	79%	8,45	79%	12,2
CLT+b_{eff}	15,5 meter	5,8	1	100%	0,8	100%	10,7	100%	17,5
Both	15,5 meter	2,6	0,12	12%	0,63	79%	8,45	79%	11,2

A7.6 Shape of openings

The shape of openings have been defined as rectangular openings of 1,74x1,74 meter in chapter 3.3. However, different shapes of openings can be required. For instance in case a door opening is needed to allow access to a balcony. That is why the façade has also been analyzed with regard to different shapes of openings.

This analysis has been done using the theoretical hand calculations that have been presented in this report. Influence of connections has not been included. As this would (in theory) be unaffected by the openings in the panels.

Three alternative openings have been considered. The first is an opening with the dimensions required for a door (1,00 x 2,40 meter). The second opening is dimensioned for a door with an additional sidelight (1,40 x 2,40 meter). Finally the third opening has been dimensioned for a wider window of 2,00 x 1,20 meter.

Figure 28, four different openings in the façade panels

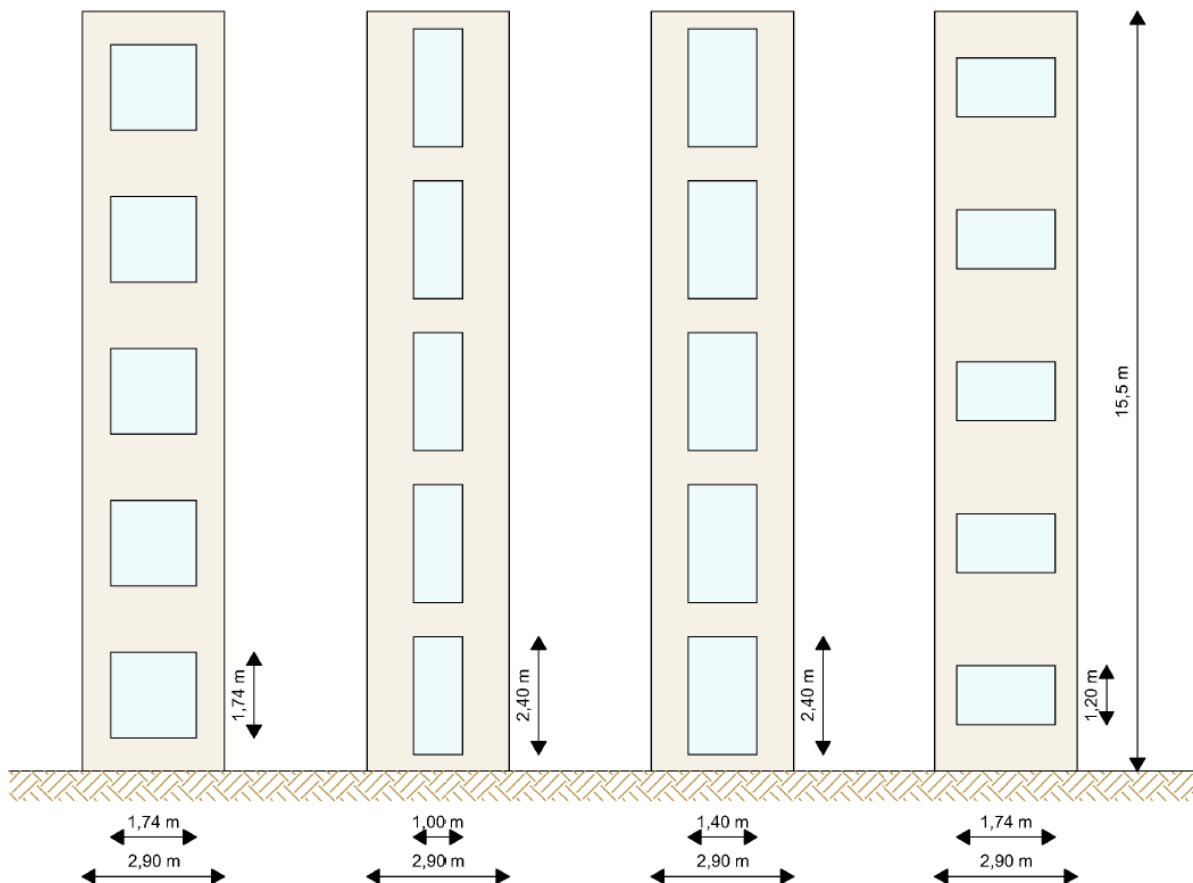


Table 46, top deformation of the façade for different type of openings

W_{top}	Rectangular	Door	Door + sidelight	Window
	1,74 x 1,74 m	1,00 x 2,40 m	1,40 x 2,40 m	2,00 x 1,20 m
15,5 meter	4,92	3,75	6,83	5,57
31,0 meter	20,1	15,2	27,1	22,9
46,5 meter	39,8	28,8	47,1	47,1
62,0 meter	100	69,8	110	120
77,5 meter	218	149	225	265

Top deformations of the façade for different openings have been calculated using the theory presented in chapter 4. The door opening shows that the top deformation is reduced compared to the rectangular openings used for the computer models. When a sidelight is added to the door the top deformations increase such that they surpass the top deformations of the rectangular openings. The increase of top deformation is primarily the result of the increased deformation as a result of deformations of the lintels.

The window openings also result in an increased top deformation when compared to the rectangular openings. This is mainly due to the reduced bending stiffness of the façade, as the bending stiffness is related to the area of the piers. Another contributor is the horizontal deformation of the piers themselves. For all other openings, the pier deformation is relative low. But for the wider windows this becomes more prominent.